Addis Ababa University
አዲስ አበባ ዩኒቨርሲቲ

SEEK WISDOM, ELEVATE YOUR INTELLECT AND SERVE HUMANITY !

Addis Ababa University

College of Natural and Computational Sciences

School of Earth Sciences

Spatial and Temporal Hydrochemical Variation of Upper Awash Sub-Basin, Central Ethiopia

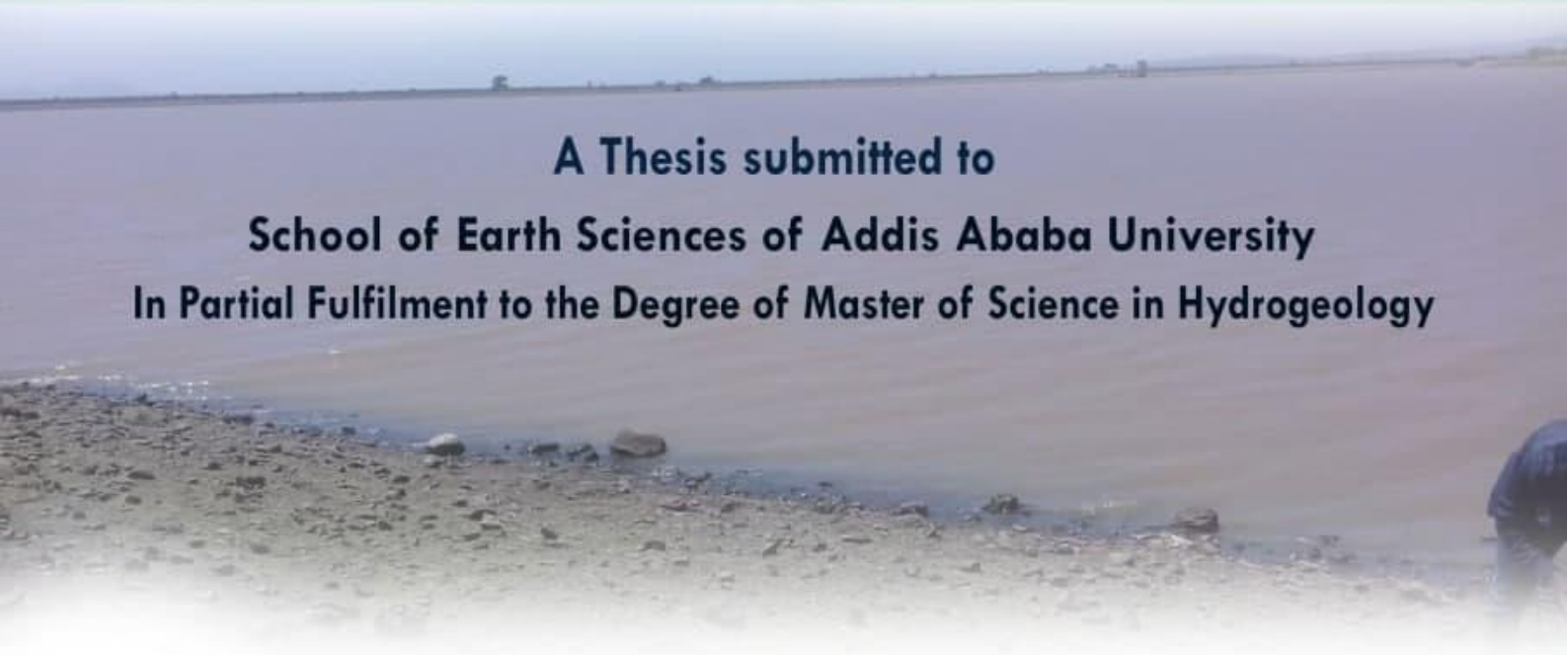

A Thesis submitted to

School of Earth Sciences of Addis Ababa University

In Partial Fulfilment to the Degree of Master of Science in Hydrogeology

By: Gebeyaw Ayele Kassaw

Advisor: Dr. Dessie Nedaw

September 2021

Addis Ababa, Ethiopia

Addis Ababa University

College of Natural and Computational Sciences

School of Earth Sciences

Spatial and Temporal Hydrochemical Variation of the Upper Awash Sub-Basin, Central Ethiopia

A Thesis Submitted to

School of Earth Sciences of Addis Ababa University in Partial Fulfilment to the Degree of Master of Science in Hydrogeology

By: Gebeyaw Ayele Kassaw

Approved by the Board of Examiners:

	Signature
Dr. Behailu Birhanu (Examiner)	_____Date_____
Dr. Tilahun Azagegn (Examiner)	_____Date_____
Dr. Dessie Nedaw (Advisor)	_____Date_____

Declaration for Originality and Quality

I undersigned declare that this thesis is my original work for the requirement of the degree of Master of Science in Hydrogeology accomplished under the supervision of Dr. Dessie Nedaw, School of Earth Sciences, Addis Ababa University, during the year 2021/22. My further declaration is that this work has not been presented and/or submitted to any other college, institution, or university for the award of any degree or Diploma. All the secondary data sources and materials used in the thesis work have been duly cited and acknowledged.

Gebeyaw Ayele Kassaw (MSc Candidate)

Signature_____ Date: _____

Advisor: Dr. Dessie Nedaw

Signature_____ Date: _____

Abstract

In countries like Ethiopia, regular hydrochemical variation follow-up is not common. The Upper Awash Sub-Basin is found in a region with high population density, high water demand, and is a highly vulnerable water resource that requires regular hydrochemical follow-up. This study was aimed to assess the spatial and temporal hydrochemical variation in the Upper Awash Sub-Basin conducted by combining previous hydrochemical data from various sources, and the present two year's data analyzed in 2019 and 2021. The major cation variation is mainly attributed to the rock-water interaction due to the availability of complex geology in the area comprising highly weathered, olivine, pyroxene, and feldspar bearing basaltic rocks and acidic volcanic rocks that can alter the composition of water making the concentrations of calcium, magnesium, sodium, and potassium ions variable both spatially and temporally with minor effects from anthropogenic sources taken under consideration. The temporal variation of major cations in groundwater is due to the residence time of groundwater in the area, and the circulation of groundwater along the regional and local fault lines. Bicarbonate is the most abundant and varying anion in the area resulting from a high rate of carbon dioxide outgassing from thermal aquifers like Filwuha and from the reaction between dissolved carbon dioxide with the rocks to produce bicarbonate and clay or mica. Sulfate, chloride, and nitrate concentrations in both groundwater and surface water are increasing through time mainly due to anthropogenic factors from nitrate and sulfate fertilizers. In addition to the anthropogenic factors, chloride concentration is also related to the stagnation of water at compacted clay along fault zones. Despite their concentration below the acceptable standards, the concentration of toxic heavy metals like lead, zinc, and manganese show both spatial and temporal variation. The hydrochemical variation analysis depicted that groundwater is more stable with relatively lower hydrochemical variation than the lakes and Rivers as it is a hidden resource. On the other hand, Lakes and Rivers in the area show temporal hydrochemical variation due to their proximity to the controlling factors. Water-supply reservoirs in the Addis Ababa area have relatively stable hydrochemical parameters whereas Debrezeit Lakes and the Rivers have relatively higher spatial and temporal variation. Groundwater in most areas of Upper Awash is suitable for drinking and agricultural activities. Regarding water quality for irrigation, Mojo and Holeta Rivers, Lake Hora, and Lake Hora Hoda are highly saline that may affect soil fertility and crop yield.

Key Words/Phrases: Concentration, Spatial Variation, Temporal Variation, Upper Awash Sub-Basin, Water Quality

Acknowledgment

I would like to express my sincere gratitude to my advisor Dr. Dessie Nedaw for his tireless support, inspiration, enthusiasm, and willingness to share his vast knowledge throughout my research work. Not only experience sharing but also this thesis is part of the currently undergoing project in the Upper Awash Sub-Basin entitled 'Sound Groundwater Management under a Changing Climate for the Upper Awash Basin (UAB) Using Isotope Enabled Water Balance Modeling' by Dr. Dessie Nedaw and everything required for this thesis is covered by the above project.

I want to acknowledge all Addis Ababa University, School of Earth Sciences instructors who supported me in gaining very important knowledge about the subject matter and other related fields.

I would like to express my greatest thanks to Water Works Design and Supervision Enterprise, Addis Ababa Water and Sewerage Authority, Ethiopian National Meteorological Agency, and Ministry of Water Irrigation and Energy for their kindness in providing the necessary data to carry out this research work.

I would like to acknowledge different organizations and their officers who allowed me to take water samples and for in-situ measurements.

My deepest gratitude goes to Ato Worku and our driver Ato Hailu Dibabe for their cooperation in allotting field materials and field scheduling.

My greatest appreciation goes to my beloved friends Belay Molla, Amanuel Godie, Amanuel Habtamu, Asfie Meshesha, Xhaka Mebratu, and Behailu Girma for their tireless support throughout my research work.

My greatest gratitude goes to my beloved family for their inspiration and encouragement throughout my study.

Table of Contents

List of Figures

List of Tables

List of Acronyms

°C	Degree Celsius
µS/cm	Micro Siemens per Centimeter
AAWSA	Addis Ababa Water and Sewerage Authority
BDL	Below Detection Limit
DEM	Digital Elevation Model
EARS	East African Rift System
EC	Electrical Conductivity
EPA	Environmental Protection Agency
GSE	Geological Survey of Ethiopia
ITCZ	Intertropical Convergent Zone
Km	Kilometer
m	Meter
MER	Main Ethiopian Rift
mg/l	Milligram Per Liter
mm/a	Millimeter Per Annum
NMA	National Meteorological Agency of Ethiopia
NMSA	National Meteorological Service Agency
pH	Hydrogen-ion Activity
TDS	Total Dissolved Solids
UAB	Upper Awash Sub-Basin
UTM	Universal Transverse Mercator
WFB	Wonji Fault Belt
WWDSE	Water Works Design and Supervision Enterprise

Chapter One

Introduction

1.1. General Background

Water is a valuable natural resource without which life on Earth would be impossible, and its presence is the main factor that distinguishes our planet, the Earth, from others in the solar system. Our day-to-day activities depend on the availability of cheap and clean water resources, useful for domestic, agricultural, and industrial activity (Hiscock & Bense, 2005). Human development and well-being largely rely on the availability of pure water and its usefulness is determined by the chemical, physical, and biological qualities.

The amount of ionic species in natural waters is determined by several factors, including the type of soil and rock through which the water passes, the degree of weathering and solubility of the mineral components of rocks and soils, the extent and duration of contact with rocks and soils, temperature conditions, and the type of dissolved and suspended solutes that falls with precipitation and anthropogenic factors (Tenalem Ayenew, 2006).

The Upper Awash Sub-Basin comprises various rock units including basalts, rhyolites, ignimbrites, pyroclastic materials, and unconsolidated sediments to some extent. As a result, the chemical composition of groundwater flowing through these geological materials can be altered both spatially and temporally.

The solubility of minerals in water is determined by the temperature and pressure condition of the environment. The change in temperature and pressure conditions results in weathering of rocks and soil formation, loose minerals from the resulting soils can be easily dissolved in water. The residence time of groundwater in an area determines the duration of rock-water interaction and this, in turn, controls the amount and number of its hydrochemical parameters.

The quality of surface water and shallow groundwater can be controlled by anthropogenic factors since these water bodies are close to the source of such factors. One of the country's largest rivers, Awash and its tributaries emerge from the highland areas with various geologic formations and flow down to Afar. The major tributaries of the Awash River including the Akaki, Mojo, and Holeta rivers pass through one of the most densely populated and industrialized urban centers of the country. These surface water bodies could be vulnerable to anthropogenic factors.

1.2. Objectives

1.2.1. General Objective

- To assess the possible spatial and temporal variation in the hydrochemistry of the Upper Awash Sub-Basin by the combination of the present hydrochemical analyses with the previous data from various sources.

1.2.2. Specific Objectives

Specific objectives include:

- To Generate a tabular hydrochemical data of the Upper Awash Sub-Basin from the earliest analysis to present-day laboratory results;
- To evaluate the suitability of the water resource for drinking and agricultural activities;
- To estimate the annual groundwater recharge of the sub-basin.

1.3. Problem Statement

The Upper Awash Sub-Basin is a densely populated and urbanized area, which is also home to major industries of the country where there is a high water demand for domestic, industrial, and agricultural purposes. The water supply sources for the city of Addis Ababa are mainly from surface waters like Legedadi, Gefersa, and Dire reservoirs; groundwater sources are mainly in the Akaki well-field. The groundwater resource is also used by other towns and rural communities within the sub-basin. Different springs and rivers are also used for several purposes including agricultural activities and domestic consumption. These surface water and groundwater supply sources could be vulnerable to different anthropogenic influences and other factors. However, there is a lack of detailed regular follow-up and continuous trend analysis studies conducted to analyze the variation in the hydrochemistry of surface water and groundwater resources of the area, except a two-year water quality monitoring conducted by Water Works Design and Supervision Enterprise (WWDSE) in 2006 and 2007. As a result, this study will try to address whether there is hydrochemical variation in surface waters and groundwater resources of the sub-basin based on previous hydrochemical data and present laboratory analysis.

1.4. Significance of the Study

Understanding the hydrochemical variation through time is crucial to follow-up on each hydrochemical parameter so that they remain within the acceptable water quality standards for

domestic, industrial, and agricultural purposes. If the presence of a hydrochemical variation is detected, it can be used to identify the possible source of that variation and to take a remedial measure, especially if the variation is related to anthropogenic influences. On the other hand, the presence of a change in hydrochemistry with time may imply what will happen after some time in the future if it continues with the current trend. In general, understanding the hydrochemical variation through time may lead to the formulation of a more grounded policy on water safety and quality.

1.5. Previous Works

Regarding hydrochemistry, various academic as well as non-academic researches, have been conducted by many scholars in the Upper Awash Sub-Basin. Hydrochemical investigation in the area started back in the late 1930s. The hydrochemical analysis of Lake Hora in Debrezeit shows high bicarbonate and sodium ions (Omer, 1938).

According to the Greek Water Engineering Company (WATENCO, 1951), Filwuha thermal spring in Addis Ababa has a high concentration of sodium, bicarbonate, and sulfate ions. In 1951, the concentration of sodium was about 715.7mg/l as investigated by the above organization, and in 952, it was 641mg/l. Bicarbonate was a highly concentrated ion in the thermal spring, which was about 1873mg/l in 951 measurements and dropped to 1743mg/l after one year. The third dominant ion in the spring was sulfate, having a concentration of variable concentrations ranging from 47mg/l to 60mg/l. The other earliest analysis on hydrochemistry in the Upper Awash Sub-Basin was carried out by Chuzo Kondo in 1958, 1967, and 1975. In 1967, the concentration of sodium was dramatically increased to 1182mg/l in the spring water and bicarbonate had shown temporal variation after its concentration was increased to 2440mg/l. potassium ion concentration had also shown temporal variation within 16 years gap (3.1mg/l in 1951 and was 60mg/l in 1967 measurement).

Many types of research had been conducted in the Upper Awash Sub-Basin by the Ministry of mines including Igzaw Solomon (1974), Gebretsadik Eshete (1978), and Getahun Kebede (1980), Berhane Melaku (1982).

Bicarbonate and Magnesium ions are dominant in Lake Babugaya whereas Lake Bishoftu is characterized by high bicarbonate and sodium ions (Tamiru Alemayehu, 1992). Bishoftu Guda and Kuriftu lakes are chemically similar to the groundwater whereas Lake Hora contains a large amount of chloride concentration (Tamiru Alemayehu, 1992). The presence of a large amount of bicarbonate in Lake Bishoftu depicts its maturity. As a result of a low degree of

water-rock interaction, most of the waters in the Debrezeit area have low total dissolved solids ranging between 300 and 700mg/l. However, Lake Bishoftu is highly concentrated with a salinity level of 1600mg/l (Tamiru Alemayehu, 1992). Debrezeit Lakes have different chemistry mainly controlled by the rate of groundwater flow, especially Lake Babugaya is highly affected by the inflow and outflow of groundwater whereas highly saline lakes including Arenguade, Kilole, and Lake Hora are least affected by groundwater flux and Bishoftu Lake is chemically intermediate (Seifu Kebede, 1999).

As a result of the differences in rock-water interactions related to lithology and groundwater residence time, geomorphological setting, and climate, there are wide spatial variations in the hydrochemistry of natural waters in Ethiopia's broad volcanic topography (Tenalem Ayenew, 2006). Following regional groundwater flow directions towards areas of low rainfall and high evaporation and groundwater residence time, TDS increases from the highlands to the rift valley. The highland waters, in contrast to the rift valley waters, have a more homogeneous chemical composition and have a low total dissolved solids content. Highland waters are predominantly Ca-Mg bicarbonate, whereas rift valley waters are mainly Na-bicarbonate, with high total dissolved solids and fluoride levels. The escarpment waters are heterogeneous in composition and have a moderate total dissolved solids content. (Tenalem Ayenew, 2006).

The dominance of acidic volcanics, high temperatures in geothermal regions, and high CO_2 outgassing resulted in high fluoride concentration in the rift water. The presence of high nitrate in some major urban centers of the rift including Addis Ababa depicts anthropogenic pollutions.

Akaki catchment is an ideal place to understand groundwater hydrochemical evolution along flow paths as a result of water-rock interaction and anthropogenic effects (Molla Demlie et al., 2007). Very dilute Ca–HCO_3, Ca–Na–HCO_3 type water draining the Entoto silicic; Ca–Mg–HCO_3, Mg–Ca–HCO_3 type water draining the Addis Ababa basalt in the center sector and the Bishoftu basalt aquifers in the south. On the other hand, The Filwuha thermal system produces Na–HCO3 type water with rock-dominated hydrochemistry.

Anthropogenic factors result in a Ca–NO_3 and Ca–Cl-type water circulation in the middle section of the catchment, suggesting pollution (Molla Demlie et al., 2007). The systematic increase in EC and all major ions from Entoto to the Akaki well-field in the south reveals hydraulic continuity between the various aquifers and hydrochemical evolution from north to south along the flow direction. Cold-water in the northern portion of the Akaki catchment has lower sodium to total cations ratio, Ca+Mg / Na+K, TDS or EC, PH, and a greater Ca / Mg

ratio, but this changes as we move south (Ebasa Oljira, 2006). Groundwater salinity is influenced by Na, HCO_3, SO_4, and K, and the positive correlation between NO_3, Cl^-, and SO_4 reveals anthropogenic influence. The change in groundwater chemistry is mainly due to the dissolution of silicate minerals in the carbon dioxide open system and precipitation of Kaolinite and chalcedony except for the distribution of Cl^-, NO_3, and SO_4 to the chemical evolution in the central sector having anthropogenic origin. In Addis Ababa, improper waste disposal resulted in high levels of chromium, manganese, and nitrate in shallow groundwater infiltrated from contaminated surface water (Tamiru Alemayehu, 2001). According to the extensive hydrochemical investigation, most shallow wells, springs, and rivers are polluted by heavy metals and nitrates (Tenalem Ayenew et al., 2008).

The Ethiopian rift groundwater is found in a circumstance where aquifer heterogeneity and thermodynamically controlled geochemical reactions throughout the groundwater flow path can produce a comparable geochemical pattern. The composition of the Ethiopian rift waters follows a definite geochemical zonation that follows the geography(Kebede et al., 2008). This zone is defined by a shift in cation species from Ca and Mg-dominated waters near the mountains to Na-dominated waters near the rift bottom. Anions move from HCO_3 to Cl and SO_4 in a similar way. Rather than the extensively documented suggestions, regional geochemical zonation is mostly caused by aquifer composition variation.

Groundwater from the Rift floor is more chemically evolved than recently recharged waters from the escarpments, and its hydrochemical characteristics are linked to its spatial distribution in the escarpment, escarpment-rift transition zone, Rift floor (Bretzler et al., 2011).

According to Andarge Yitbarek et al., (2012), water in the Upper Awash Sub-Basin is classified into five major groups of chemical facies: Ca-Mg-HCO_3, Ca–Na–HCO_3, Na-Ca-MgHCO_3, Na-HCO_3, and Ca–HCO3. The Na-HCO_3 water types in Filwuha springs are characterized by high TDS (800-2250mg/l), high EC, and HCO_3. Groundwater draining the plateau parts of the Upper Awash Sub-Basin dominated by basaltic outcrops with thin paleosols intercalations are characterized by Na-Ca-HCO_3 with few Na-HCO_3 type water and TDS less than 235mg/l. groundwater draining the transitional rift part of the area has moderately mineralized water (TDS<470>238mg/l) is characterized by Ca-Na-HCO_3 type in the transitional part of the rift and evolves to Na-Ca- HCO_3 in the rift part. Recently recharged shallow groundwater systems in the plateau part of the Upper Awash Sub-Basin have diluted chemistry (TDS<200mg/l) with Ca-HCO3 type waters. Some groundwater wells from the transitional and rift parts of the Upper Awash may have this characteristic. Groundwater wells near scoria cones are in the transitional

rift part of the Upper Awash Sub-Basin have moderately diluted chemistry (TDS<450>130mg/l). These water classes are mainly Ca-Mg-HCO_3 type waters influenced by basic volcanic rocks.

Sodium and calcium are the dominant cations in the spring waters of the Upper Awash Sub-Basin and are more or less equally abundant

Sodium and Calcium as the dominant cations and they are more or less equally abundant with the predominant water type of bicarbonate type (Mg-HCO_3, Ca-HCO_3, and $NaHCO_3$ type (Mekdes Nigatie, 2012). A detailed hydrochemical investigation of Upper Awash Sub-Basin was done by the Water Works Design and Supervision Enterprise (WWDSE, 2008) in general, and specifically, the hydrochemistry of Addis Ababa and its surrounding is also investigated by Addis Ababa Water and Sewerage Authority (AAWSA).

1.6. Methodology and Materials Used

For this research, a lot of time and effort was put into gathering relevant primary hydrochemical data and secondary data from concerned institutes and previous studies. In general, all the activities performed in this study can be classified into three phases. During the first phase, the available literature related to the title was reviewed; secondary data such as meteorological data (precipitation, temperature, wind speed, and duration of sunshine hours) were collected from the National Meteorological Agency of Ethiopia (NMA); Previous hydrochemical data of Upper Awash were collected from Water Works Design and Supervision Enterprise (WWDSE), Addis Ababa Water and Sewerage Authority (AAWSA) and from different kinds of literature. The second phase was field water sample collection for laboratory analysis and in-situ field measurements. 15 water samples were systematically collected in different parts of Upper Awash Sub-Basin with different considerations taken into account including selected sites that are vulnerable to hydrochemical variation, taking samples from both discharge area and recharge area to know the spatial variation of ions and the corresponding water quality. Water samples were taken from rivers, groundwater, Lakes, and spring. Insitu measurements such as pH, temperature, electrical conductivity (EC), total dissolved solids (TDS), and titration of a 50ml filtered water sample were carried out to measure the alkalinity of the water (bicarbonate concentration analysis). Site geological and hydrogeological description was also made in terms of lithological description, identification of geological structures like faults and joints which may act as a conduit for groundwater and its contaminant flow.

The third phase was attributed to the interpretation of laboratory analysis results. The hydrochemical analysis of fifteen water samples was analyzed in the laboratory in 2019 and 2021 to know the concentration of Calcium ion (Ca^{2+}), Magnesium ion (Mg^{2+}), Sodium ion (Na^{+}), Potassium ion (K^{+}), Chromium (Cr), Cadmium (Cd), Lead (Pb), Zinc (Zn), Iron (Fe), and Manganese (Mn). By combining the previous hydrochemical data collected from different institutions/organizations and literature with the present laboratory analyses and in-situ field measurements, the temporal and spatial hydrochemical variation of groundwater and surface water were determined from the concentration-time graph and spatial variation maps respectively. Depending on the nature of the environment, the possible sources of hydrochemical variation were indicated. Water type classification was made using Aquachem 2014.2 software and hydrochemical trend analysis graphs were prepared by using the Scientific Data Analysis and Visualization (SciDAVis). To show the spatial hydrochemical variation, spatial distribution maps of the Upper Awash Sub-Basin were also prepared by interpolation on ArcMap.

The materials used for this research work were GPS, EC Meter, and Sulphuric acid having 1.6 and 0.16 acid concentration, Filter paper, Syringe, Reagent, beaker, and funnel. The software used for this research is ArcGIS, Aquachem2014.2, SciDAVis, and New_LocClim_1.10.

GPS: was used for recording the location (Geographic coordinates) of sampling sites, for finding travel direction, and to know the elevation of the area above mean sea level.

EC Meter: a multifunctional Electrical Conductivity Meter (EC-Meter) was used to measure the temperature, electrical conductivity, pH, and Total Dissolved solids of the water samples.

Sulphuric Acid: Sulphuric acid (1.6 and 0.16 acid concentration) was used for measuring the Alkalinity of the water sample. Titration was done to know the concentration of unknown components (Bicarbonate concentration) with the known concentration of Sulphuric acid droplets.

Filter Paper: water samples taken from lakes and rivers contain many suspended materials and were not clean. So filtering was required before doing titration since such turbid water samples may lead to the wrong measurement result. For this purpose, the filter paper was used to purify 100ml of water sample for alkalinity measurement.

Syringe: syringe was used to bypass water samples onto the filter paper and also to take 50ml of filtered water for titration.

Reagent: six droplets of reagent were added to 50ml of water sample and the color of the water sample will be changed to purple color. The Sulphuric acid concentration added to this sample was measured until this purple-colored water sample is changed to cloudy color.

Beaker and Funnel: beaker and funnel were used as a container for water samples during in-situ field measurements.

Softwares applied for this study were:

ArcGIS: location maps, climate, soil, land use and land cover maps, geological and structural maps, drainage and hydrochemical distribution maps were prepared using ArcGIS Software.

Aquachem 2014.2 software: was used for hydrochemical analysis and water type classification and for preparing different hydrochemical graphs which simplify the interpretation in terms of ionic dominance and water quality.

New_LocClim_1.10: 21 years of meteorological data from each of the thirteen stations were taken from the National Meteorological Agency of Ethiopia (NMA) for climatic description and recharge estimation of the area. However, this daily meteorological data taken from NMA contains some missing data. These missing data were filled with the average climate data obtained from New_LocClim software.

Scientific Data Analysis and Visualization (SciDAVis) was used to prepare graphs showing temporal variations of different chemical species.

Finally, interpretations in terms of temporal and spatial ionic variations in both groundwater and surface water bodies were carried out; water type classification was made and the sources of ionic variations were forwarded; the quality of water for domestic, agricultural, and industrial applications was checked based on the standard guidelines.

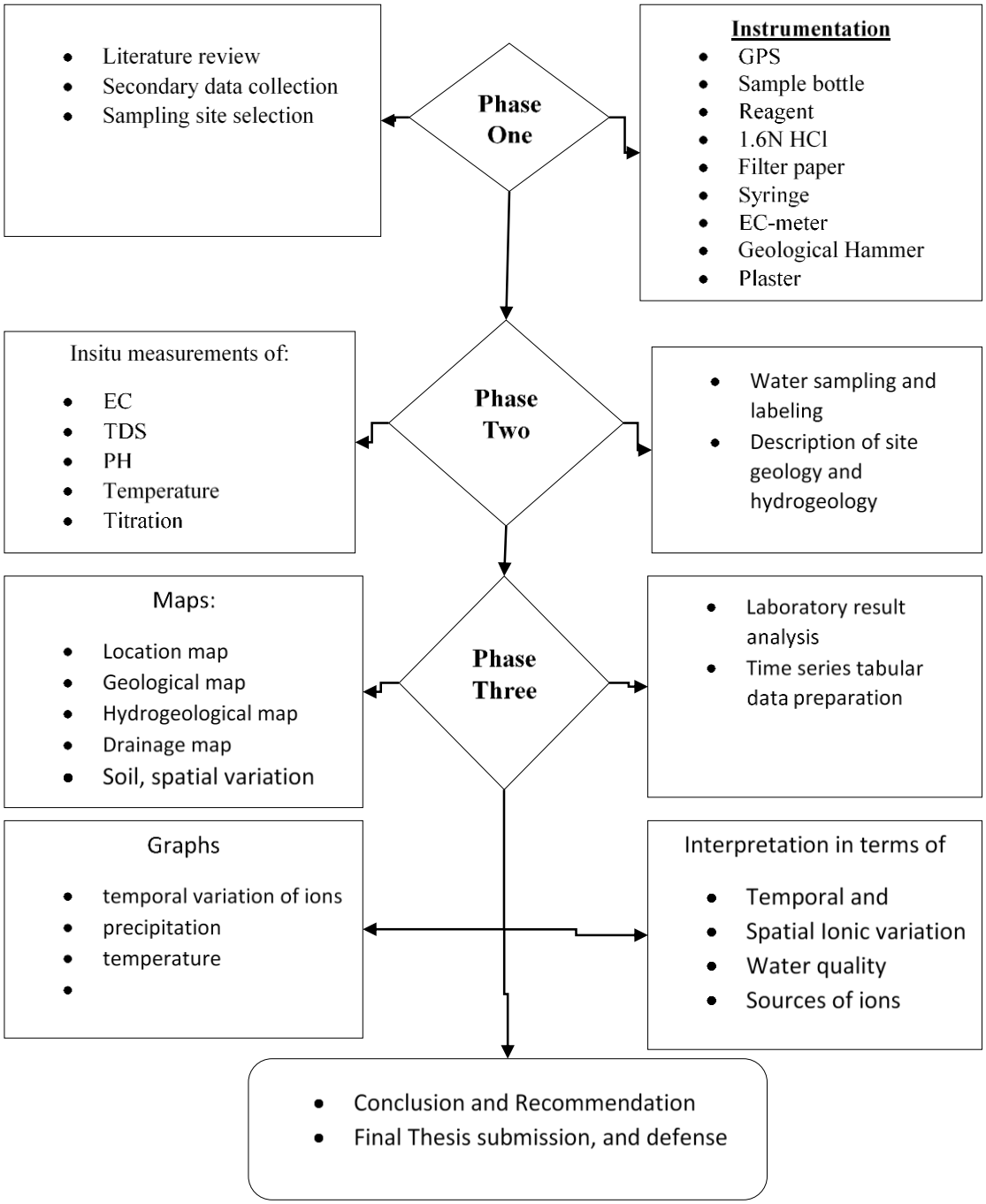

Figure 1. 1: Activity Flow Chart

Chapter Two

Literature Review

The mineralogy of rocks, chemical weathering, evaporation, atmospheric precipitation, geomorphology, the residence time of groundwater, and anthropogenic influences all play a major role in hydrochemistry (Freeze & Cherry, 1979; Morán-Ramírez et al., 2016). The composition of groundwater in Ethiopia is a function of lithologic variation, evaporative enrichment before recharge, and thermodynamic control (Seifu Kebede, 2013). The hydrolysis of rocks in the presence of atmospheric or soil carbon dioxide produces Na^+, K^+, Ca^{2+}, Mg^{2+}, and HCO_3^- in groundwater. In addition, the texture, porosity, regional structures, degree of fissuring, and other factors might influence the composition of groundwater passing through the rock (HEM, 1985).

Since rock temperature increases with depth, water circulating at a greater depth substantially attains higher temperature and this temperature raises both solubility and rate of dissolution of most rock minerals. As a result, the solute content of thermal water is commonly higher than non-thermal water (HEM, 1985). Thermal groundwater in and around Main Ethiopian Rift contains high $_PCO_2$, Na^+, HCO_3^-, SO_4^{2-}, and Cl^-. The recent increase in NO_3^- and Cl^- in groundwater might be due to the lack of wellhead protection (Tenalem Ayenew, 2006; Tilahun Azagegn, 2014, 2014; Seifu Kebede, 2013). The groundwater in younger volcanics in the rift and its neighboring areas is characterized by high HCO_3^- and Na^+ with TDS ranging from 500mg/l to 2000mg/l (Seifu Kebede, 2013).

There are substantial temporal and spatial variations in groundwater chemistry as it flows from recharge to discharge areas, representing various hydrochemical processes in aquifer systems (Rumuri & Manivannan, 2020). All groundwater arises from rainfall and snowmelts that are chemically altered in the atmosphere as well as in the soil horizons which can alter the chemistry of groundwater (Freeze and Cherry, 1979). The evaporation, weathering, precipitation, mixing, ion exchange, redox, and dissolution are some of the main hydrochemical processes that govern its chemistry (Krishna Kumar et al., 2017). The composition of groundwater in and near the Ethiopian rift environment is relatively variable with dilute waters having a high Ca^{2+}, Mg^{2+}, and HCO_3, and become Na^+, and HCO_3 dominated with increasing Cl^- in concentrated waters (Tesfaye Chernet et al., 2001; Tenalem Ayenew, 2006; Seifu Kebede et al., 2008).

Differences in rock-water interactions related to lithology and groundwater residence time, geomorphological context, and climate cause spatial variation in ionic concentration in both groundwater and surface water systems in Ethiopia's volcanic landscape (Tenalem Ayenew, 2006). The hydrochemistry of groundwater in the Main Ethiopian Rift is a function of hydrolysis of silicate-containing minerals and cation exchange. The groundwater evolves from Ca-Mg-HCO_3 type water in the plateau areas to Na-HCO_3 type towards the rift floor (Muhammed Haji et al., 2021).

The plateau areas in the Upper Awash Sub-Basin with shallow groundwater systems that have low TDS, high Ca/Na ratio and $CaHCO_3$ water type signifies that the aquifer is newly recharged and is at the early stage of groundwater evolution (Tilahun Azagegn, 2008). The shallow systems of groundwater in the highland areas of the Upper Awash Sub-Basin are characterized by Ca-Mg-HCO_3 water types with lower total dissolved solids. Such water types might be found in some parts of the transitional and rift areas. The evidence from the depth of groundwater and water facies implies their contact with recently recharged water or their early stage of chemical evolution (Andargie Yitbarek et al., 2012; Tilahun Azagegn, 2014). According to Tenalem Ayenew (2006), streams and rivers flowing across the Ethiopian highland volcanic provinces have similar major ion chemistry with shallow groundwater systems in the same region. The chemistry of river water is resulting in either groundwater or precipitation (Tilahun Azagegn, 2008). The occurrence of $NaHCO_3$ and low TDS in the deeper aquifers of plateau areas may be due to the absence of deep circulating old water mixing with such groundwater systems. The deep aquifer has a higher Cl^- concentration than the shallow aquifer and this very high value is linked to water entrapment at compacted clay along faults and recent eruption centers (Tilahun Azagegn, 2008).

The deeper aquifer systems having higher pH than the shallow groundwater suggests the process of hydrolysis as groundwater flows from a shallow aquifer to deep aquifer systems. The thermal groundwater in the Weliso-Addis Ababa and Addis Ababa-Ambo regional fault systems with different lithologic units have variable chemical compositions (Tilahun Azagegn, 2014). The presence of permeable geological formation along the Weliso-Addis Ababa and Dukem-Abusera fault systems results in a low TDS thermal groundwater. This permeable geologic formation may act as a conduit for high TDS deep groundwater and fresh meteoric water mixing. The deep thermal groundwater in the Filwuha areas has high TDS. These thermal

groundwaters are overlain by impermeable massive ignimbrite, tuff, and trachyte units that impede freshwater and deep-water mixing (Tilahun Azagegn, 2008).

When compared to plateau zone aquifers, shallow cold water aquifers in the transition zone have chemical behavior that is substantially similar but slightly evolved (Tilahun Azagegn, 2008; Tenalem Ayenew, 2006). The variation in a geologic formation, stratigraphy, structural setup and its relation with the shallow aquifer system result in variable chemical behavior of deep aquifer systems in the transition zones. Deep aquifer systems in the transition zones found along the Inchini-Becho-Koka flow path characterized by high TDS, high F^-, and $NaHCO_3$ water type are generally different from shallow aquifer systems of both plateau and transition zones (Tilahun Azagegn, 2008). The chloride concentration in these aquifer systems is higher than the plateau aquifers due to the stagnation of water at compacted clay along fault zones. Along the other flow paths, local recharge to the deep groundwater along with rigorous local faulting and highly permeable geological formation makes them have similar hydrochemistry to the shallow aquifers. The water type in these aquifer systems varies from $CaHCO_3$ to $NaHCO_3$ with variable TDS.

Carbon dioxide outgassing along the east-west oriented Ambo-Filwuha and Weliso-Addis Ababa fault systems resulted in high TDS with $NaHCO_3$ rich groundwater (Tilahun Azagegn, 2008). The groundwater that circulates through NNE-SSW faults systems are characterized by high pH and $NaHCO_3$ water type reflecting discharge zone waters and highly evolved groundwater.

The transitional rift environments are characterized by Ca-Na-HCO_3 type waters. According to Andargie Yitbarek et al., (2012), such water types are evolved as groundwater flows from highland recharge areas with Ca-HCO_3 and Mg-HCO_3 type waters to the rift environment having Na-Ca-HCO_3 type due to the ion exchange of Ca^{2+} for Na^+ as manifested in the negative correlation between the two ions that supplies Na^+ to deep groundwater in plateau areas. On the other hand, Ca-Na-HCO_3 type water in the transitional environment is not from such processes since they do not show a negative correlation that implies the source of Na is from the dissolution of sodium-rich plagioclase that supplies Na^+ to the groundwater.

The presence of stagnant surface water bodies, variation in geological formations, and structural setting of the area results in a variation of hydrochemical behaviour in the rift zone (Tilahun Azagegn, 2008). The shallow aquifer systems in the rift zone have high TDS and F^- with highly evolved $NaHCO_3$ water type, and low Ca/Na ratio with some exceptions of

groundwater that are getting recharged from meteoric water through spatter scoria cones and from the Mojo river. Generally, the hydrochemistry of plateau and transition aquifer systems is controlled by silicate hydrolysis and cation exchange processes whereas the rift zone groundwater is influenced by calcite precipitation (Tilahun Azagegn, 2008).

The Ca-Mg-HCO_3 water types are distributed in rift floor, transition, and plateau areas. These water types are characterized by moderately dilute chemistry (130mg/l<TDS<430mg/l). Since these water types are characteristics of the groundwater wells in scoria cones found in the transition zones, this may imply the influence of basic volcanic rocks on groundwater chemistry (Andargie Yitbarek et al., 2012).

According to Tenalem Ayenew (2006), few groundwaters in the major urban centers of the Ethiopian rift including Addis Ababa have high NO_3^- that might be related to anthropogenic influences. According to Mekdes Nigatie (2012), the high NO_3^- in groundwater in highly populated areas of the Upper Awash Sub-Basin might be due to contamination from municipal wastes whereas the high Cl^- in groundwater is probably from pit Latrines, waste disposals, and from the city water supply.

Long-term monitoring of groundwater hydrochemical characteristics in an area will reveal the source contribution and future changes in groundwater hydrochemical features (Gayathri et al., 2021). The spatial and temporal variability in the hydrochemistry of groundwater is related to rock weathering, the use of excessive fertilizers, and wastewater (Pashaeifar et al., 2021).

The Chemical composition and distribution patterns in rivers can tell more about the sources of chemicals in river water, its relationship with the natural environment, and the impact of human activities on the river (Pazi, 2008; Tripathee et al., 2014). According to Amare Shiberu et al., (2017), the increase in EC, TDS, Na, alkalinity, $SO4^{2-}$, NH_3, K, and Cl, K, and Mg, through time in Awash River may deteriorate the quality of the river and it may not be suitable for the intended use.

Chapter Three

Description of the Upper Awash Sub-Basin

3.1. Location and Accessibility

Upper Awash Sub-Basin is located in Central Ethiopia, within the Oromia National Regional State incorporating the capital city Addis Ababa at the western margin of Main Ethiopian Rift (MER) that extends from Entoto ridge in the north to Lake Koka in the south and from Debrezeit in the east to Guraghe highlands in the west. It comprises the upper portion of the Awash river basin with the following grid coordinates: "8° 10' - 9°19'N & 37°55' – 39°18'E". It is bounded by the Blue Nile basin from north and west; the Omo basin from Southwest, by the rift valley lakes basin in the south, and by the Middle Awash basin in the east. The estimated surface area of the Upper Awash Sub-Basin is about 10,550km^2 which comprises the headwater area of the Awash River basin which flows from the central part of the country towards the northeast and disappears in Afar. The Upper Awash Sub-Basin is accessible along the roads starting from the capital of the country, Addis Ababa in all directions; along Addis Ababa-Nazret road; Addis Ababa-Ambo road; Addis Ababa-Welkite and Addis Ababa- Meki roads.

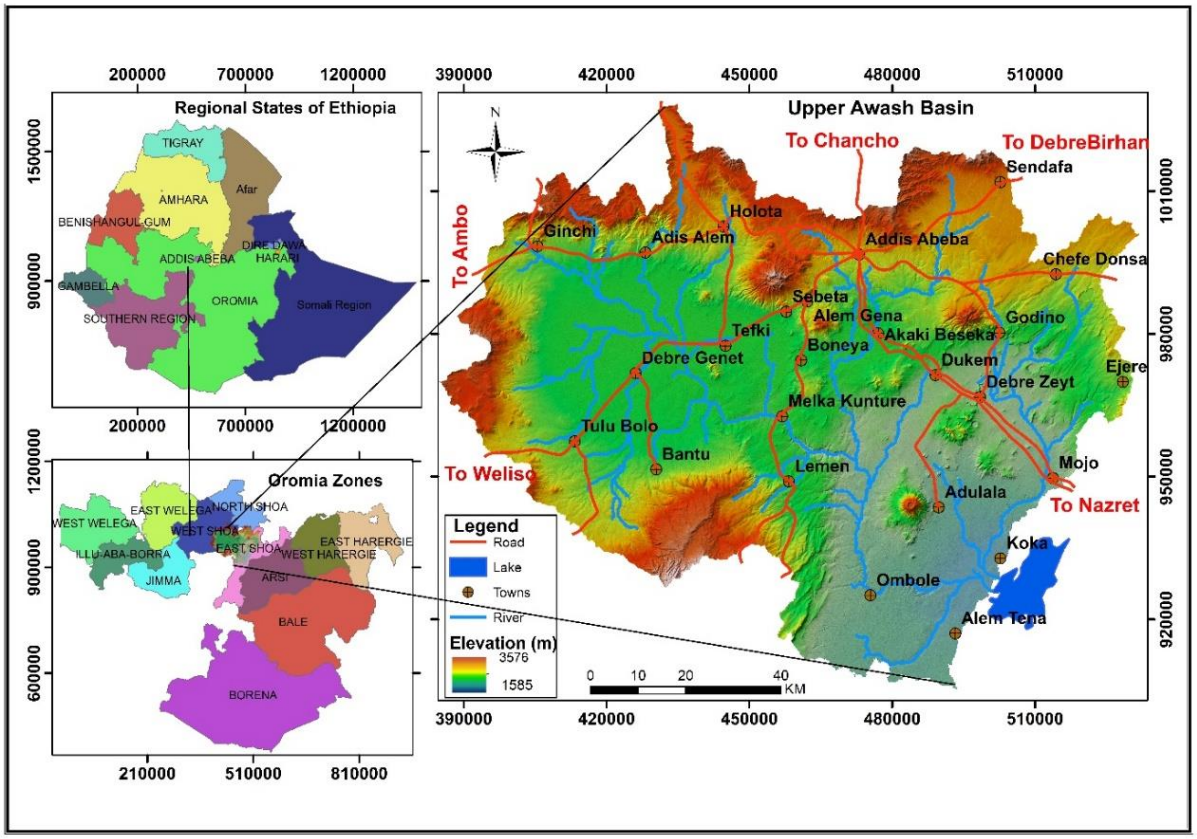

Figure 3. 1: Location Map of the Study Area

3.2. Physiography and Elevation of Upper Awash Sub-Basin

Since the area is found within the rift margin characterized by silicic volcanism and associated rifting, Upper Awash Sub-Basin comprises variable topography. The Upper Awash Sub-Basin is characterized by escarpments and plateaus containing Entoto Ridge, Mount Furi, Mount Yerer, Mount Wechecha, Mount Ziquala, and Guraghe, and Weliso highlands controlled by volcano-tectonic activities and erosional processes. On the other hand, the southern part of the area is characterized by a flat surface that is occupied by Lake Koka, and the western part of the area around Debregenet is characterized by a relatively flat surface. The northern, eastern, and western parts of the area are mainly steep slopes; undulating topography in the central part, and more or less gentle slope in the south and some western parts of the area.

The Elevation ranges from 1575m at the outlet near Koka reservoir to 3565m at Gurage highlands and it generally consists of the central (Becho) and eastern (Koka) plain surrounded by plateau and escarpments making the western shoulder of the main Ethiopian rift system.

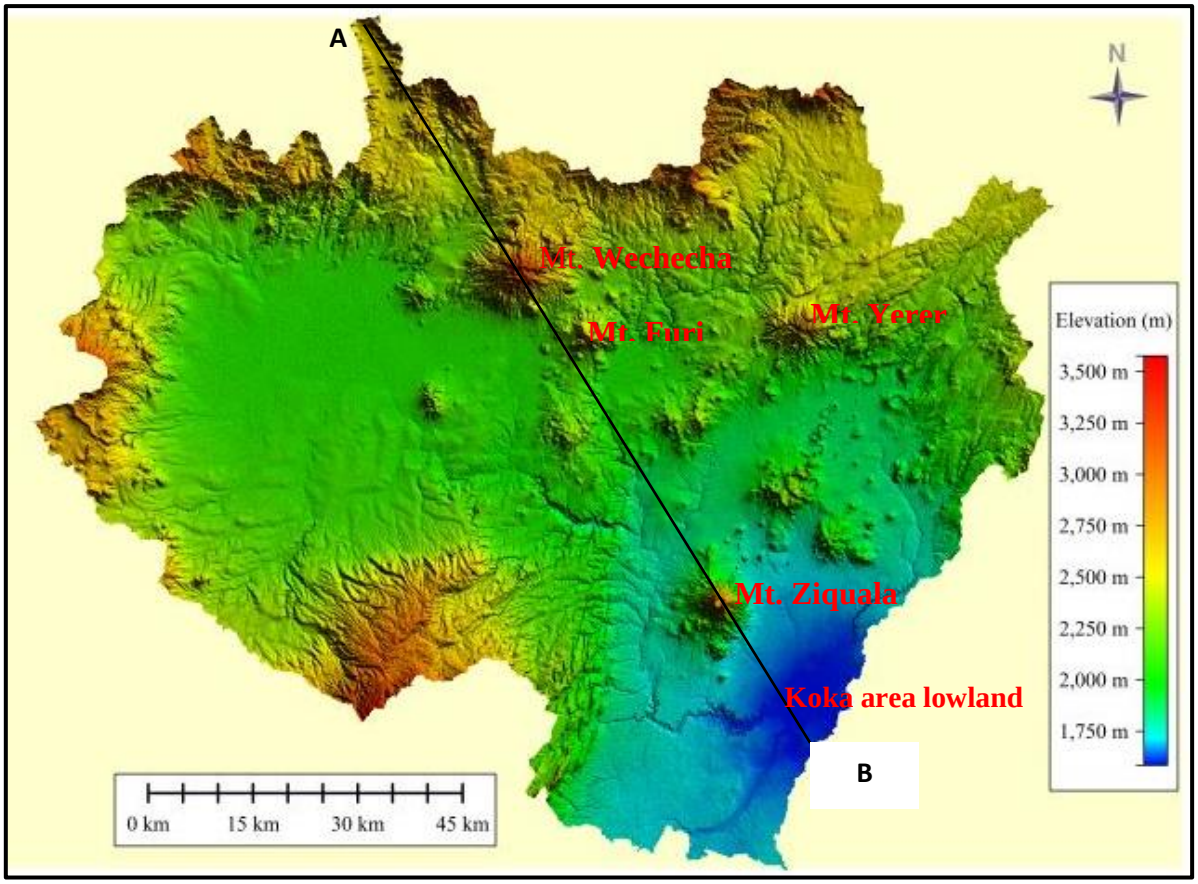

Figure 3. 2: Physiographic Map of Upper Awash Sub-Basin

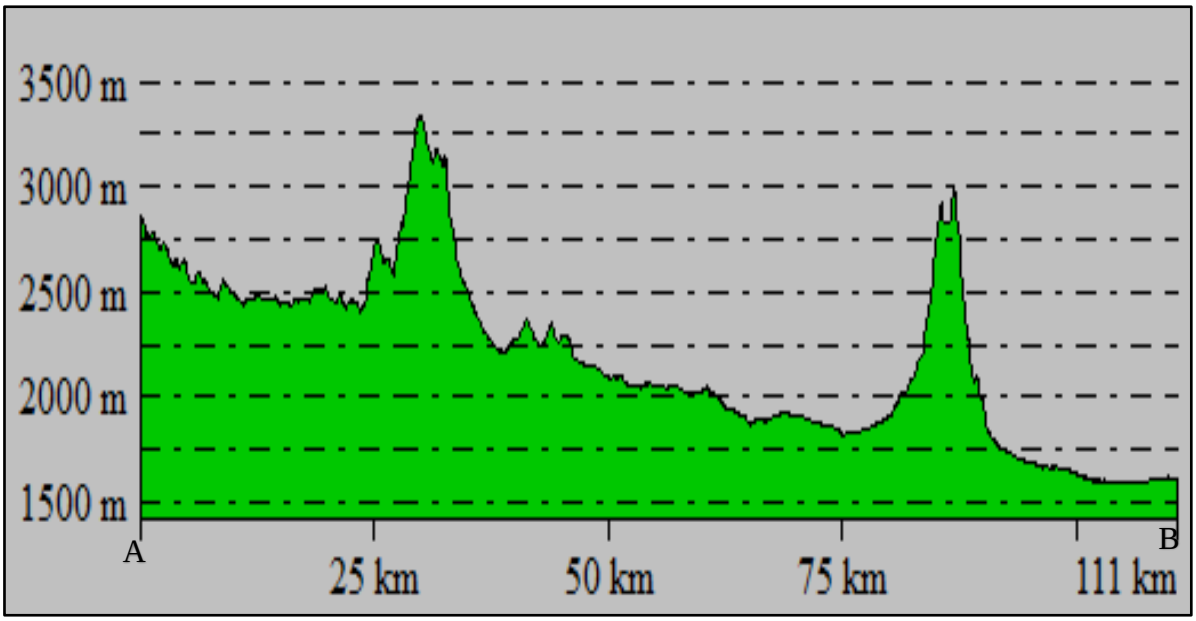

Figure 3. 3: Profile from A to B (from Entoto ridge to Koka)

3.3. Drainage Characteristics of Upper Awash Sub-Basin

Many seasonal and perennial tributaries feed the Upper Awash Sub-Basin that originates in different areas of the upper parts of the Basin. The surface water divide of Awash Basin and the Blue Nile basin is the mountainous part of the Upper parts of the study area which extends from Entoto ridge to Ginchi is the beginning of many tributaries and the Awash River itself. The northeastern tributary of the Upper Awash Sub-Basin is the Akaki River that originates at the base of Entoto ridge and flows down to Lake Aba Samuel. On the northwestern part, Ginchi, Holeta, and Berga rivers are the other tributaries to the Awash River. Mojo river in the east; Teji river, Bantu, and Lemen rivers are also tributaries of Upper Awash Sub-Basin on the western part that originate at the foot of Guraghe highlands. Generally, Upper Awash and its tributaries form a dendritic pattern as shown on the map below. Crater lakes are also common in the area including Ziquala Lake found on top of Mount Ziquala; around Bishoftu town there are many crater lakes including Lake Bishoftu, Hora Hoda, Kilole, Hora, and Kuriftu Lakes. Artificial Lakes such as Legedadi, Dire, and Gefersa Lakes are used as water supply units for the city of Addis Ababa. Lake Abasamuel found at the outlet of Akaki catchment is also used for hydro-power generation and irrigation purposes.

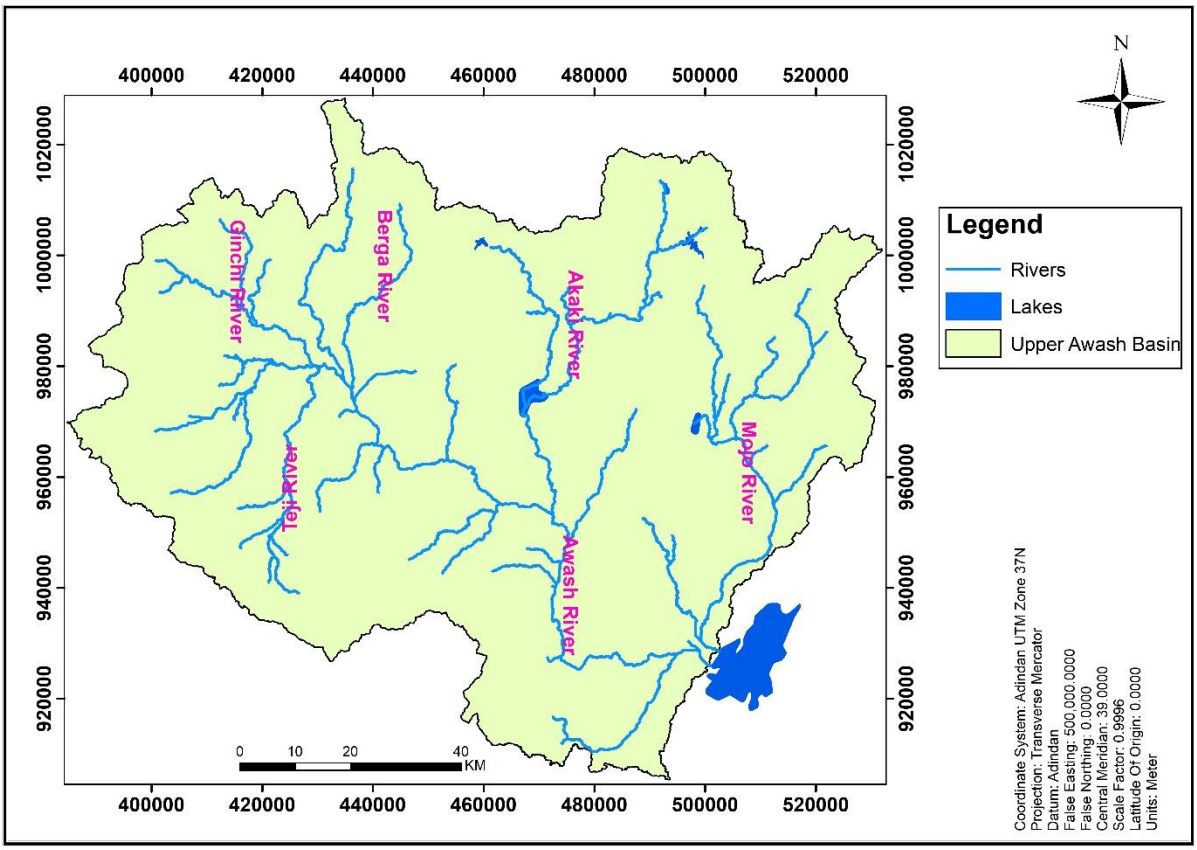

Figure 3. 4: Drainage Map of Upper Awash Sub-Basin

3.4. Climate

The topographic variation in Upper Awash Sub-Basin resulted in a variable climate system in the area. In addition to its complex topography, the other climate determining factor is the Inter-Tropical Convergence Zone (ITCZ). It is an east-west oriented equatorial low-pressure region where surface northeast and southeast winds converge. When these low-pressure winds meet, moist air is forced upward to produce cumulus clouds which in turn produces heavy precipitation. The position of this zone changes following the position of the sun relative to the Earth and associated atmospheric circulation (NMSA, 2001). Seasonal rainfall in Ethiopia mainly occurs due to the migration of the Inter-Tropical Convergence Zone (ITCZ) over the year. The migration of ITCZ is mainly related to the variation of the Indian Ocean Sea surface temperature.

In Ethiopia, there is one main wet season called Kiremt that extends from mid of June to September in which most parts of northern Ethiopia receive precipitation (up to 350mm/month). During this season, Inter-Tropical Convergence Zone (ITCZ) is found in its northernmost position.

There is also a lesser amount of precipitation in the northern and central parts of Ethiopia from February to May (called "Belg"). The southern parts of Ethiopia experience two wet seasons which occur as the Inter-Tropical Convergence Zone shifts to its southernmost position. The Belg season (March to May) is the main rainfall season for those areas which yields about 100-200mm per month and little rainfall occurs in October to December (called the "Bega" season), yielding around 100mm per month.

Traditionally by relating altitude and temperature, there are five climatic zones in Ethiopia namely: Wurch (cold climate at more than 3000m a.m.s.l), Dega (temperate like climate high lands with 2500-3000m a.m.s.l), Weina Dega (warm, 1500-2500m a.m.s.l), Kola (hot and arid type areas less than 1500m a.m.s.l) and Bereha (hot and hyper-arid type) climates (NMSA, 2001). Based on this classification, the three climatic zones (Wurch, Dega, and Weina Dega) exist in Upper Awash Sub-Basin. Entoto, Guraghe mountains, and the western edge of Ginchi are classified as Wurch; the upper central parts of Upper Awash Sub-Basin around Addis Ababa, Sendafa, Holeta areas, and the southern parts of Tulubolo area, and western parts of Ginchi are traditionally classified as Dega climatic zones whereas most southern and eastern parts of the area are classified as Weina Dega climatic zone as shown on the map below.

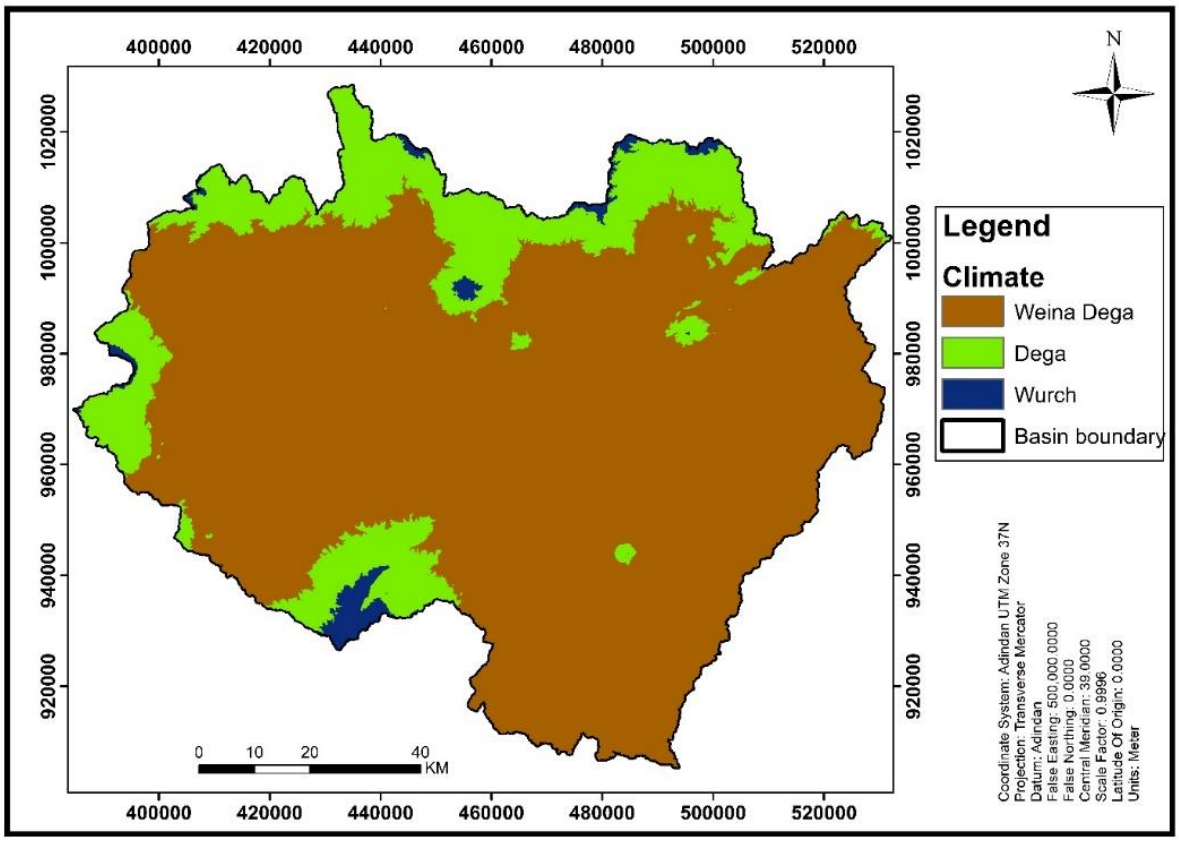

Figure 3. 5: Traditional Climate Classification Map of Upper Awash Sub-Basin

3.5. Soil

Various soil types are available in the Upper Awash Sub-Basin including Pellic Vertisol, which is the dominant soil type in the central part of the area. These types of Soils are characterized by a high content of clay minerals which are sensitive to change in water content. These clay minerals swell by absorbing water and increase their volume when they get wet and they shrink when the soil dries which produces deep cracks. This type of soil has higher natural fertility, higher water holding capacity, and can respond well to several crop requirements. The other soil type found in the area is fluvisol which is river sediment found around Bantu and Lemen towns. The texture of this soil type is sandy clay loam that is formed when Bantu and Lemen rivers flow from the foothills of Guraghe highlands down to the flat land. Cambisol and Orthic Solonchakes have sandy loam to sandy clay loam texture are found in Lemen, Sebeta, Godino, and Entoto ridge. Leptosols with high gravel content are also distributed in different areas. Leptosols are mostly loamy sand to sand in texture (MoWR, 2008).

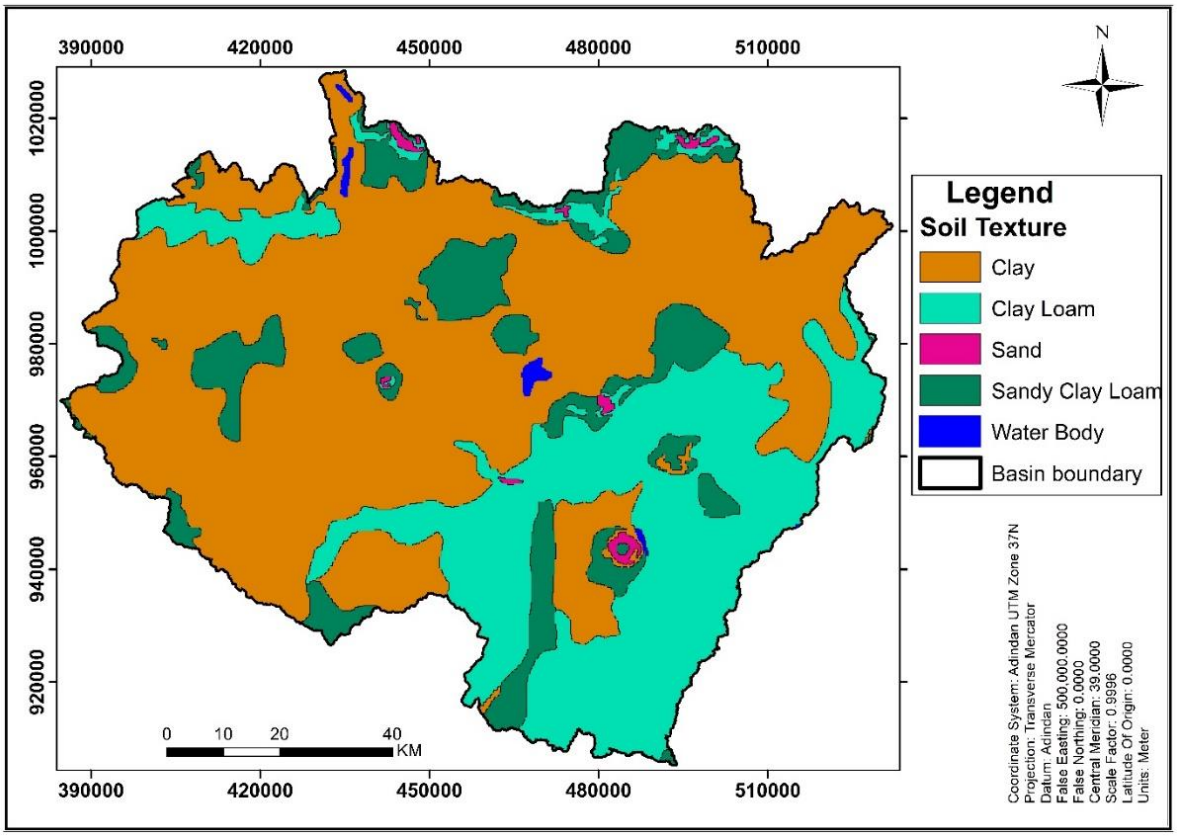

Figure 3. 6: Textural Classification of the Soil in the Area

3.6. Land Use and Land Cover

Since the country's economy largely relies on agriculture, most of the Upper Awash Sub-Basin is cultivated land. In some parts of the area farmers apply irrigation for example around the Akaki River near AbaSamuel, the river water is diverted into the farmland for the production of onion, cabbage, and other cereals. The northern edge of the study area is urbanized since the country's capital, Addis Ababa is within the Upper Awash. Manmade and crater lakes also occupy a small part of the area especially in Debrezeit, Lake Ziquala, Lake Aba Samuel, Legedadi, and Gefersa. Grasslands, shrubs, and trees cover some parts of Upper Awash. Aquatic vegetation occurs near open water bodies. About 89.7% of Upper Awash is cultivated land; 4.7% of the total area is grassland; 2.6% has urbanized as shown in the table below (Sentinel, 2016).

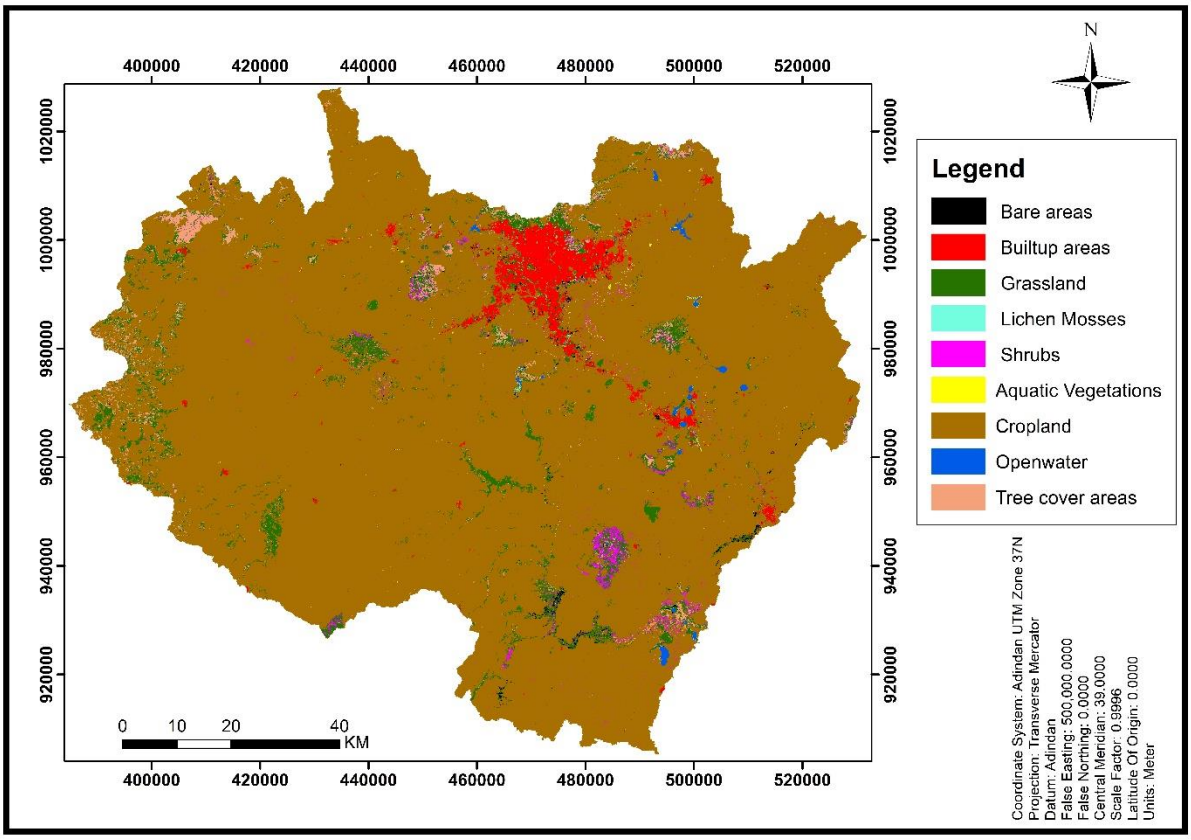

Figure 3. 7: Land Use and Land Cover Map of Upper Awash Sub-Basin

Table 3. 1: Land Use and Land Cover Percentage

Land Use type	Area (km^2)	Area Coverage (%)
Grassland	497	4.71
Tree cover	177	1.68
Cropland	9465	89.72
Shrubs	96	0.91
Bare land	5	0.05
Built up areas	272	2.58
Aquatic Vegetation	12	0.11
Open Water	25	0.24

3.7. Geology

3.7.1. Regional Geology and Tectonics

The East African Rift System (EARS) is a divergent plate boundary between Nubia and Somalia plates that extends from Djibouti to Mozambique (Bonini et al., 2005). The Ethiopian Rift (ER) is part of the East African Rift System (EARS), comprises a series of rift zones extending over a distance of about 1000km from the Afar Triple Junction at the Red Sea-Gulf of Aden intersection to the Kenya Rift which is characterized by huge volcanic products since its appearance (Boccaletti et al., 1999).

According to Giday Woldegabriel et al., (1990), Volcanism in the Ethiopian Rift began in the Eocene-Late Oligocene, and the rift tectonic history corresponds to modern times. The Ethiopian Rift is divided into two main sectors, namely the Main Ethiopian Rift and Southwestern Ethiopian Rift (Boccaletti et al., 1999). The Southwestern Ethiopian Rift is marked by large volumes of the oldest volcanic rocks. The north-south trending faults are its main characteristics.

The Main Ethiopian Rift, which is about 90Km wide, is the sector where recent volcanic products are prevalent. It divides the north-western and southeastern plateaus of Ethiopia. It is developed during the late Miocene. The Main Ethiopian Rift is a roughly NE trending sector of the East African Rift system that includes a series of rift segments extending from the Afar Triple Junction at the Red Sea-Gulf of Aden intersection to the Kenyan Rift (Bonini et al., 2005; Tsegaye Abebe et al., 2010). The main Ethiopian Rift is characterized by well-developed quaternary faulting mainly of the Wonji Fault Belt (WFB) and Quaternary rocks are commonly

affected by faulting along this belt, which defines an important active volcano-tectonic axis located within the broader rift valley bounded by border faults trending north-northeast to the northeast (Boccaletti et al., 1999). The MER is characterized by active extensional tectonics accommodating ~6-7mm/yr relative movement between the African and Somalian plates (Chu and Gordon, 1999; Fernandes et al., 2004 as cited in Bonini et al., 2005).

Traditionally, the Main Ethiopian Rift is subdivided into Southern Main Ethiopian Rift, Central Main Ethiopian Rift, and Northern Main Ethiopian Rift (Mohr, 1983). The Northern Main Ethiopian Rift (MER) covers the true Afar depression up to the Lake Koka region following the middle course of the Awash River valley. The main boundary faults in this region show an average N50° trend and formed since about 10–11Ma (Kazmin et al., 1980; Mohr, 1983; Hayward and Ebinger, 1996; Chernet et al., 1998; Wolfenden et al., 2004 as cited in Bonini et al., 2005).

The Central Main Ethiopian Rift covers most of the Lakes Region, up to the Lake Awassa area and the main boundary faults trend roughly N30°–35°; the age of faulting onset is estimated to be around 8.3–9.7 Ma, while the age of the earliest syn-rift volcanic deposits is ~8Ma (Giday Woldegabriel et al., 1990).

The Southern Main Ethiopian Rift extends south of Lake Awassa into the ~300km wide system of basins and ranges (referred to as broadly rifted zone that characterizes the overlapping area between the Ethiopian and Kenya Rifts (Davidson and Rex, 1980; Ebinger et al., 2000 as cited in Bonini et al., 2005). Faults in the Southern MER show a dominant N-S to N20° trend and were well established after ~18 Ma (Levitte et al., 1974; Zanettin et al., 1978; WoldeGabriel et al., 1991; Ebinger et al., 1993 as cited in Bonini et al., 2005).

These three segments represent different stages of the extension process, from early rifting in the Southern MER to more evolved stages in the Central and Northern MER preceding the incipient seafloor spreading in Afar (Hayward & Ebinger, 1996).

3.7.2. Geology of Upper Awash Sub-Basin

Upper Awash comprises variable lithologic units of igneous rocks and alluvial deposits. These lithologic units are classified as Tertiary acidic and basic volcanic rocks and quaternary ages of acidic and basic volcanic rocks, lacustrine and alluvial deposits. Rock units found in the Upper Awash Sub-Basin are categorized as tertiary volcanic rocks, quaternary volcanic, lacustrine, and alluvial deposits.

Addis Ababa Basalt

This unit is exposed in the Addis Ababa area which is a fine-grained rock mainly composed of plagioclase, pyroxene, and opaque minerals (Assiged Getahun, 2007). According to WWDSE (2008), it is fine to coarse-grained composed of olivine and plagioclase phenocrysts with thin lava flows overlying the Addis Ababa ignimbrites. On fresh outcrops, Addis Ababa basalt is predominantly olivine basalt with a distinctive grey appearance, although it weathers to a reddish-brown color. It usually appears as a rock, with secondary minerals filling the vesicles (Assiged Getahun, 2007).

Addis Ababa Ignimbrite

It is composed of ignimbrite and non-welded pyroclastics, such as Ash and Tuff. It is grayish and white which demonstrates fiamme texture, elongated rock fragments of various colors when welded (WWDSE, 2008). According to WWDSE (2008), this rock unit is outcropped around Addis Ababa, Chefedonsa, and Becho areas

Akaki Basalt

It comprises scoria fallouts and phyric basalt lava flows (Efrem Beshawered, 2010). This unit is a coarse-grained porphyritic olivine basalt that is strongly vesicular, with carbonate minerals filling the vesicles in some areas (WWDSE, 2008). It is mainly composed of scoria and spatter cones, as well as lava flows.

Tarmaber Basalt

The basalt covers the upper sandstone in a non-conformable manner and the bottom ignimbrite in a conformable manner. It has layers that are stratified and have different compositions and structures (Assiged Getahun, 2007). Tarmaber basalt is primarily transitional to Na-alkaline basalts in composition, with small benmoreites and trachyte (Peccerillo et al., 2007). Mostly, Tarmaber basalt consists of scoriaceous lava flow with pockets of columnar olivine bearing basalt within the scoriaceous components. It's worn, cracked, and pinkish to grayish (WWDSE, 2008). It is characterized by lenticular, zeolitized alkali basalts including a significant quantity of tuff, scoriaceous lava flows per-alkaline rhyolites, and characteristic red paleosols (Abbate et al., 2015).

Nazret Unit

It is composed of a sequence of welded peralkaline rhyolitic ignimbrite crystals. Numerous rhyolitic and trachytic domes make up the unit. The ignimbrites are mostly eutaxitic, with oblate glassy particles. There are many shattered rock fragments and crystals; the most prevalent crystals are alkali feldspars, quartz, aegirine, and amphiboles (WWDSE, 2008). A sequence of ignimbrite sheets is alternated with paleosol layers and aphyric flood basalts in this unit. The ignimbrite units are unwelded at the top, whereas the bottoms are highly welded. They are made up of glassy fiamme and basaltic lithic pieces in abundance (Boccaletti et al., 1999).

Wechecha-Furi-Yerer Trachytes

These rock units are also known as central volcanic units composed of trachyte and pyroclastic materials. The trachyte is coarse-grained, light gray, brown-grey to dark grey in fresh samples, and pinkish yellow to reddish-brown in weathered samples (WWDSE, 2008; Efrem Beshawered, 2010). Quartz, feldspar, and mica are the principal rock-forming minerals on a macro scale (Efrem Beshawered, 2010). Other units found in these areas include pyroclastic materials found near and around Wenchi and Dendi lakes, as well as the products of Mount Dendi, an isolated elliptical cone with a NE-SW direction (Efrem Beshawered, 2010).

The Entoto Ridge and Becho Area Rhyolites

The Entoto silicic formation, which lies beneath the Entoto Mountain range, includes the rhyolite mountain (Tesfaye Asresahagne and Asmelash Abay, 2016). It is grayish pink in fresh specimens and reddish-brown to yellowish-grey in weathered specimens. Rhyolites create isolated cones on the Becho plain (WWDSE, 2008).

Tulu Rie Basalt

Black aphyric basalt lavas constitute Tulu Rie basalt. The unit unconformably overlies Nazret pyroclastic deposits at the type locality. This unit is outcropped in the eastern portion of the plotted area, forming northeast-trending escarpments at Chefedonsa and Ejere (WWDSE, 2008). Lavas are mostly olivine basaltic, with a few rare plagioclases–rich basaltic andesite thrown in for good measure. The texture of the basalts is porphyritic or sub-aphyric, and the phenocrysts are mostly olivine. Because of its stratigraphic position and composition, the Tulu Rie Basalt is classified as part of the Bofa Basalt, and sub-horizontal or slightly slanted tabular lava flows constitute the Tulu Rie basalt (Kazmin and Seifemichael Berhe, 1978).

Chefe Donsa Pyroclastic Deposits

These rock units are ash, tuff, and pumice with fine-grained, poorly welded rock with vitrophyric fiamme and lithic pieces interspersed with ash and unwelded tuffs, as well as related rhyolitic lava flows (WWDSE, 2008). Fresh samples are pale to dark grey, while weathered samples are reddish to yellow to pink.

Weliso-Ambo Basalt

It comprises lava flow composed of porphyritic basalt, basalt breccia, and small tuff, with big crystals of plagioclase, olivine, and pyroxene. There is scoriaceous basalt in the Weliso area. This unit is mapped as basalt lava flows connected to volcanic centers in the Abay Master Plan report, and it ranges in age from the Pliocene to the present day (WWDSE, 2008).

Ziquala Trachyte

This unit is outcropped at Ziquala Mountain. It is dark grey, mildly porphyritic to coarsely porphyritic, and contains scarce pyroclastic deposits (Efrem Beshawered, 2010). Anorthoclase, sanidine, minor clinopyroxene phenocrysts, and glassy alkali feldspar groundmass make up the Ziquala trachyte, which is grayish pink in color, coarse-grained, and petrographically made of anorthoclase, sanidine, minor clinopyroxene phenocrysts, and glassy alkali feldspar (WWDSE, 2008).

Bede Gebaba Volcanic Units

The core part of the volcanic complex comprises spatter cones and basaltic lava flows from the younger Bishoftu Volcanics. Rhyolitic obsidians are the most recent products (WWDSE, 2008). The composition of pumice and lavas ranges from rhyolites to minor trachytes. In a glassy to microcrystalline groundmass, the lava contains micro phenocrysts and rare phenocrysts of sanidine and quartz, as well as scattered plagioclase and clinopyroxene (Gasparon et al., 1993).

Bishoftu Volcanic Unit

Like the portions further south, the Bishoftu volcanic area is composed of aligned maars and cinder cones. Megacrysts abound in Debrezeit cinder cones, as are uncommon mantle xenoliths (Rooney et al., 2005). There are spatter and cinder cones in the Bishoftu Volcanic area, as well as tabular basaltic lavas, flows, and phreatomagmatic deposits. With olivine phenocrysts, the basalt is vesicular and coarse-grained. Surges and highly fragmented deposits linked with

maars and tuff rings make up the phreatomagmatic deposits (WWDSE, 2008). It is commonly found interspersed with lacustrine sediments and distal silicic volcanic ashes surrounding the maar craters.

Alluvial Deposits

These deposits are found in Becho areas forming flat-lying topography and marshy areas. Regolith, reddish-brown soils, talus, and alluvium comprised the alluvial layer, which mostly outcropped above the Tertiary volcanics on the plateaus and the Becho Plain (WWDSE, 2008). It is composed of loose sand, silt, and clay-bearing clasts that range in color from brown to grey. Basalt, rhyolite, and scoria boulders are among the clasts. Also frequent are thick black, brown, and reddish-brown soils (Efrem Beshawered, 2010).

Lacustrine Deposits

It is exposed in AlemTena, Koka, Hombole, Mojo, Dukem, and Debrezeit to Godino areas. It is composed of loose, brown to grey color sand, and silt (Efrem Beshawered, 2010). These deposits are fine-grained, brown-yellowish deposits that are poorly stratified and typically contain volcanic materials (WWDSE, 2008). Volcanic layers are common in these successions, becoming dominating and coarse-grained around the maars. In the lakes region and on the rift shoulders in general, and in Mojo and its surrounds in particular, lacustrine beds are interbedded with Pliocene-Pleistocene ignimbrite. These units include redeposited volcanic sands, siltstone, sandstone, calcareous minerals, and diatomite predominate, with water-laid tuffs intercalated. These deposits are brown-yellowish in color, fine to medium-grained in texture, thinly stratified, extremely friable, and less compacted, these deposits are often brown-yellowish in color, fine to medium-grained in texture, thinly stratified, very friable, and less compacted.

Geological Structures

The vicinity of the Upper Awash Sub-Basin to the Main Ethiopian Rift makes it have complex geological structures. The main secondary geological structures are lineaments and faults, and the primary structures include bedding and volcanic layering (Assiged Getahun, 2007).

Faults

Four types of fault systems were recognized in the Upper Awash Sub-Basin trending in NE-SW, NW-SE, N-S, and rarely E-W directions (WWDSE, 2008; Efrem Beshawered, 2010). The

NW-SE fault systems are the oldest fault systems that affected all rock types in the Upper Awash Sub-Basin. They are crustal scales that acted as a conduit for substantial volcano activity in the area. Their age ranges from the early Paleozoic to the present, but they were reactivated later with the major tectonic event in the area (WWDSE, 2008). The Bede Gebaba-Wechecha fault systems are examples of such fault types. The E-W fault systems are also known as the Yerer-Tuluwelel volcanic lineaments that extend the Addis Ababa-Ambo-Nekemte road (Tsegaye Abebe et al., 1998). These are the major fault systems highly affecting Tarmaber basalt in the Upper Awash Sub-Basin (WWDSE, 2008). The other fault systems are NE-SW faults that are trending parallel to the major rift axis highly affecting younger volcanic rocks of Tulu Rie basalts (WWDSE, 2008). The N-S fault system is a relatively newer fault system that acts as a conduit for young volcanic rocks, such as Addis Ababa basalt (WWDSE, 2008).

Primary and Secondary Structures

Flow layering in rhyolites, ignimbrites, ash falls, and lacustrine deposits. Secondary structures, tilting of the flow layering, and bedding plane due to faulting are also observed in rhyolites and ignimbrites (WWDSE, 2008).

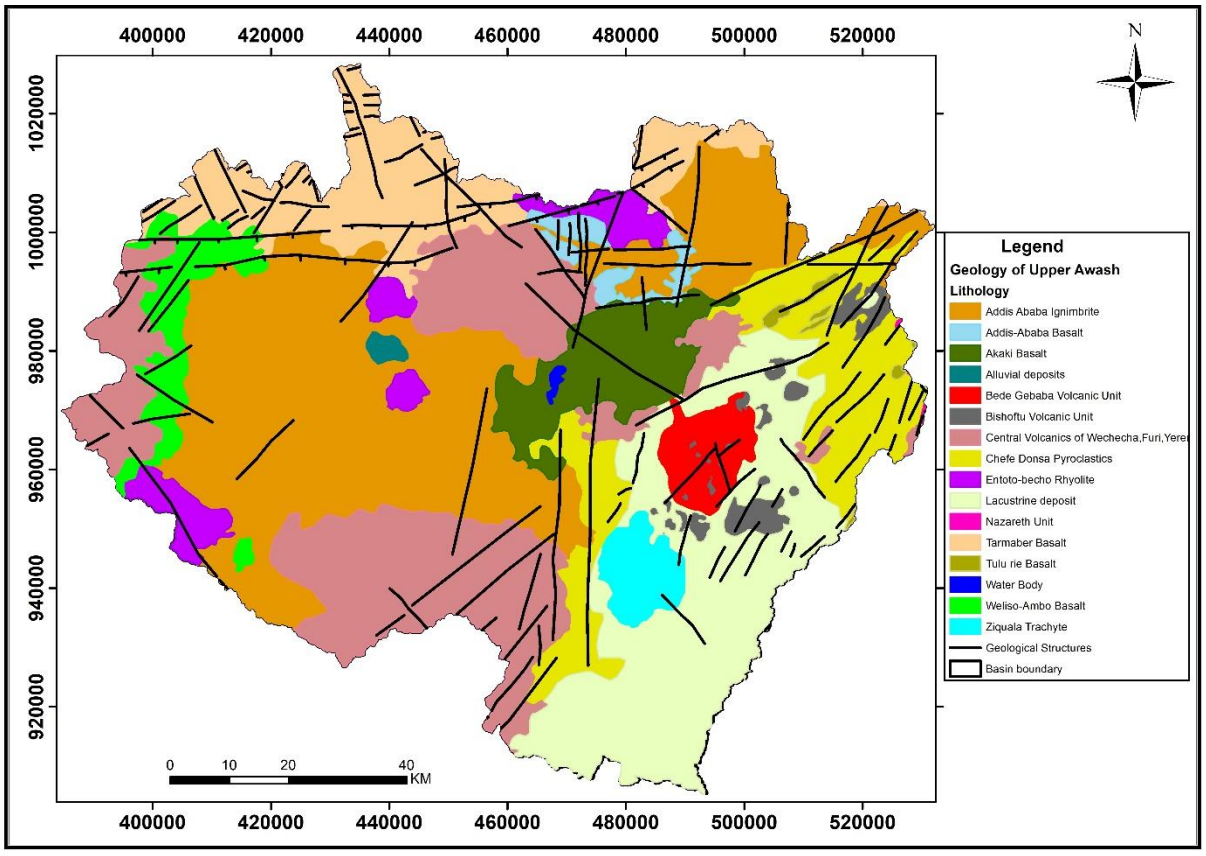

Figure 3. 8: Geological Map of Upper Awash Sub-Basin (Modified from WWDSE, 2008)

Chapter Four

Hydrometeorological Characteristics of Upper Awash Sub-Basin

4.1. Meteorological Parameters

Meteorological parameters collected from the National Meteorological Agency of Ethiopia (NMA) are Precipitation, Temperature, wind speed, Relative humidity, and Sunshine hour. More than 30 meteorological stations are found in the Upper Awash Sub-Basin which is controlled by the National Meteorological Agency of Ethiopia (NMA). Most of these stations are fourth-class stations in which the data available are precipitation and Temperature only. Meteorological data obtained from the National Meteorological Agency are incomplete. All meteorological parameters were obtained from first-class stations like Addis Ababa, Debrezeit, and Holeta. For this study, data from 13 meteorological stations were taken for areal recharge estimation and climatic classification of the area.

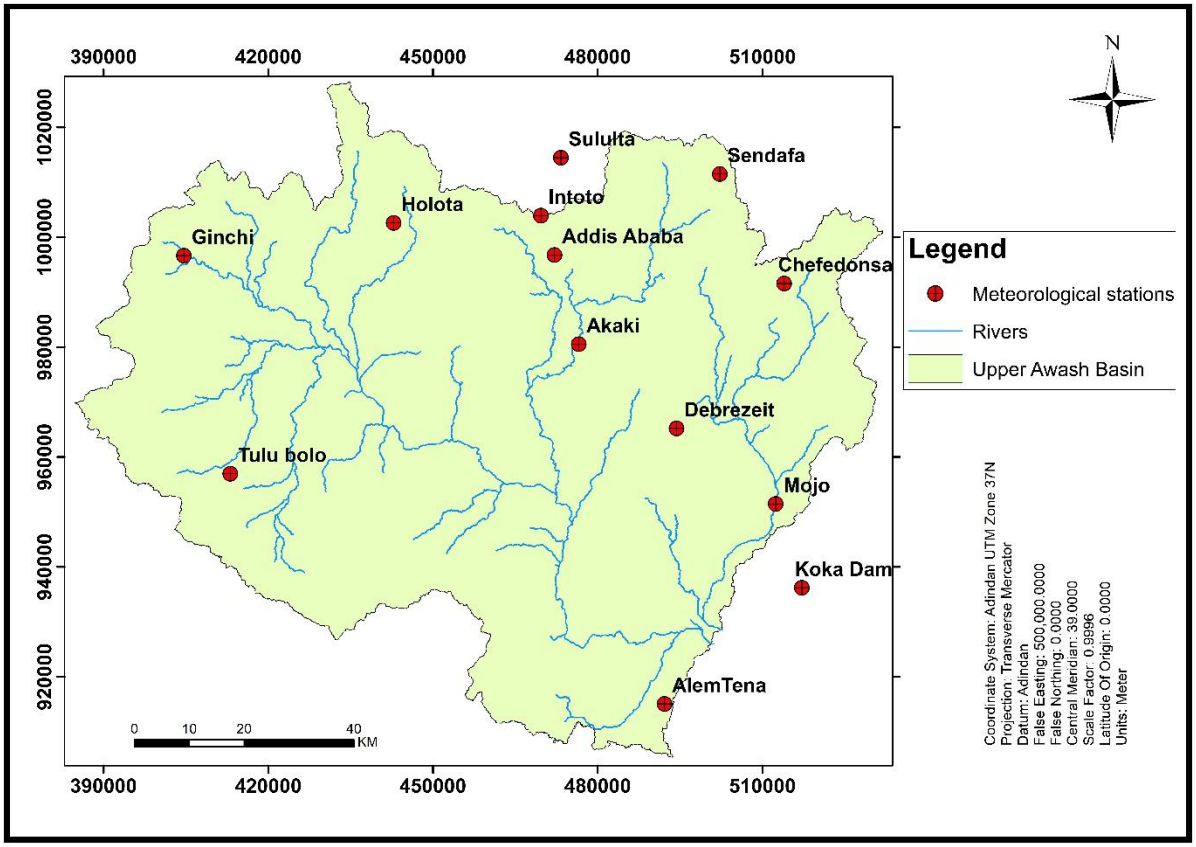

Figure 4. 1: Meteorological Stations within the Upper Awash Sub-Basin

Table 4. 1: Mean annual rainfall and mean annual temperature at each meteorological station

Stations	year	class	UTME	UTMN	Elevation (m)	Mean Annual Rain fall (mm)	Mean Annual Temp (°C)
Addis Ababa	2000-2020	1st	996775	472153	2386	1230	17.4
Akaki	2000-2020	2nd	980500	476595	2057	954	19.8
Sendafa	2000-2020	4th	1011481	502261	2558	1207	16.4
Intoto	2000-2020	4th	1003919	469681	2903	1305	13.5
Holeta	2000-2020	1st	1002609	442829	2400	1165	14.9
Sululta	2000-2020	4th	1014697	473114	2595	1238	14.3
Ginchi	2000-2020	4th	996582	404567	2132	1055	18.5
Chefedonsa	2000-2020	4th	991562	513951	2402	935	17
Debrezeit	2000-2020	1st	965202	494365	1900	868	18.7
Koka Dam	2000-2020	4th	936175	517181	1625	916	22.4
Mojo	2000-2020	3rd	951434	512447	1771	1076	20.4
Tulubolo	2000-2020	2nd	956925	413095	2190	1089	17.8
AlemTena	2000-2020	4th	915051	492187	1725	835	19.3

4.2. Areal Precipitation

The amount of precipitation Upper Awash receives vary with seasonal variation. The Upper Awash Sub-Basin gets precipitation in two different seasons as the Inter-Tropical Convergence Zone (ITCZ) shifts its position following the position of the sun relative to the Earth and associated atmospheric circulation. This zone is the convergence between low-pressure winds from Tropical easterlies of Indian Ocean origin and equatorial westerlies from the Atlantic Ocean. The amount and distribution of precipitation in Ethiopia are largely affected by the location of that area relative to the moisture source. At the end of May, the ICTZ moves towards northern Ethiopia. During this time, high-pressure wind develops in the Atlantic Ocean in which most parts of Ethiopia are influenced by this Atlantic equatorial westerly where wind originated from this ocean starts to ascend over the highlands of southwestern Ethiopia which results in Kiremt season rain in most parts of Ethiopia including the study area. This season lasts for four months from June to September. In April, the ITCZ shifts to its southernmost position in southern Ethiopia. At this time high-pressure wind develops in the Indian Ocean which generates moist easterly wind over Sudan and neighboring southern Ethiopia. This moist air current ascends over the highlands of southern Ethiopia and neighboring countries to produce small “Belg” rains in southern Ethiopia including the study area.

The mean Areal rainfall depth of the Upper Awash Sub-Basin was calculated by using the Thiessen Polygon method. 21year daily precipitation data were taken from National Meteorological Agency and each station's daily precipitation was multiplied by the corresponding polygon area weighting factor. The daily weighted rainfall was summed to get

the monthly precipitation at each station. Annual precipitation for each station was calculated by adding the monthly weighted precipitation. The mean annual precipitation of Upper Awash calculated from 21 meteorological stations was 1025.23mm.

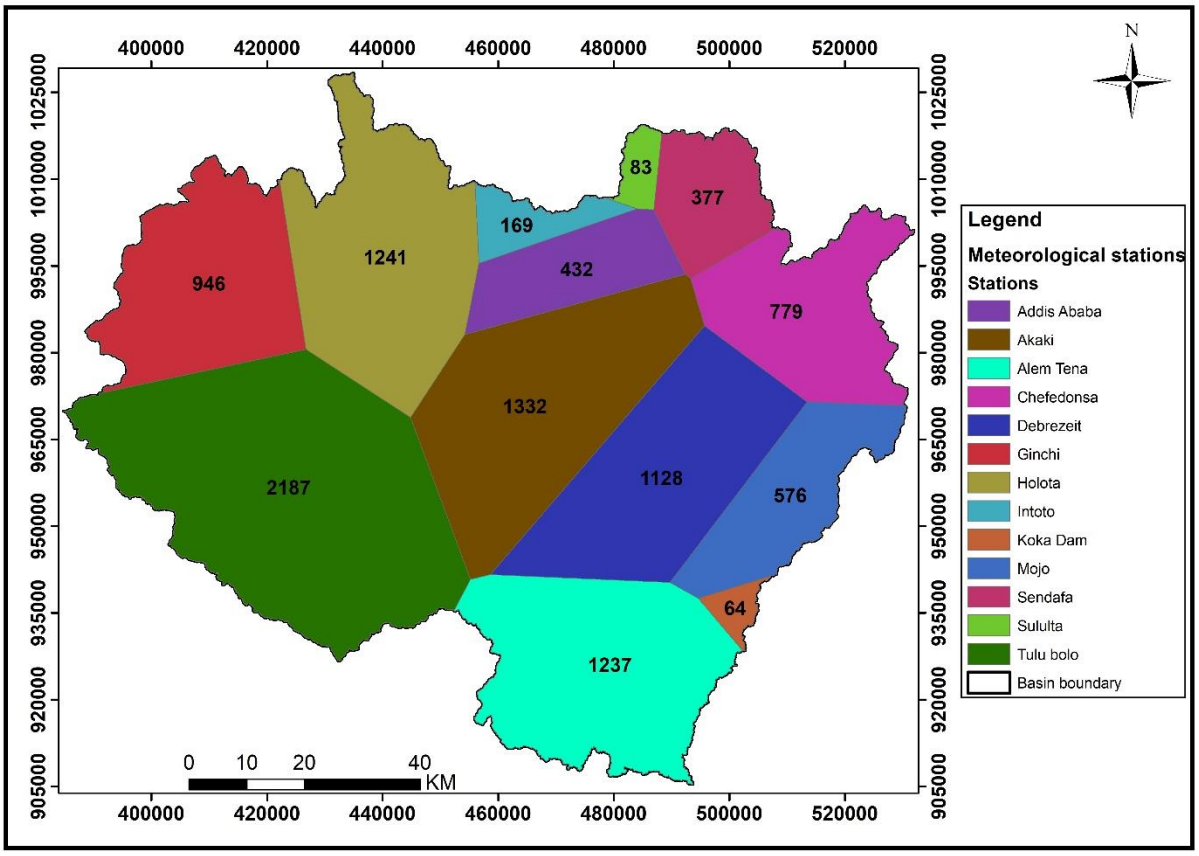

Figure 4. 2: Thiessen Polygon Map of Upper Awash Sub-Basin

As we can see from the graph, the area receives higher mean monthly precipitation during the "Kiremt" season (June, July, August, and September) and the second moist season is the "Belg" season (March, April, and May) where a smaller amount of precipitation occurs relative to the "Kiremt" season. Other months such as October, November, and December are regarded as "Bega" seasons. These months are considered as dry months in which most of the time there will not be precipitation or precipitation occurs rarely and the least amount of precipitation is recorded during these months.

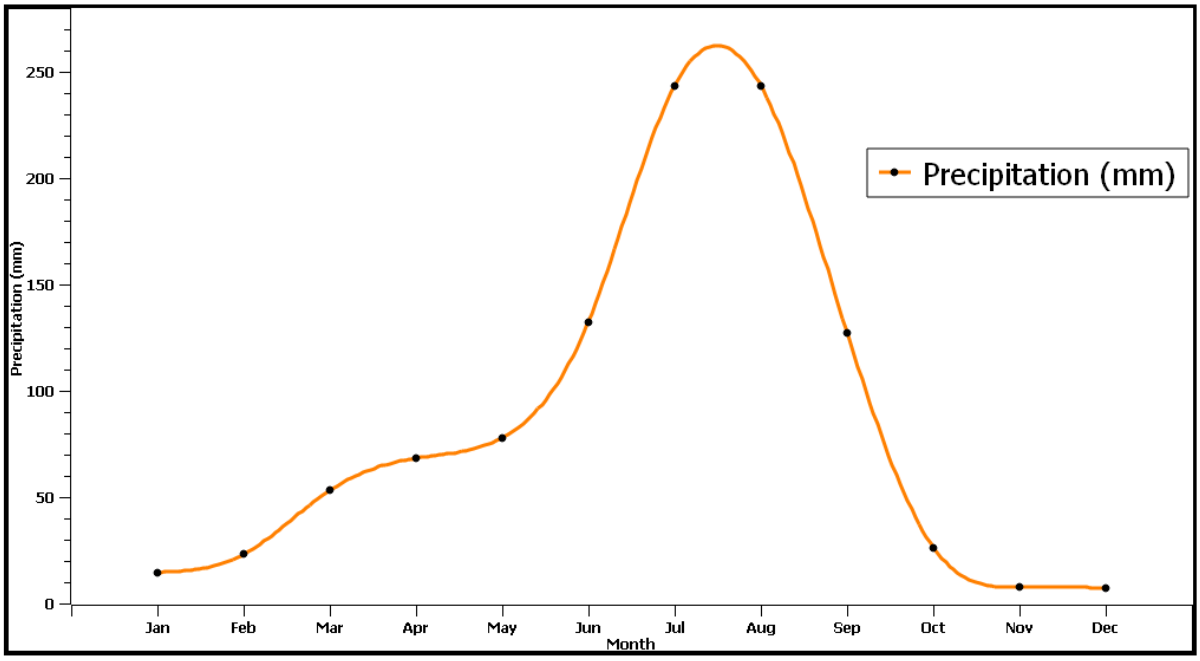

Figure 4. 3: Mean Monthly Precipitation of Upper Awash Sub-Basin

4.3. Temperature

The mean monthly temperature was calculated from 13 meteorological stations of 21 years (2000-2020 GC) daily maximum and daily minimum temperature. The mean annual temperature of Upper Awash varies from 16.49°C to 19.27°C. As we can see from the table, the coldest month is December and May is the warmest month.

Table 4. 2: Mean monthly temperature of Upper Awash Sub-Basin

Month	Jan	Feb	Mar	Apr	May	Jun e	Jul	Aug	Sep	Oct	Nov	Dec
Temp (°C)	17.2	18.2	19.1	19.1	19.3	18	17.1	17	17	16.98	16.6	16.5

4.4. Potential Evapotranspiration (PET)

In the water budget study of any catchment, determination of the amount of Potential evapotranspiration is essential in maintaining the water balance of the catchment. Potential Evapotranspiration is defined as the maximum amount of water that would be Evapotranspired if there is enough water available from precipitation and soil moisture. It is an ideal quantity of water that can be evaporated per unit area, per unit time from an idealized unlimited free water surface under existing atmospheric conditions (Yates & Strzepek, 1994). The potential Evapotranspiration of the area was estimated using the Thorenthwaite method. The

Thorenthwaite method mainly uses air temperature as an index of the energy available for evapotranspiration (THORNTHWAITE, 1948). The monthly potential evapotranspiration is calculated using the mean monthly temperature calculated from 13 stations of 21-years daily maximum and minimum temperature using the following Thorenthwaite formula.

$$E_t = 1.6b\left[\frac{10Ta}{I}\right]^a$$

Where: Et = Potential Evapotranspiration in cm/Month

Ta = Mean Monthly air temperature (°C)

I = Annual heat index

b = Latitude correction

The annual heat index (I) is calculated from the mean monthly temperature using the following formula. The annual heat index is the sum of monthly heat indices.

$$I = \sum_{i=1}^{12}\left(\frac{Tai}{5}\right)^{1.5}$$

Where Ta_i is the mean monthly air temperature (°C) in this case the mean monthly temperature is shown in the table above. Using the formula, the value of the Annual heat index (I) is estimated to be **81.43**. The exponent "**a**" is calculated from the annual heat index using the following formula.

$$a = 0.49 + 0.0179I - 0.0000771I^2 + 0.000000675I^3$$

$$= 0.49 + 0.0179(81.43) - 0.0000771(81.43)^2 + 0.000000675\,(81.43)^3$$

$$\mathbf{a = 1.8}$$

The amount of annual potential evapotranspiration of the Upper Awash Sub-Basin was estimated to be **787.7mm/a.**

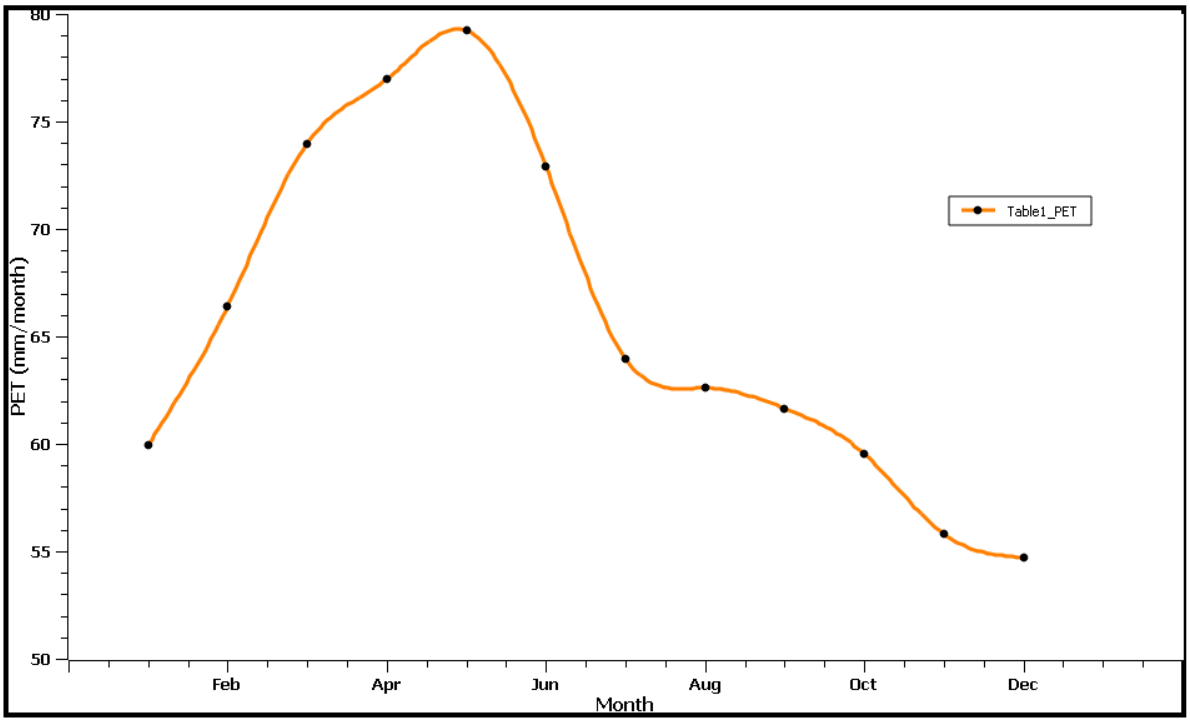

Figure 4. 4: Mean Monthly Potential Evapotranspiration (mm/month)

4.5. Actual Evapotranspiration

In the real world, evapotranspiration occurs under available moisture and atmospheric condition. Actual evapotranspiration is defined as the evaporation from the bare land, soil moisture, and water bodies combined with transpiration from plants under the available moisture, precipitation, and atmospheric condition. Actual evapotranspiration is controlled by the amount of precipitation, temperature condition, and duration of sunshine, wind speed, soil type, vegetation, and soil moisture. In this regard, in Upper Awash Sub-Basin, the dominant soil type is Pellic Vertisol (light and heavy Clays) which has a maximum water holding capacity of 150mm. the other factor under consideration was the vegetation type and types of crops. Moderately deep-rooted crops such as corn, cereals, onion, Garlic, and others are common in the area. The amount of actual evapotranspiration was estimated by the soil water balance method. The actual Evapotranspiration of the Upper Awash Sub-Basin was estimated to be 660.91mm/a, which is about 65% of the mean annual precipitation of the area under investigation.

Since Actual evapotranspiration is related to temperature higher evapotranspiration occurs in May as this month is the hottest whereas the lowest evapotranspiration is recorded in December.

Table 4. 3: Actual Evapotranspiration calculated by soil-water balance method

mm	Jan	Feb	Mar	Apr	May	Jun	Jul	Aug	Sep	Oct	Nov	Dec	Annual
P	14.57	23.08	53.21	68.32	77.89	132.50	240.00	243.33	127.33	26.33	7.75	7.36	1021.67
PET	59.93	66.40	73.98	76.95	79.24	72.91	63.95	62.60	61.64	59.53	55.80	54.71	787.64
P-PET	-45.36	-43.32	-20.77	-8.63	-1.35	59.59	176.05	180.73	65.69	-33.20	-48.05	-47.35	
AccPot WL	-173.96	-217.28	-238.05	-246.68	-248.03					-33.20	-81.25	-128.60	
SM Retained	47.03	35.23	30.68	28.96	28.70	88.29	150.00	150.00	150.00	120.22	87.27	63.64	
ΔSM	-16.61	-11.80	-4.56	-1.71	-0.26	59.59	61.71	0.00	0.00	-29.78	-32.95	-23.62	
AET	31.18	34.88	57.77	70.03	78.15	72.91	63.95	62.60	61.64	56.11	40.70	30.98	660.91

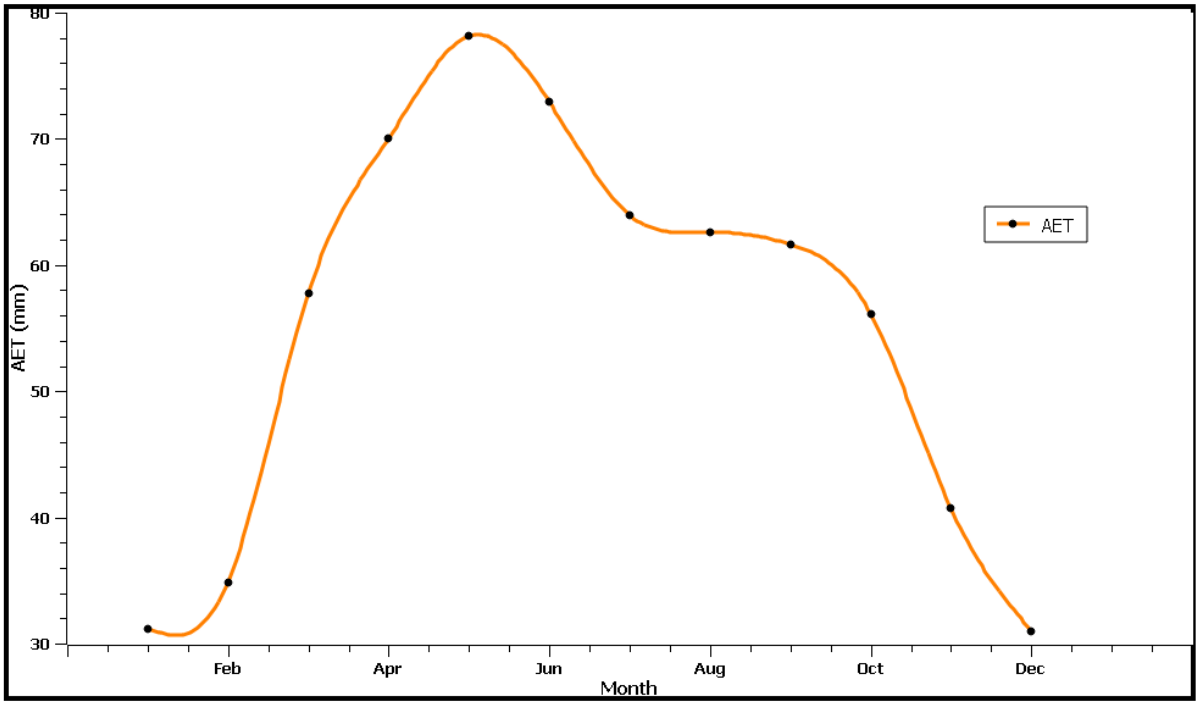

Figure 4. 5: Mean Monthly Actual Evapotranspiration

4.6. Surface Runoff

When precipitation occurs, rainwater infiltrates into the subsurface either joins the groundwater or it may follow the subsurface horizontal flow (interflow). When the soil layer reaches its maximum infiltration capacity, excess precipitation starts to flow on the surface of the Earth which is considered as surface runoff. Runoff is the major component of the hydrologic cycle which is influenced by different factors such as rainfall intensity, climate, vegetation cover, topography, geology, soil type and characteristics, slope, and surface roughness (Rezaei et al.,

2019). In the case of the Upper Awash Sub-Basin, urbanization in Addis Ababa has a pronounced influence on the amount of surface runoff since artificial surface coverages such as asphalt and concrete surfaces block the infiltration of rainwater in the soil horizon. Impervious and smooth surfaces have lower permeability which results in higher surface runoff. Soil texture is the other factor influencing surface runoff. The dominant soil types in Upper Awash Sub-Basin are Clay and Clay loams and the presence of clay reduces the pore between grains which reduces infiltration thereby increasing the risk of surface runoff. Southern and central parts of Ethiopia experience dual rainy seasons (Kiremt and Belg) with greater intensity of precipitation at a time. The higher the intensity of the precipitation and the wetter the environment, the higher the surface runoff.

Table 4. 4: Soil Groups

Soil group	Description
A	(Low runoff potential) Soils that have a high infiltration rate even when wet. Deep, well-drained sands and gravels make up the majority of these. Water transmission is high in these soils (final infiltration rate more than 0.3 in. /h). **Soil Texture: Sand, loamy sand, or sandy loam**
B	When thoroughly wetted, soils with moderate infiltration rates. These primarily consist of soils with moderately fine to moderately coarse textures that are moderately deep to deep, moderately well-drained to well-drained. Water transmission is moderate in these soils (final infiltration rate 0.15–0.30 in. /h). **Soil Texture: Silt loam or loam**
C	When thoroughly wetted, soils exhibit slow penetration rates. Soils with a layer that prevents water from flowing downward or soils with a moderately fine to fine texture are the most common. Water transmission is slow in these soils (final infiltration rate 0.05–0.15 in. /h). **Soil Texture: Sandy clay loam**
D	When thoroughly wetted, soils with a high runoff potential have very sluggish penetration rates. Clay soils with a high swelling potential, soils with a constantly high water table, soils with a claypan or clay layer at or near the surface, and shallow soils over nearly impermeable materials are the most common examples. Water transmission is exceedingly slow in these soils (final infiltration rate less than 0.05 in. /h). **Soil Texture: Clay loam, silty clay loam, sandy clay, silty clay, or clay**

The amount of surface runoff is calculated by the Curve Number method developed by the Natural Resource Conservation Service (Mockus, 1972). The Curve Number (CN) method was developed to estimate the depth of surface runoff from the areal rainfall depth. The Curve Number is dependent upon the soil type and land use type of the area. The dominant soil texture

is Clay in this regard which is categorized into soil group D, and most of the area is cultivated for agricultural purposes. By considering such conditions, the Curve Number (CN) for Upper Awash Sub-Basin was estimated to be **91 (**Table 4.5**).**

$$\frac{(P-0.2S)^2}{P+0.8S} \quad \text{For P > 0.2S}$$

Where: **Q** is a Surface runoff in inches

P is daily rainfall depth in inches

CN is Curve Number Suggested by American Soil Conservation Service

S is potential Maximum retention after runoff begins

Potential Maximum Retention (S) is the infiltration that occurs after the rainfall has been started. For the calculation of Runoff, 21 years of daily precipitation from 13 meteorological stations were used. The potential maximum retention (S) is calculated from Curve Number (CN) using the following formula:

$$S = \frac{1000}{CN} - 10$$

$$= \frac{1000}{91} - 10 = 0.99$$

Table 4. 5: Curve Number Determination from Land Use and Soil Groups

Land Use Description	**Soil Grouping**			
Land Use Type	**A**	**B**	**C**	**D**
Commercial, town houses	80	85	90	95
Cultivated with conventional tillage	72	81	88	91
Woods or forest, thin stand, and poor cover	45	66	77	83
Pavement and roofs	100	100	100	100
Pasture or range poor condition	68	79	86	89
Farmsteads	59	74	82	86

As described from the above formula, surface runoff for each daily runoff was calculated for P>0.2*S (P>0.198), and finally summed up to get the annual runoff for the given sub-basin. The amount of surface runoff of Upper Awash calculated using the above method is about **205.6mm/a**, which is about 20% of the total mean annual precipitation of the sub-basin.

4.7. Groundwater Recharge Estimation

Groundwater recharge takes place when water infiltrates at the earth's surface, percolates through the soil horizon passing the water table. Groundwater is a finite resource that needs management by controlling abstraction and means of replenishment. Understanding how much water is withdrawn from storage and how much water is added to groundwater is the key

component of groundwater management. Groundwater recharge amount can be estimated by different methods; Ground Water table fluctuation method, Catchment Soil-water balance method, Chloride mass balance method, and hydrograph separation. In Upper Awash Sub-Basin, different scholars have tried to estimate the amount of groundwater recharge using different methods. Molla Demlie et al. (2007) estimated the mean annual recharge of Akaki catchment using Semi distributed catchment soil-water balance method (Thornthwaite & Mather, 1957) and Chloride mass balance methods. Using these methods, the groundwater recharge amount of the Akaki catchment was about 105.4mm and 205mm respectively. WWDSE (2008) estimated the mean annual recharge of Upper Awash Sub-Basin using the Water balance (WATBAL) model developed by David Yates (Yates & Strzepek, 1994), and the estimated value was about 47mm. In this study, the method applied for recharge estimation is the catchment Soil water balance method.

$$\mathbf{P = AET + R + Q}$$

Where

P = precipitation (mm/yr)

AET = Actual Evapotranspiration (mm/yr)

Q = runoff expressed as millimeters over the catchment (mm/yr)

R = groundwater recharge (mm/yr)

$$\mathbf{R = P - AET - Q}$$

Table 4. 6: Water Budget Components

Hydrologic components	Precipitation	Actual evapotranspiration	Surface runoff	Recharge
Estimated amount (mm/year)	1021.67	660.91	205.6	155.16

The mean annual recharge was estimated to be 155.16mm/year, which is about 15% of the total annual precipitation.

4.8. Water Budget Analysis

The water budget is the analysis and consideration of the amount of water that enters and leaves the system (Stanton et al., 2011). It is the determination of all inflow and outflow components of a catchment, transfer between the components, and their relative contribution within the catchment which is very helpful to define how much water is available in a store, how much

water is already consumed, to decide where the water is coming from and at what rate is the groundwater getting replenished. Water budget components include Precipitation, Evapotranspiration, Surface runoff, and Groundwater Recharge. In this study, these components were determined using the soil-water balance method. The mean annual precipitation of the catchment was 1025.23mm/a. From this annual precipitation, about 660.91mm (65%) was evaporated back to the atmosphere, about 205.6mm (20%) of water flows over the Earth's surface as runoff and 158.69mm (15%) of the total precipitation has been infiltrated to replenish the groundwater.

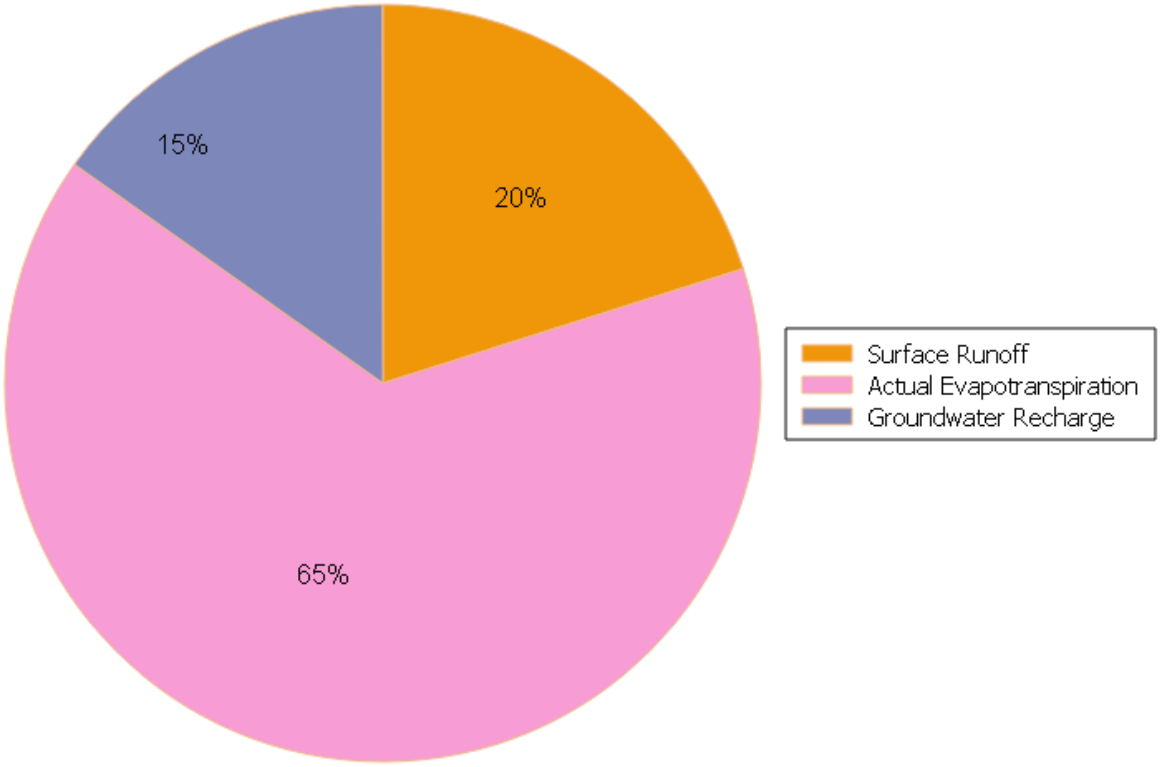

Figure 4. 6: Water Budget Components

Chapter Five

Hydrogeology

The hydrogeological classification of local rock units is based on quantitative data like permeability, yield, aquifer thickness, and transmissivity, while the qualitative investigation includes field observations of the geological, hydrogeological, geomorphological, physical, and geographical setup (Bereket Fentaw and Mihret Manaye, 2019). Based on their qualitative and quantitative characteristics, rock units in the Upper Awash Sub-Basin are classified into the following aquifer types:

Extensive and Moderately Productive Porous Aquifers

This aquifer the quaternary alluvial deposits. The grain size of these alluvium deposits varies greatly, ranging from clay and silt to sand and gravel, and occasionally boulder size. These deposits have relatively good permeability and productivity with sand to gravel grain size as well as with some fine-grained undifferentiated sediments.

The swamp deposits and lakes resulted in lacustrine deposits in the low-lying areas with variable permeability that relies on the grain size, sorting and recharge conditions (Bereket Fentaw and Mihret Manaye, 2019). The permeability and productivity of lacustrine deposits with silt and sand grain sizes are better, whereas those with very fine ash and massive tuff interbreeding layers have low permeability and productivity.

Extensive and Highly Productive Fissured Aquifers

The Tarmaber and Addis Ababa basalts are typical examples of this aquifer system. The degree and intensity of fracturing, the enhancement of jointing, and the interconnection of primary porosity all have a role in the permeability of this aquifer. The Tarmaber basalts have good fracturing, hence it has good hydraulic properties (Bereket Fentaw and Mihret Manaye, 2019). The scoriaceous composition of the aquifer makes it ideal for groundwater storage and transport. In addition, secondary cracks and weathering strengthen the columnar joints, resulting in the development of springs in the highlands. Faulting increases permeability and leads to the formation of a groundwater conduit in some areas, particularly along the rift escarpment, and greatly improves the water-bearing qualities of the aquifer. The groundwater in the Tarmaber basalt is manifested by the springs discharged from it. The geological, geomorphological, and climatic factors of the area result in high groundwater discharge layers

in the Tarmaber basalt. Apart from the extreme fracturing, the presence of secondary material infilling is a common issue that reduces permeability. The average yield of springs and shallow and deep wells varies greatly, with an average of 18.7 l/s. The static water level ranges from artesian to 50 m b.g.l., but it can reach as high as 120 m b.g.l. in some areas (Bereket Fentaw and Mihret Manaye, 2019).

Following Akaki basalt, where the well-field was built, and the Addis Ababa basalt is a major groundwater source for the city. This lava flow is mostly porphyritic to aphanitic in texture. The concentrated joints created during lava cooling, lava tubes, interconnecting vesicles, and voids left between lava flows are responsible for this high water storage, transmissivity, and permeability. The presence of a major Filwuha fault and numerous localized fractures also affects the hydraulic properties of this unit. The principal water-bearing structures are formed where secondary cracks alter and enhance the primary porosity as a result of tectonic and weathering processes (Bereket Fentaw and Mihret Manaye, 2019).

This aquifer is overlain by fresh and substantial ignimbrite in most parts of Addis Ababa, resulting in artesian conditions and the fact that most boreholes must dig through this ignimbrite to reach good discharge. In addition to direct infiltration, the Entoto rhyolitic trachyte ridge is the principal recharge source for this aquifer. In most cases, soil development improves groundwater recharge; however, in the northern section of Addis Ababa, steep slope topography leads to soil erosion and increased runoff. The secondary permeability of Akaki basalt, which is the result of fracturing and weathering, is extremely important for its water-bearing properties. The interconnections of many vesicles in Akaki basalt are poor or may be filled with secondary infilling materials. As a result, vesicles play a minor role in the permeability of the rock. However, fractures in certain vesicles cause them to connect, increasing permeability (Bereket Fentaw and Mihret Manaye, 2019). The remarkable permeability of Akaki basalt scoria fallout is entirely dependent on vesicles and pour gaps. Rainfall recharges this aquifer directly, while groundwater flows from the northern portion of Addis Ababa city, and local watercourses recharge it indirectly.

Aquicludes

The structures and weathering conditions of the Ziquala, Wechecha, Furi, and Yerer trachytes vary, as do the presence of water, and storage capacity. The absence of thick soil facilitates surface runoff and decreases infiltration. As a result, little groundwater is stored, except for the formation of springs with variable, generally low discharge. The water-bearing characteristics

of Chefedonsa pyroclastic deposits and the Nazret unit are concentrated on weathering cracks and weathering zones, which modify the limited primary porosity and permeability. These units are usually large, with little fracturing and weathering. As a result, they have lower permeability, yet they can occasionally transmit water to the underlying aquifers. They can serve as a regional aquiclude in most cases (Bereket Fentaw and Mihret Manaye, 2019). The pore spaces developed on the Chefedonsa pyroclastic rocks are insufficient to store and transfer groundwater. The grain sizes vary from clay to gravel, which makes it difficult to sort and has low permeability. This unit is also found as an intercalated layer in lacustrine sediments and operates as an impermeable layer in the majority of cases. However, it has developed linked pore spaces in some locations, resulting in good permeability and allowing for some groundwater storage.

Extensive and Moderate Productive Mixed Aquifers

The volcanic rocks classified under this type of aquifer are frequently intercalated by sediments, resulting in mixed units. The Chefedonsa pyroclastic deposits, rhyolitic and trachytic lava domes, Wechecha, Furi, Yerer volcanic rocks in some areas intercalated with superficial deposits are grouped into this aquifer type. The permeability and productivity of this aquifer are highly variable, with significant spatial variation. The wide range of spring yields suggests that the permeability varies greatly depending on the manner of occurrence, the severity and degree of weathering and fracturing, the type of materials in the pyroclastic flows, the availability of sufficient recharge, and the topographic environment. The vertical and lateral non-homogeneity of volcanic rocks partly intercalated by various sediments causes these semi-confined situations (Bereket Fentaw and Mihret Manaye, 2019).

This unit is occasionally massive and fresh, with less fracturing and weathering. This unit acts as a confining layer for the underlying basaltic aquifer on the plateau, particularly around Addis Ababa (Bereket Fentaw and Mihret Manaye, 2019).

Extensive and Moderately Productive Fissured Aquifer

This aquifer is comprised of basalts, ignimbrites, trachytes rhyolites, and tuffs and ash mainly in Addis Ababa and other highland recharge areas comprising Addis Ababa basalt, Akaki basalt, Addis Ababa ignimbrite, Tarmaber basalt, Entoto trachyte, and rhyolite. Although most of the wells are underwater table conditions, a considerable number of them have semi-confined circumstances. The vertical and lateral non-homogeneity of volcanic rocks partly intercalated by diverse sediments causes these semi-confined situations. Basaltic lavas are fluid

and generate thin flows with a lot of pore space at the tops and bottoms (Bereket Fentaw and Leta Alemayehu, 2010). This aquifer is local or discontinuous but highly productive aquifers in which flow is mainly through regularly developed systems of fissures and joints of sedimentary and volcanic rocks with transmissivity (T = 1.1–10 m^2/d, q = 0.011–0.1 l/s.m, with spring and well yield Q = 0.51–5 l/s) (Bereket Fentaw and Leta Alemayehu, 2010).

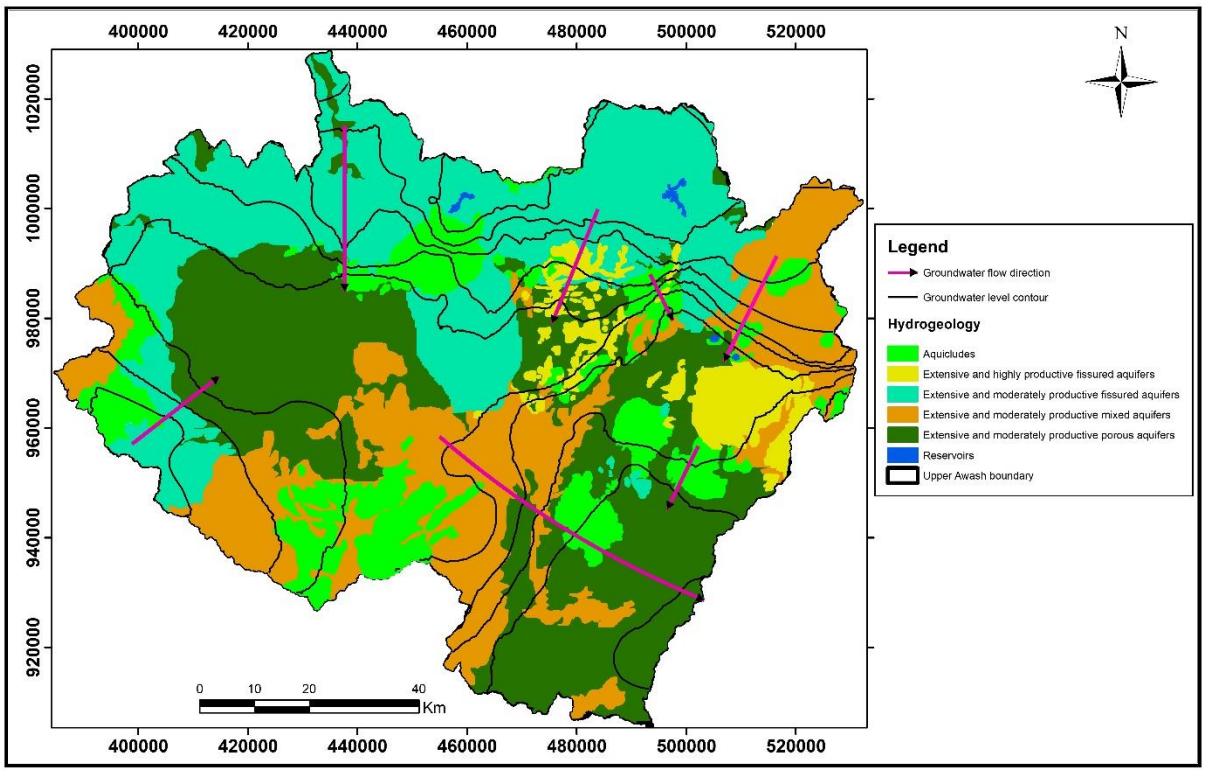

Figure 5. 1: Hydrogeological Map of Upper Awash Sub-Basin (Modified from Geological Survey of Ethiopia, 2010; WWDSE, 2008)

Chapter Six

Hydrochemical Variation and Water Quality of Upper Awash Sub-Basin

6.1. Introduction

Hydrochemical data were analyzed in two years 2019 and 2021 from fifteen selected sites. Four groundwater samples were taken from Mojo slaughterhouse well, Sendafa public water supply well, Holeta public water supply well, and Melkakunture (Balchi Jimjima) well, and five samples were collected from the lakes; Lake Aba Samuel, Legedadi reservoir, Dire reservoir, Gefersa reservoir, and Lake Koka; five river water samples taken from Legetafo river, Mojo river upstream, Holeta river, Mojo river at the inlet to Lake Koka and Awash river at Melkakunture. One spring water sample was taken from Chefedonsa spring which is used for both domestic, irrigation, and animal watering purposes.

These fifteen water samples of each year were analyzed for sodium ion (Na^+), potassium ion (K^+), calcium ion (Ca^{2+}), magnesium ion (Mg^{2+}), and total iron (Fe_tot), manganese (Mn^{2+}), zinc (Zn^{2+}), cadmium (Cd), chromium (Cr) and lead (Pb) in Addis Ababa University, Chemistry Department laboratory. The other physical parameters such as pH, electrical conductivity (EC) and total dissolved solids (TDS), alkalinity, and temperature were measured at the site (in situ measurement). In addition to the primary data, the hydrochemical variation of groundwater is also conducted using secondary data at different sites including Akaki wellfield, Shegole well, Filwuha well, Hilton Hotel well, Debrezeit Airforce well, Debrezeit veterinary school well, Debrezeit Blue Nile plastic factory well, Debrezeit Hora tannery well, Mojo tannery well, and Debrezeit Dire tannery well.

6.2. Groundwater Chemistry of Upper Awash Sub-Basin

6.2.1. Hydrogen-ion Activity (pH)

The pH measurements from 776 primary and secondary water samples have a range of 6.0 to 9.42. About 85% of the total groundwater samples have a pH value greater than 7 (i.e. slightly basic near-neutral water). Higher pH is observed in the southern, central, and to some extent in the northern part of the study area. Despite its fluctuation, there is no significant temporal variation in pH observed from monitoring data. The high pH values in highland areas with deep

groundwater systems, and in areas close to the rift might be related to the silicate hydrolysis as groundwater flows from shallow aquifers to deeper aquifer systems. Deeper aquifers in the transition and highland areas, and lowland areas including Koka, and Alem Tena have high pH values whereas shallow aquifers in newly recharged groundwater of the three zones have lower pH.

The pH has no direct impact on water consumers. However, to provide adequate water clarity and disinfection, pH must be controlled. The pH of the water should be less than 8.0 for chlorine disinfection to be effective. To prevent corrosion of water tanks and pipelines in residential water systems, the pH of water entering the distribution system must be adjusted. The pH range set by World Health Organization for drinking water is 6.5-8.5. About 95% of the total water samples have pH values within this range that fulfill the required criteria. Some water samples have lower pH (pH <6.5) and higher pH value (pH >8.5) but the deviation is negligible.

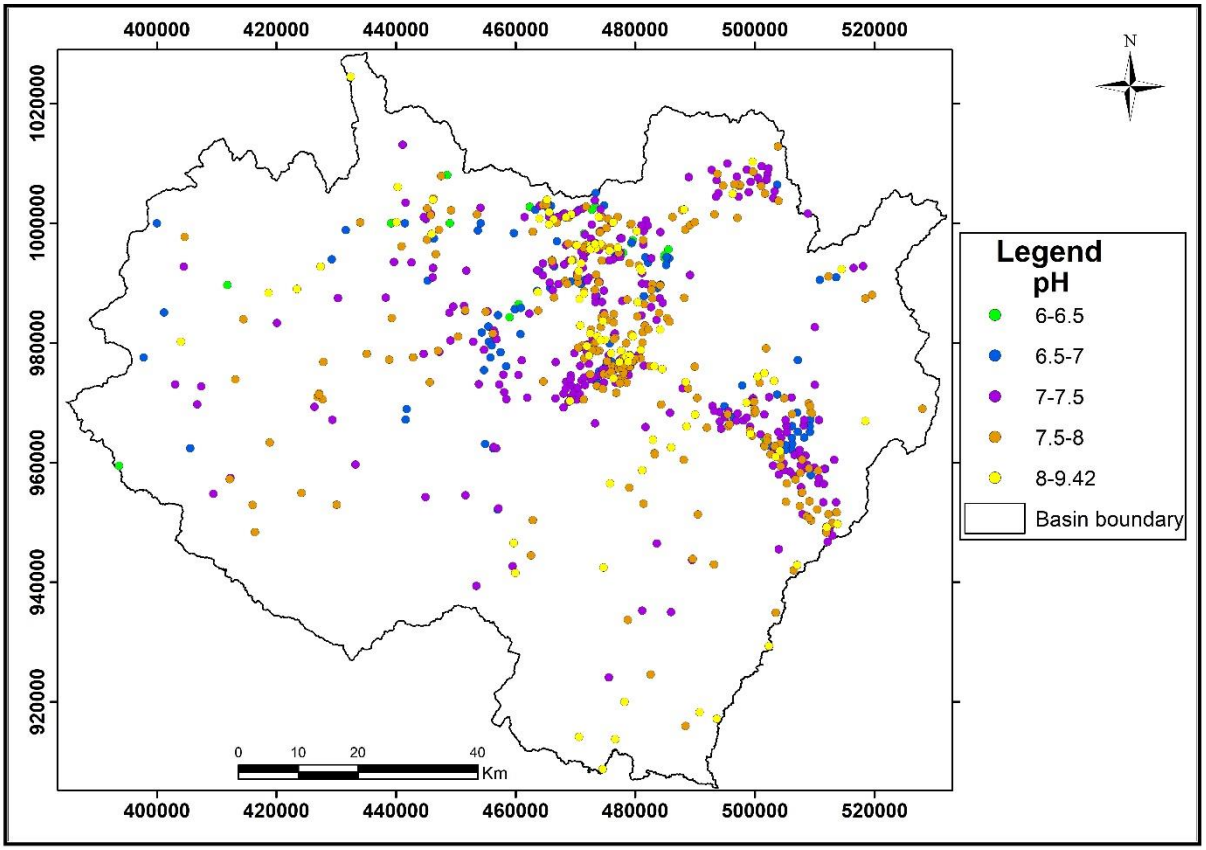

Figure 6. 1: Spatial Variation of Hydrogen-ion Activity (pH)

6.2.2. Spatial and Temporal Variation of Total Dissolved Solids in Groundwater

Spatial Variation of Total Dissolved Solids

The total dissolved solids of groundwater samples in the Upper Awash Sub-Basin show a slight

change over time with higher spatial variation due to the rock-water interaction and anthropogenic influences. The highest total dissolved solids in the area are attributed to the Filwuha wells in Addis Ababa where there is high geothermal activity along the Filwuha fault that can affect the groundwater composition. Relatively high total dissolved solids (600-1200mg/l) are observed from wells found in Debrezeit, Koka, Akaki wellfield, Ginchi, and Bantu towns. In general, newly recharged areas including Entoto ridge, Sendafa, Holeta, and Addis Alem, and some central highland areas are characterized by low TDS. The highland recharge areas in shallow aquifers including Entoto ridge, Ginchi, Holeta, and Guraghe highlands are characterized by low TDS. The circulation of groundwater along with the local fault systems in the transition, and in some highland areas make it have intermediate TDS.

The evolution of groundwater as it flows from shallow aquifer system to deeper aquifer, and its circulation along the regional fault zones of Filwuha-Ambo, Filwuha-Weliso, fault systems cause the groundwater to have higher TDS. Generally, the groundwater TDS is highly controlled by the lithology, faults, evolution, and residence time.

There is no health-based guideline value proposed for the TDS in drinking water by the World Health Organization. However, based on palatability it can be classified as excellent (TDS<300mg/l), good (300<TDS<600mg/l), fair (600<TDS<900mg/l), poor (900<TDS<1200mg/l) and unacceptable (TDS>1200mg/l). In this respect, the majority of the groundwater samples in Upper Awash Sub-Basin are categorized as good (46%) and excellent (44%); 7% are categorized as fair; 1% of it is poor and 2% of the total water samples is taken as unacceptable.

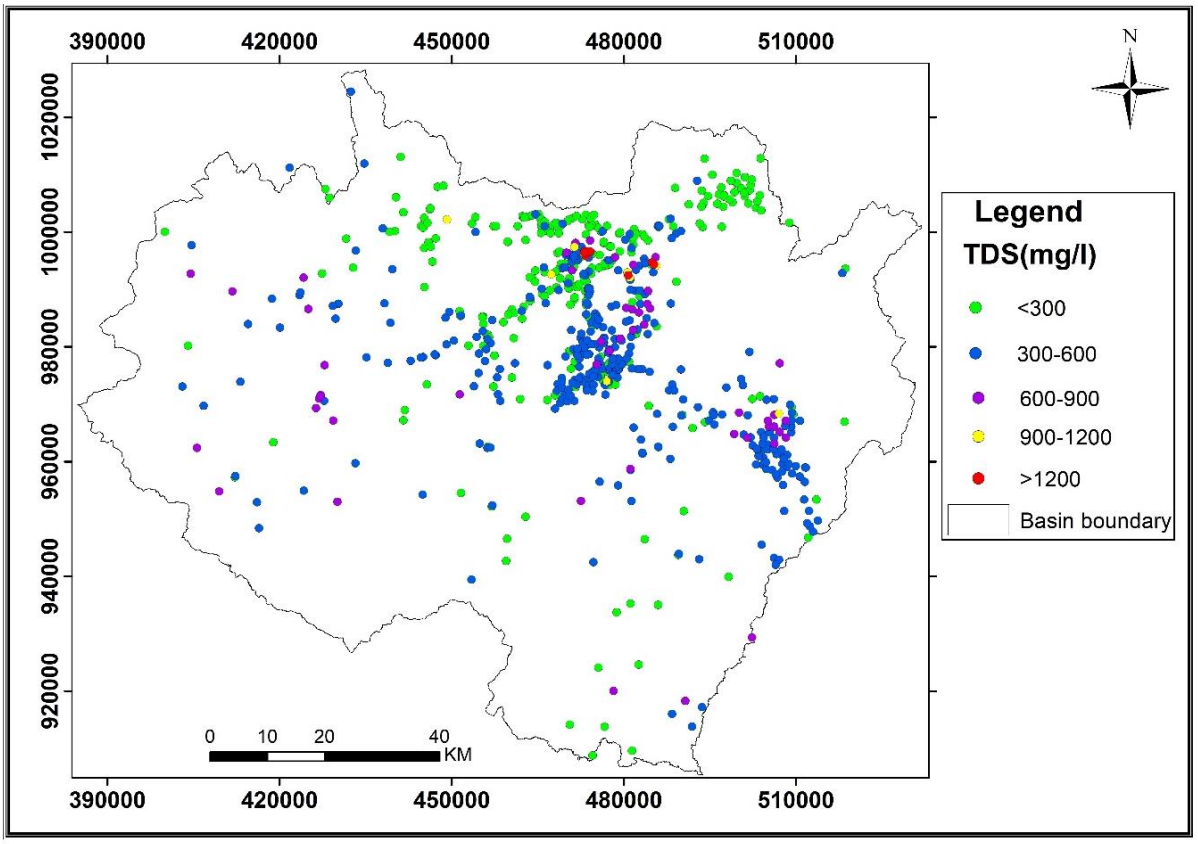

Figure 6. 2: Spatial Variation of TDS in Upper Awash Sub-Basin

Temporal Variation of Total Dissolved Solids

The total dissolved solids in groundwater were monitored at sixteen sites in the area. In some of the monitoring wells, the total dissolved solids show a slight increment over time. In Filwuha well the TDS has increased from 2240mg/l to 2846.67mg/l within five years (2006 to 2010). In other water supply wells including Shegole well, the variation was from 174mg/l (in 2007) to 311mg/l after seven years of measurement in 2015. The hydrochemistry of the water supply well in Sendafa was measured five times in the last twenty-one years including the present analysis. The total dissolved solid measured in 2000 by Water Works Design and Supervision Enterprise was 111mg/l and in the present study, it has increased to 240mg/l. The TDS in the Debrezeit Airforce well was 616mg/l in 1991, and after nineteen years in 2010, it shows an increment to 854mg/l; in Debrezeit Veterinary School well, the TDS was 452mg/l in 1974, and after twenty-six years in 2000, it has increased to 635mg/l. A slight increment in the total dissolved solids was observed in the Melkakunture water supply well, and Chefedonsa springs. However, it takes a long time to see the hydrochemical change in groundwater as it is a hidden resource. As a result, in most groundwater samples the change in TDS is not significant other than simple fluctuation or small variation over time. The temporal variation of total dissolved

solids in groundwater is mainly due to the residence time of water in a given aquifer system.

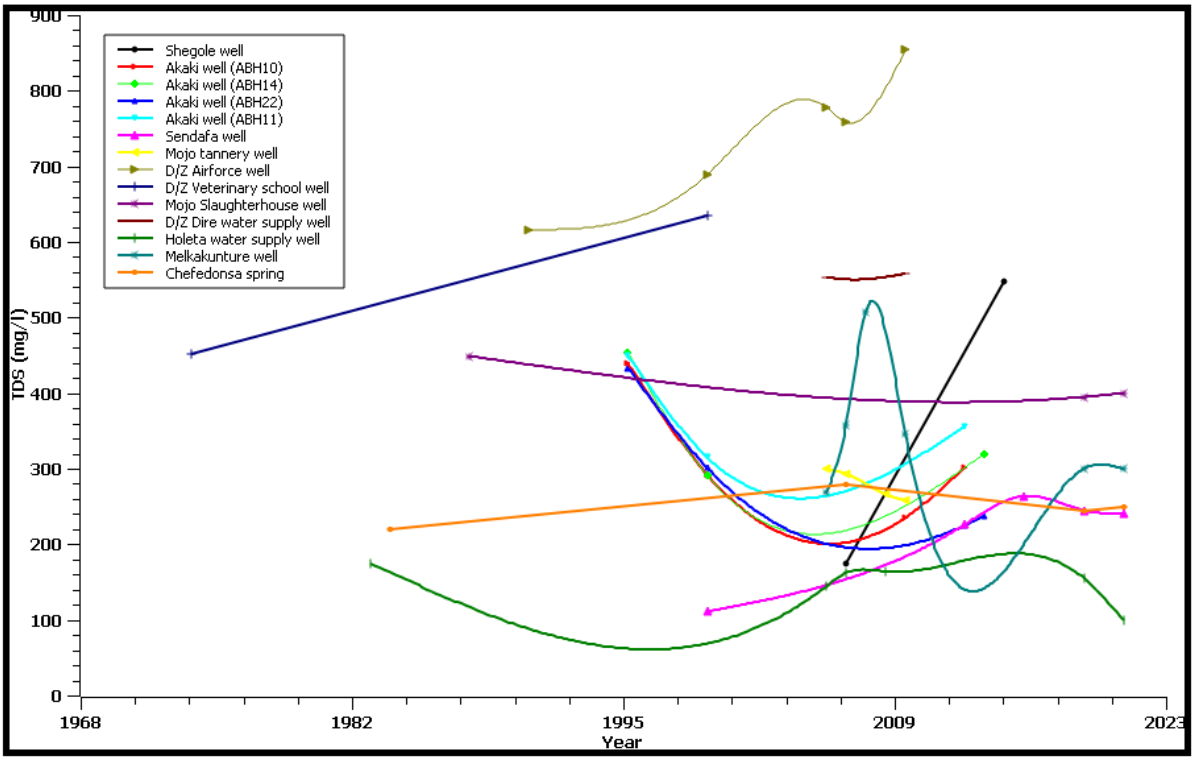

Figure 6. 3: Temporal Variation of TDS in Groundwater

6.2.3. Spatial and Temporal Variation of Groundwater Electrical Conductivity (EC)

Spatial Variation

In the same way as the total dissolved solids, high electrical conductivity is attributed to the Filwuha thermal spring water due to the thermal leaching of the surrounding rocks by highly aggressive hot water. Most parts of the recharge areas and some of the central parts of the Upper Awash Sub-Basin with shallow groundwater systems, and groundwater at its early stage of evolution have lower electrical conductivities. Shallow groundwater in the city and towns is vulnerable to the change in electrical conductivity due to the infiltration of the surface water from urban centers. Highly evolved groundwater in, and near the rift, and deep aquifers in the transition and highland areas have higher electrical conductivity. The circulation of groundwater through the local and regional faults changes its ionic composition as well as the electrical conductivity.

There is no health-based guideline value for electrical conductivity by World Health Organization. But most of the time experts forwarded that drinking water to have an electrical conductivity value less than 1000µS/cm.

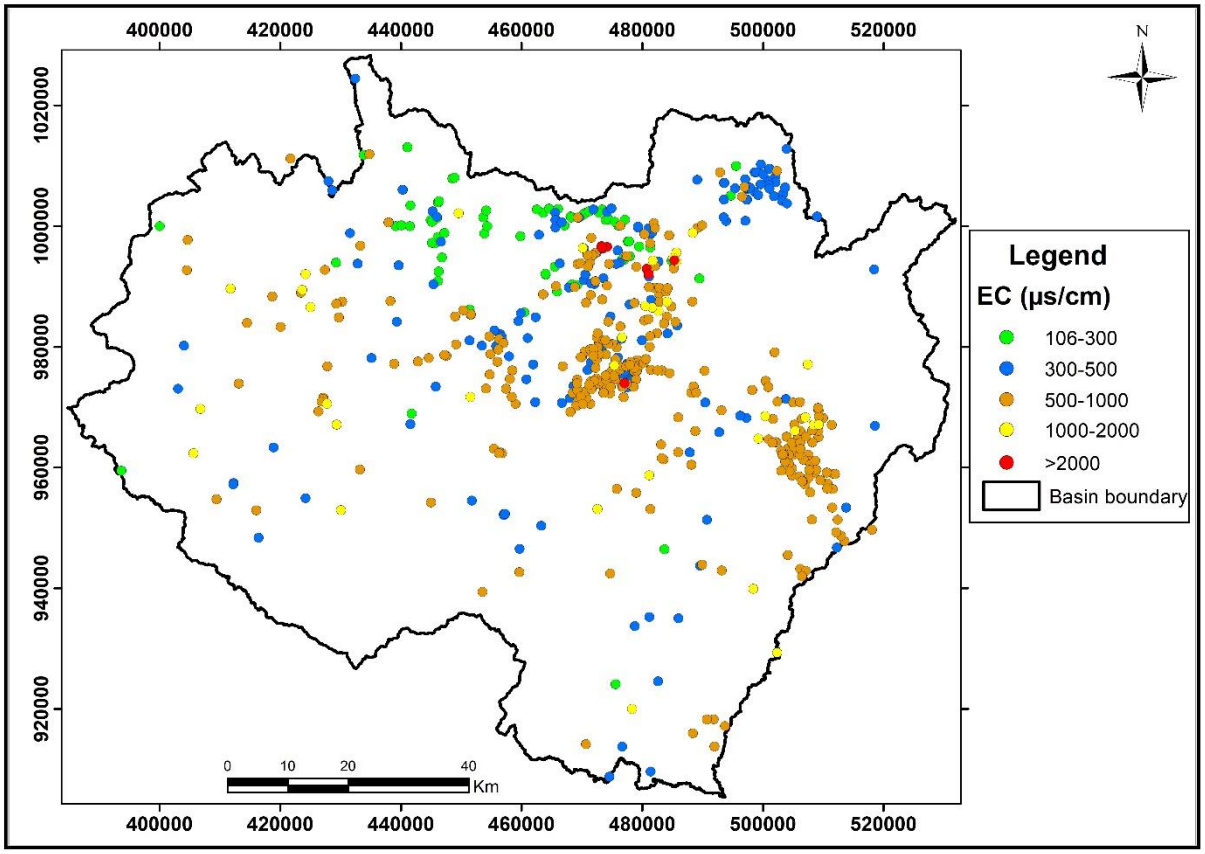

Figure 6. 4: Spatial Variation of Electrical Conductivity in Upper Awash Sub-Basin

Temporal Variation of Electrical Conductivity

Since the total dissolved solids and electrical conductivity are interrelated, the electrical conductivity has increased whenever the total dissolved solid increases. The electrical conductivity of water depends on the amount of salt dissolved in it. Thermal wells in Addis Ababa show a higher temporal variation of electrical conductivity. The EC measurement in the Shegole well has increased from 311µS/cm to 845µS/cm (2007 to 2015). From the Sendafa water supply well, the electrical conductivity was 166.5µS/cm in 2000 (WWDSE), and in the present measurement, it has increased to 480µS/cm. The Water Works Design and Supervision Enterprise reported that in 2006 that the electrical conductivity of Melkakunture public water supply well was 536µS/cm but in the present analysis, the EC has increased to 600µS/cm. In the same way, the EC in Chefedonsa spring was 361µS/cm in 1984, and it has increased to 490µS/cm in 2021. In the Mojo slaughterhouse well, the groundwater EC has increased from 736µS/cm (in 1988 measurement) to 810 µS/cm (2021). Generally, the electrical conductivity of groundwater is more or less stable and it is more convenient to say fluctuation rather than increasing over time. As groundwater lasts a long time in the area, it has a great possibility to dissolve more ions and solids that make it have higher electrical conductivity.

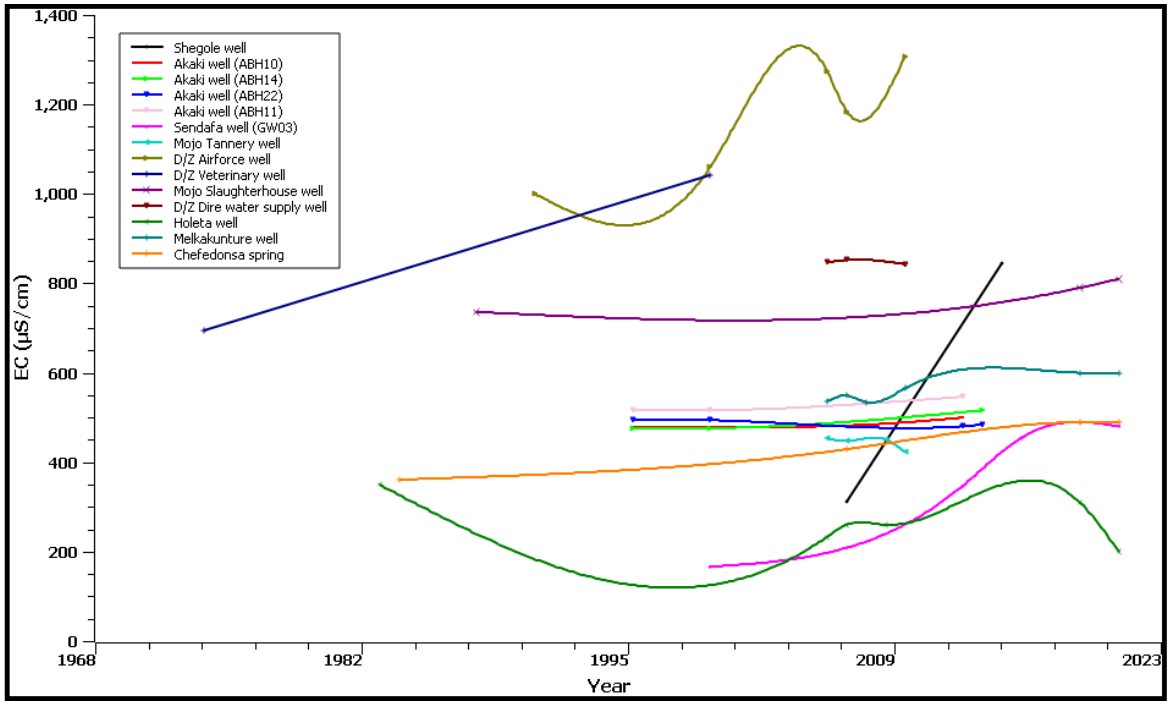

Figure 6. 5: Temporal Variation of Electrical Conductivity in Groundwater

6.2.4. Major ion Variation in Groundwater

Groundwater major ions variations were identified from the combination of previous measurements and present study at some groundwater wells.

From eight major ions, Sodium and Calcium are the most abundant and variable ions both spatially and temporally in the Upper Awash Sub-Basin.

Spatial Variation of Sodium-ion in Groundwater

As usual, sodium ion in the Upper Awash Sub-Basin is highest in Addis Ababa thermal springs. Deep groundwater in the highland recharge area also has high sodium ions (sodium type water). Due to the evolution of groundwater, areas close to the rift axis evolve from calcium to sodium dominating water in the area. Rock-water interaction is the main reason for the presence of high sodium ions in the Upper Awash Sub-Basin. Acidic volcanic rocks in the area are the major sources of sodium ion concentration in groundwater with minor anthropogenic influences taken under consideration. The increase in Na ion at the expense of Ca demonstrates the cation exchange mechanism supremacy. In areas where there is a high sodium ion, the dominant water type is sodium bicarbonate type water (Na-HCO_3 type).

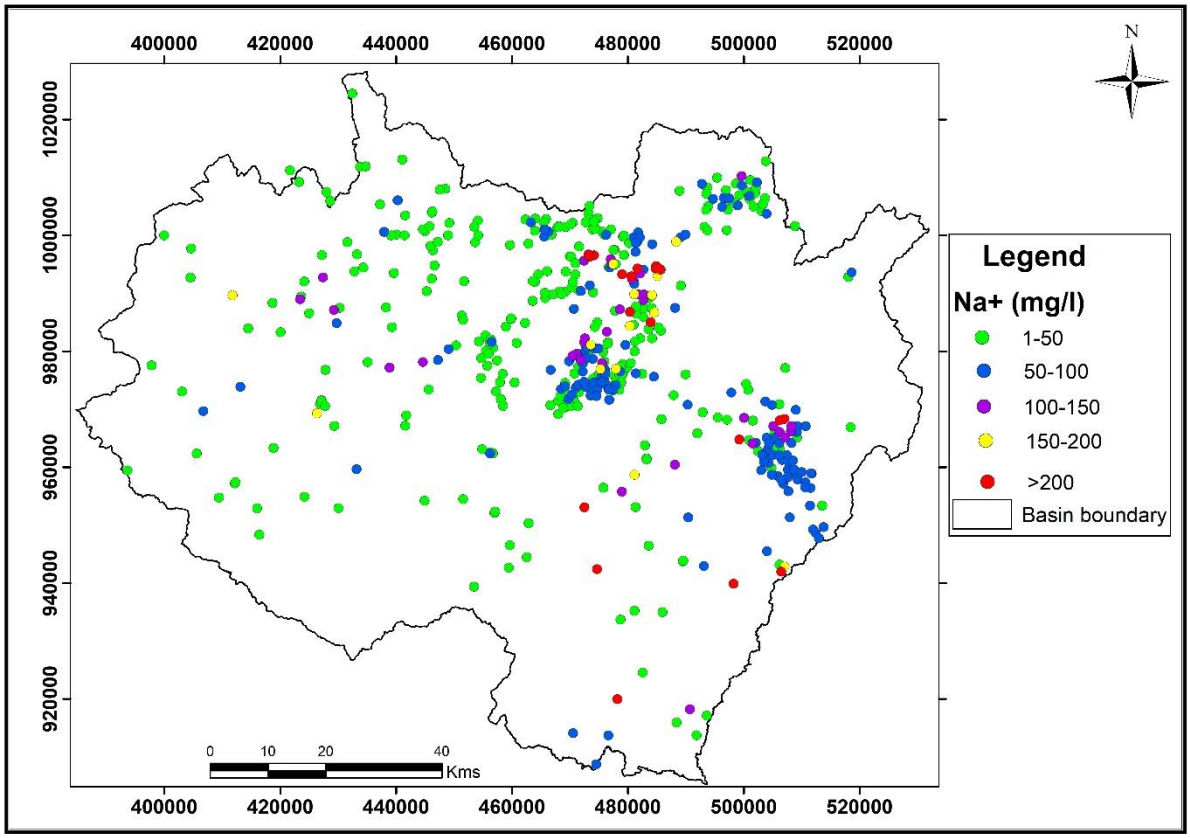

Figure 6. 6: Spatial Variation of Sodium-ion in Groundwater

Temporal Variation of Sodium-ion in Groundwater

The sodium ion is highest in groundwater at Filwuha and surrounding wells. The chemistry of groundwater in Filwuha wells was studied in 1951 by Chuzo Kondo. This thermal groundwater was studied eight times from 1951 to 2010. In the given time interval, the concentration of Sodium-ion has increased from 716mg/l to 963mg/l. However this concentration fluctuates between 1182mg/l (in 1967) and 930mg/l (in 2006). In the nearby wells from Hilton Hotel, sodium ion concentration is very high with slight variation and the concentration varies from 964mg/l to 988mg/l. The high concentration of sodium ions in these wells is attributed to the reaction between the aggressive thermal groundwater with the surrounding rocks. Sodium-ion concentration in Sendafa area groundwater varies from 6mg/l (in 2000) to 47.5mg/l (from present analysis in 2021). The other higher variation of sodium ion was recorded in Debrezeit Airforce well (6mg/l to 204mg/l) in between 1981 and 2010; from 64.5mg/l to 138mg/l at Debrezeit veterinary well; and from 63mg/l to 123mg/l at Dire water supply well. In this study, the Mojo slaughterhouse well was also taken as a monitoring station by combining the present hydrochemical data and previous research results (starting from 1988 conducted by Addis Ababa Water and Sewerage Authority. Sodium-ion concentration in the given interval of time

varies from 67.9mg/l to 88.1mg/l. Groundwater chemical analysis at Holeta well from 1983 to 2021 showed slight sodium ion variation (17mg/l to 58mg/l) and at Melkakunture well, the variation was from 38mg/l to 50.4mg/l (between 2006 and 2021 years). In some monitoring stations, for example in Akaki wells and Chefedonsa spring have lower sodium ion variation through time. Since groundwater is a concealed resource, its vulnerability to anthropogenic pollution sources is relatively minimal compared to surface waters, and it takes a long time to see ionic variation. Generally, the increase in sodium ion concentration through time is mainly due to the residence time of groundwater in the area.

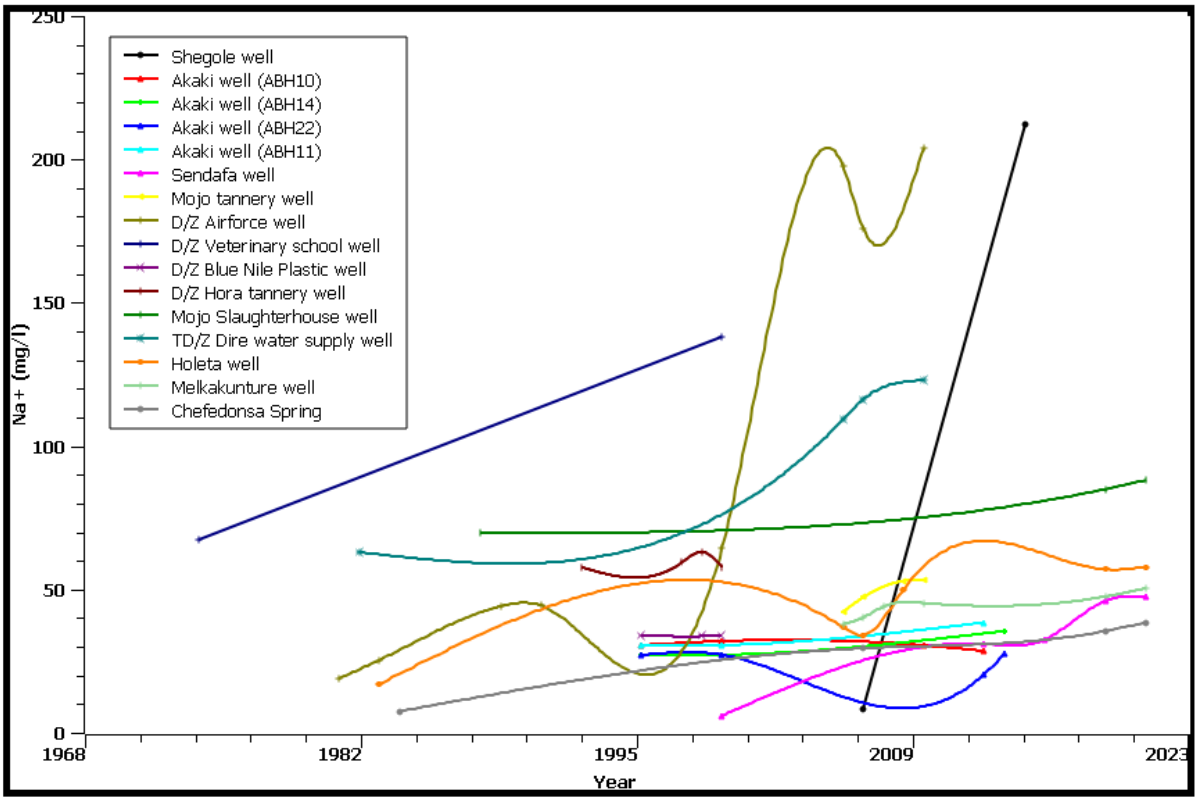

Figure 6. 7: Temporal Variation Map of Sodium-ion in Groundwater

Spatial Variation of Calcium-ion in Groundwater

Calcium ion is relatively higher in newly recharged highland groundwater. The evolution of groundwater along its flow path changes from calcium dominating to sodium ion dominating water. In areas like Akaki, Ginchi, Boneya, and Chefedonsa, calcium is the dominant cation in groundwater. In these areas, the dominant water type is calcium bicarbonate type (Ca-HCO_3 type). The reaction of highly weathered basaltic rocks with groundwater is the main source of high calcium ion concentration in groundwater. In addition, minor anthropogenic effects from industrial and domestic wastes may contribute to this concentration.

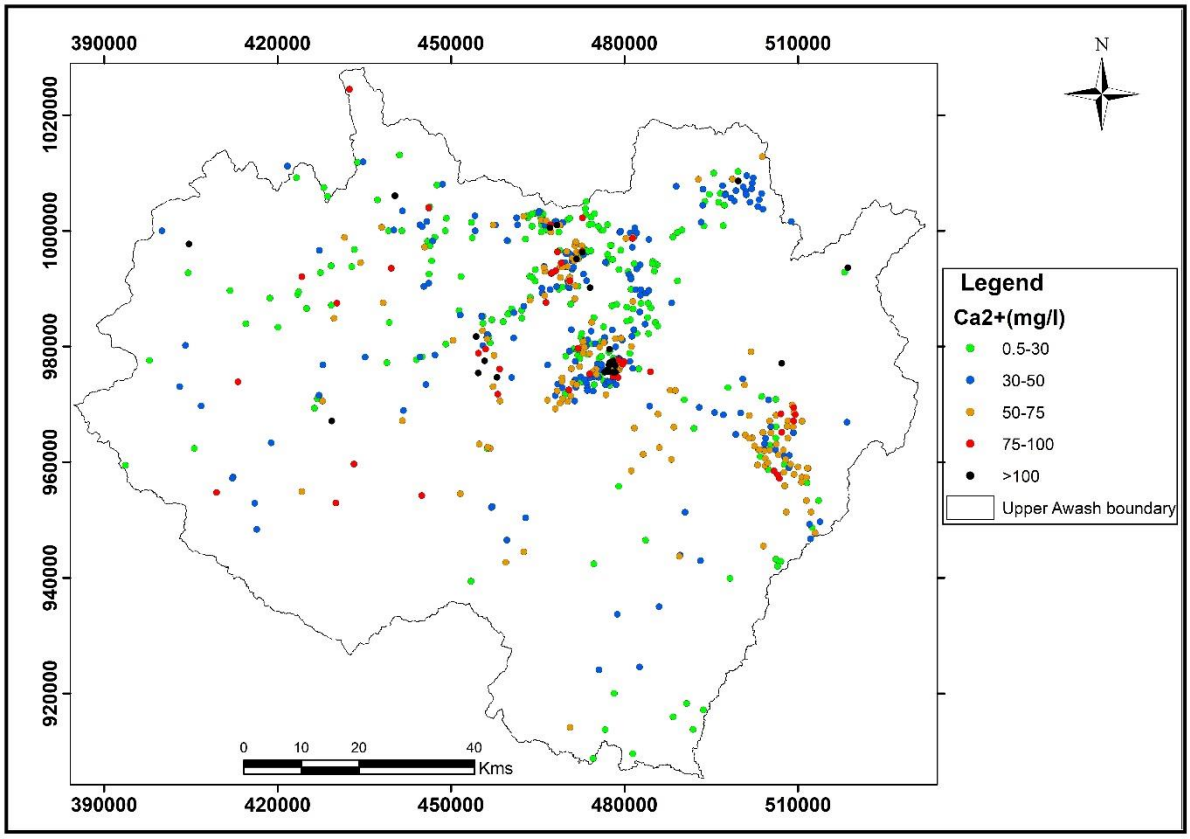

Figure 6. 8: Spatial Variation of Calcium-ion in Groundwater

Temporal Variation of Calcium-ion in Groundwater

The other highly varying ion in groundwater is the Calcium ion. Calcium ion concentration is relatively higher in and around Addis Ababa areas (recharge areas in general). In Sendafa monitoring well, Calcium ion concentration has increased from 16mg/l to 59.31mg/l within twenty-one years. The other relatively higher variation of Calcium concentration was recorded at Holeta well, which was 33mg/l in 1983 and 69mg/l in 2021. A slight variation of this ion has also been observed in Melkakunture well from 2006 to 2021 years of measurement (65.3mg/l to 81.4mg/l respectively). In general, like sodium ions, the concentration of calcium ions is also more or less stable in groundwater, and in most monitoring stations, the concentration doesn't show any significant variation over time rather it fluctuates with slight variation. In general, as the groundwater lasts a long time in a certain environment, there will be more time for rock-water interaction to take place and more calcium ions will be added to the groundwater.

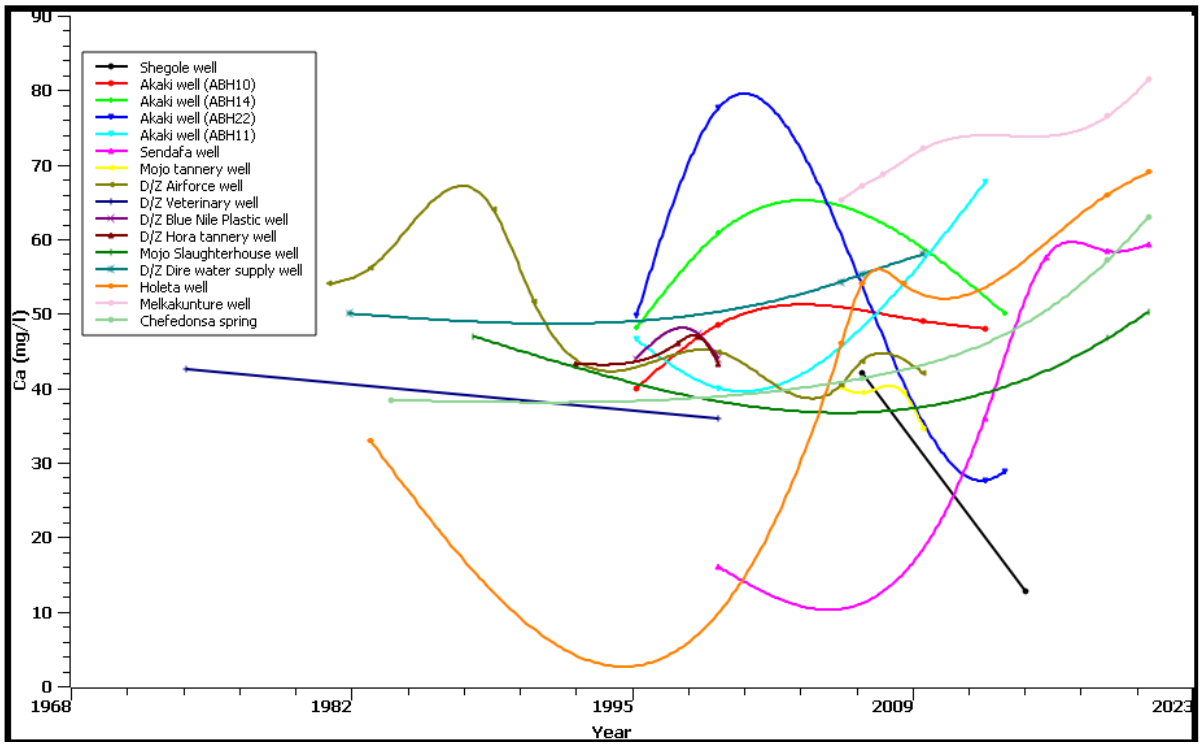

Figure 6. 9: Temporal Variation of Calcium-ion in Groundwater

Spatial Variation of Magnesium-ion in Groundwater

The concentration of magnesium in groundwater is not that much higher. The highland and transition groundwater of the Upper Awash Sub-Basin is characterized by high magnesium ion concentration. Basic rocks including Addis Ababa basalt, Akaki basalt, Tulu Rie basalt, and Weliso-Ambo basalt are the main sources of magnesium. Addis Ababa, Akaki Beseka, Debrezeit, Dukem, Godino, and Ginchi area, groundwater has high magnesium content. The groundwater found in areas close to the rift is more depleted in magnesium ions due to the evolution from calcium and magnesium bicarbonate type water to sodium bicarbonate type through the process of cation exchange. As a result, groundwater in Koka, Alem Tena, Hombole, Adulala, and Lemen areas has lower magnesium content. Groundwater in some highland areas including Holeta, Entoto, and western parts of the Upper Awash Sub-Basin have lower magnesium ions.

In general, the concentration of magnesium in the Upper Awash groundwater ranges from 1mg/l to 122mg/l. In most of the Upper Awash groundwater, the concentration of magnesium is below 20mg/l.

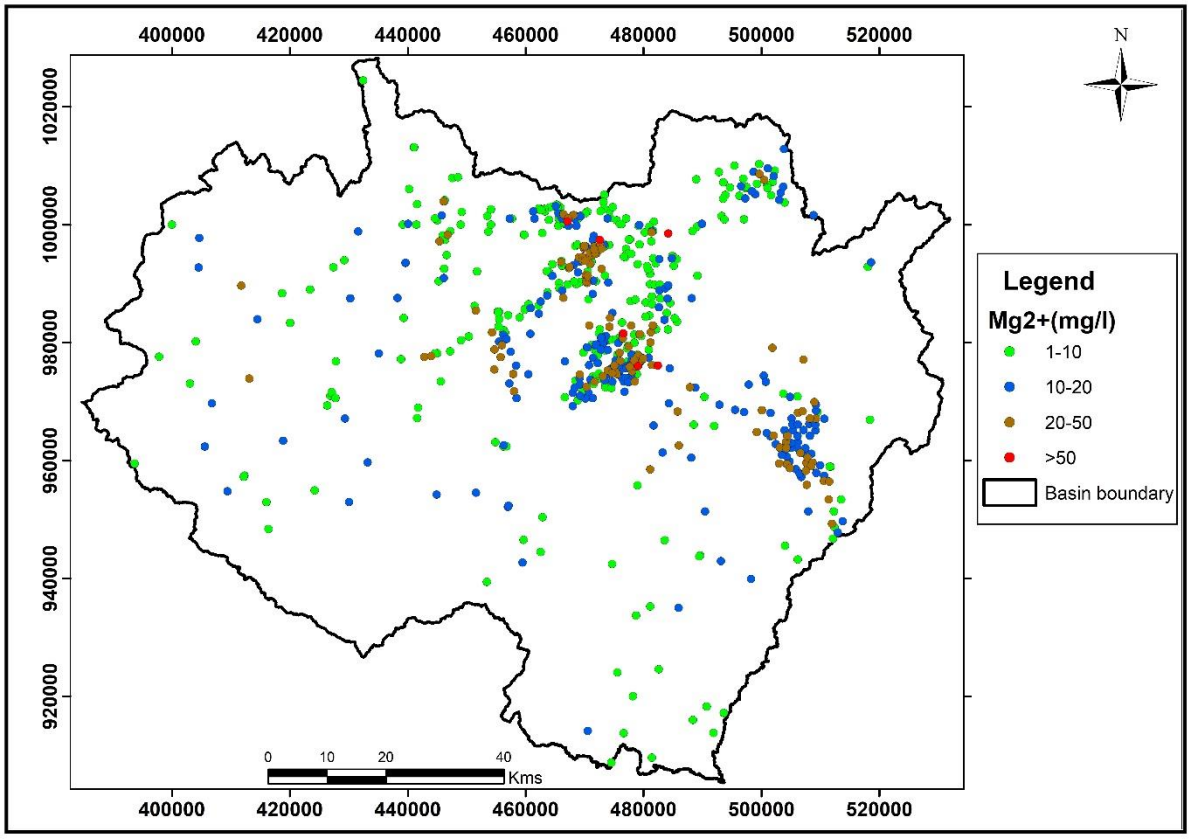

Figure 6. 10: Spatial Variation of Magnesium-ion in Groundwater

Temporal Variation of Magnesium-ion in Groundwater

Magnesium ion is the third highly concentrated ion in groundwater in the Upper Awash Sub-Basin. In Akaki wellfield, Magnesium ion showed temporal variation (23mg/l to 49mg/l) from measurements taken between 1996 and 2014. In Chefedonsa and Mojo Slaughter well, magnesium ion concentration is higher with a slight temporal variation. Generally, Magnesium ion concentration in groundwater samples is higher in Debrezeit and Mojo areas in Upper Awash Sub-Basin. In general, there is no significant temporal magnesium ion variation recorded from the monitoring wells rather the spatial variation is more pronounced. In some wells, the concentration of magnesium ions is temporarily decreasing or fluctuating. Since the main source of magnesium ions in groundwater is from rock-water interaction, the residence time of groundwater in the area affects the concentration of magnesium ions over time.

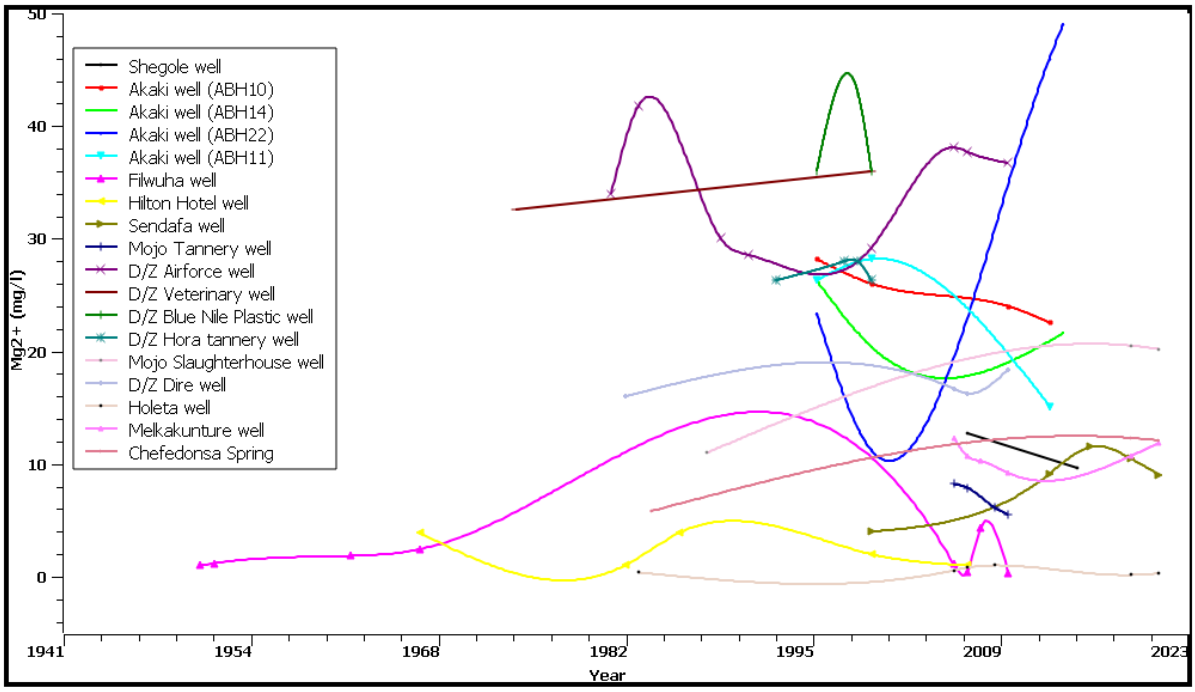

Figure 6. 11: Temporal Variation of Magnesium-ion in Groundwater

Spatial Variation of Potassium-ion in Groundwater

From the major cations, potassium is the least in groundwater. Most groundwater in the Upper Awash Sub-Basin has a lower potassium concentration (<20mg/l). In some areas including Debrezeit, Debregenet, and Addis Ababa, the concentration of potassium is higher than 20mg/l. The highest potassium ion concentration in groundwater is observed in Filwuha thermal groundwater having 65mg/l. There is no health-based guideline value proposed by the World Health Organization for potassium in drinking water. However, the Ethiopian Standards Agency set a maximum permissible limit of potassium in drinking water as 1.5mg/l.

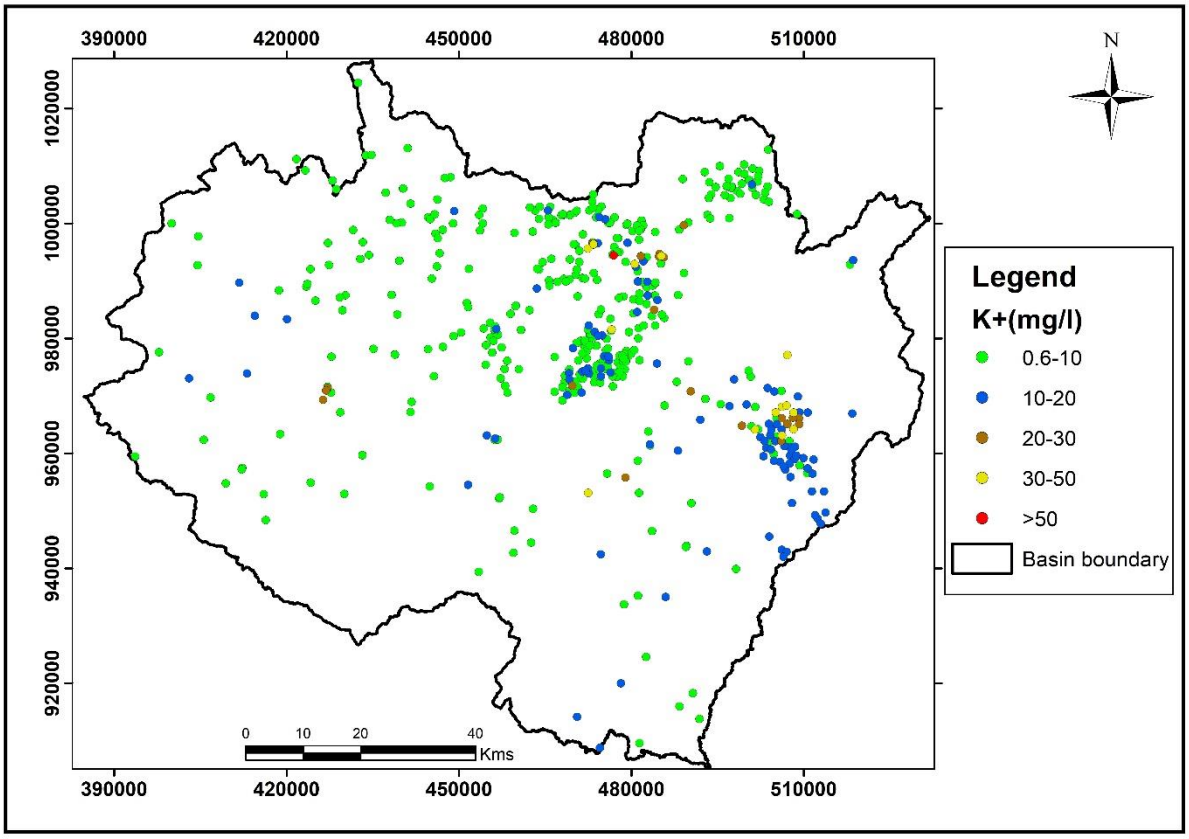

Figure 6. 12: Spatial Variation of Potassium-ion in Groundwater

Temporal Variation of Potassium-ion in Groundwater

Potassium ion is lower in concentration compared to the above three ions. In the same way as the other ions listed above, the highest temporal potassium ion variation is attributed to Filwuha thermal groundwater which varies from 3.1mg/l in 1951 to 22.7mg/l in 2007. In Sendafa well, Potassium ion concentration monitoring showed that it was 1.3mg/l in 2000 and 9.4mg/l in 2021. At Holeta groundwater the variation was 1.01mg/l (1983) and at the present analysis in 2021 its concentration raised to 9.5mg/l. Spring-water in Chefedonsa showed a slight variation in the last thirty-eight years (1984-2021) from 1.8mg/l to 13.43mg/l respectively. In general, from most monitoring stations, Potassium ion concentration is stable with minimal increase or decrease (minimum fluctuation over time). The temporal variation of potassium is influenced by the length of time for the water-rock interaction.

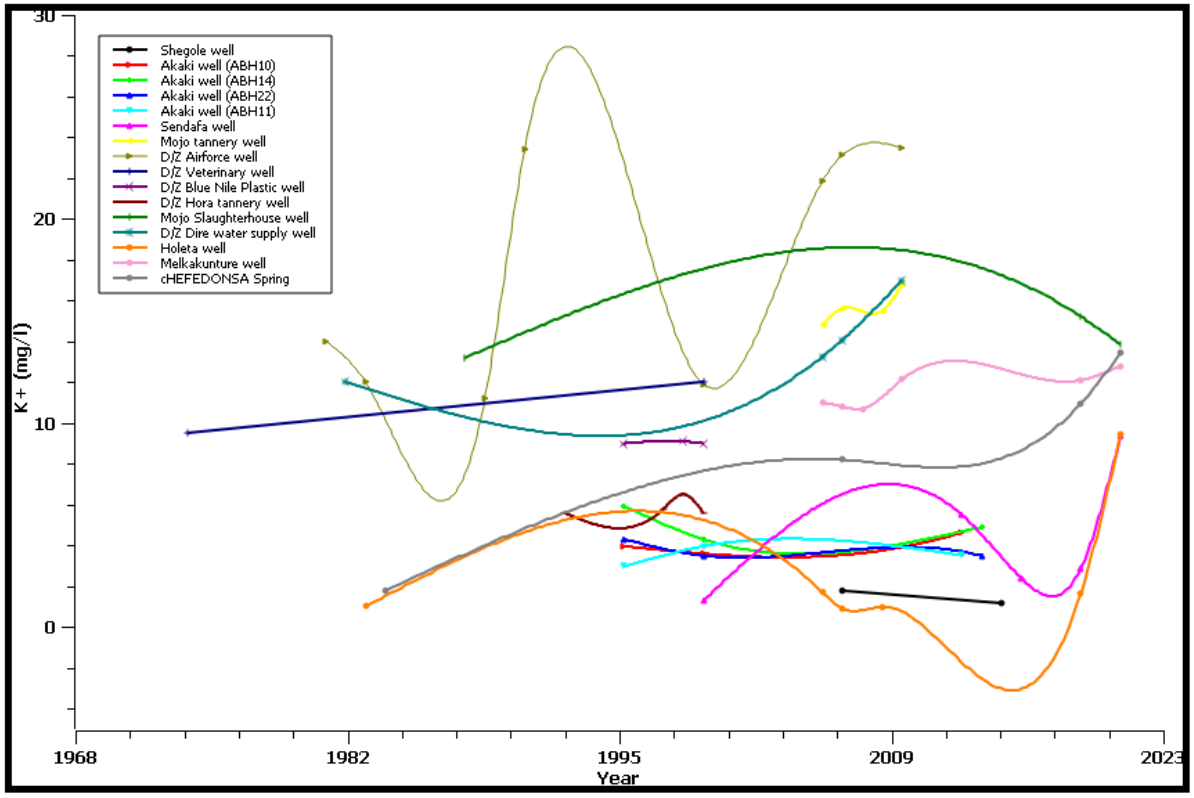

Figure 6. 13: Temporal Variation of Potassium-ion in Groundwater

Spatial Variation of Bicarbonate (HCO_3^-) in Groundwater

Bicarbonate is the most abundant anion in groundwater within the study area. The high bicarbonate concentration and its variation over time are due to the high rate of carbon dioxide outgassing from thermal aquifers like Filwuha, and in most parts of the area, it is the result of the reaction between dissolved carbon dioxide with the rocks to produce bicarbonate and clay or mica.

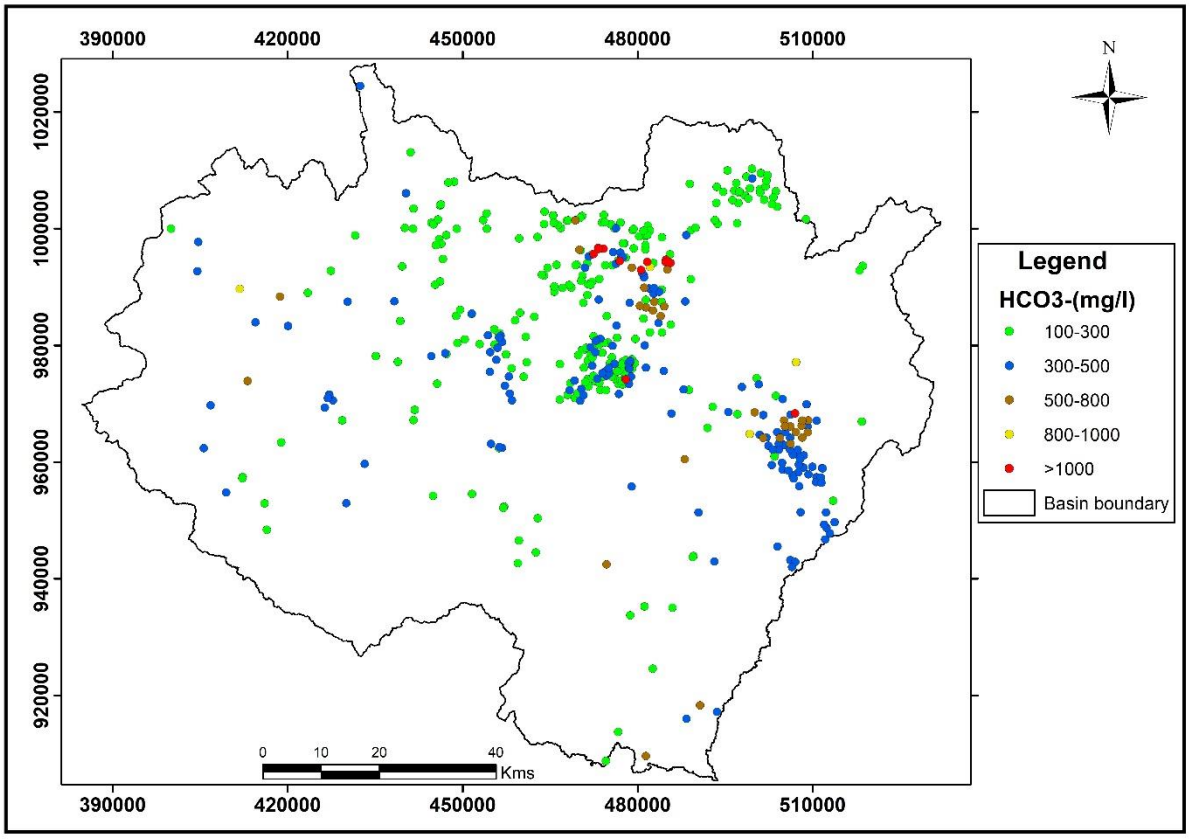

Figure 6. 14: Spatial Variation of Bicarbonate in Groundwater

Temporal Variation of Bicarbonate (HCO_3^-) in Groundwater

The Filwuha wells are characterized by a higher concentration of bicarbonate with a higher temporal variation. In Addition to Filwuha thermal wells, groundwater samples from Sendafa, Holeta, Mojo, Chefedonsa, and Melkakunture wells show temporal and spatial variation of bicarbonate ion.

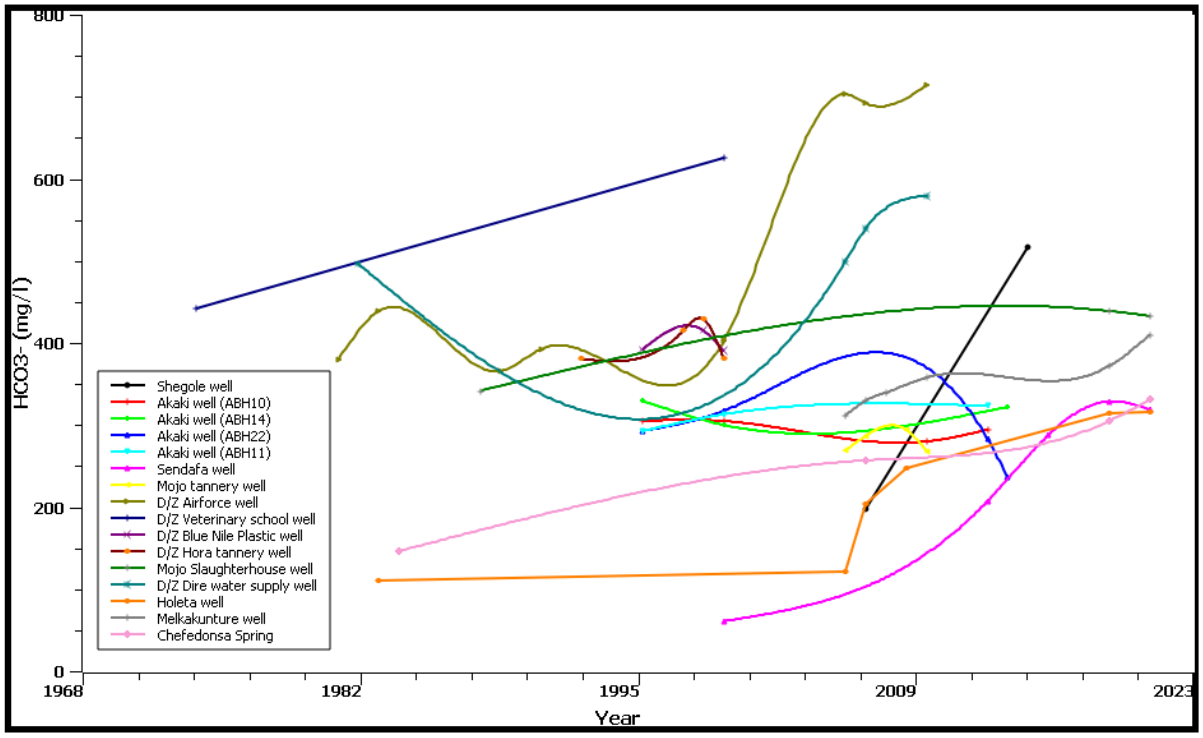

Figure 6. 15: Temporal Variation of Bicarbonate in Groundwater

Spatial Variation of Chloride in Groundwater

Chloride is one of the anions that depict the anthropogenic influences on water bodies. Based on the anion evolution sequence forwarded by Chebotarev (1955) chloride concentration in the discharge area becomes the dominant anion. However, high chloride concentration in recharge areas indicates its anthropogenic source. Chloride concentration in the Upper Awash groundwater is not that much higher but there is some implication in the increasing effects of anthropogenic factors on groundwater. Water samples from shallow, unprotected wells may occasionally exhibit elevated Cl^- ion concentrations due to surface pollution. However, a higher concentration of Cl^- in deep wells in volcanic aquifers is either from Obsidians or ion stagnation and retardation due to its enormous ionic size at fault gauges at regional faults or fluids circulating through deep-seated sedimentary rocks.

The major anion in water type classification is the bicarbonate but some water types incorporate chloride extension. Anthropogenic influences are manifested by the higher concentration of chloride from water samples taken in the city and towns as shown in the map below.

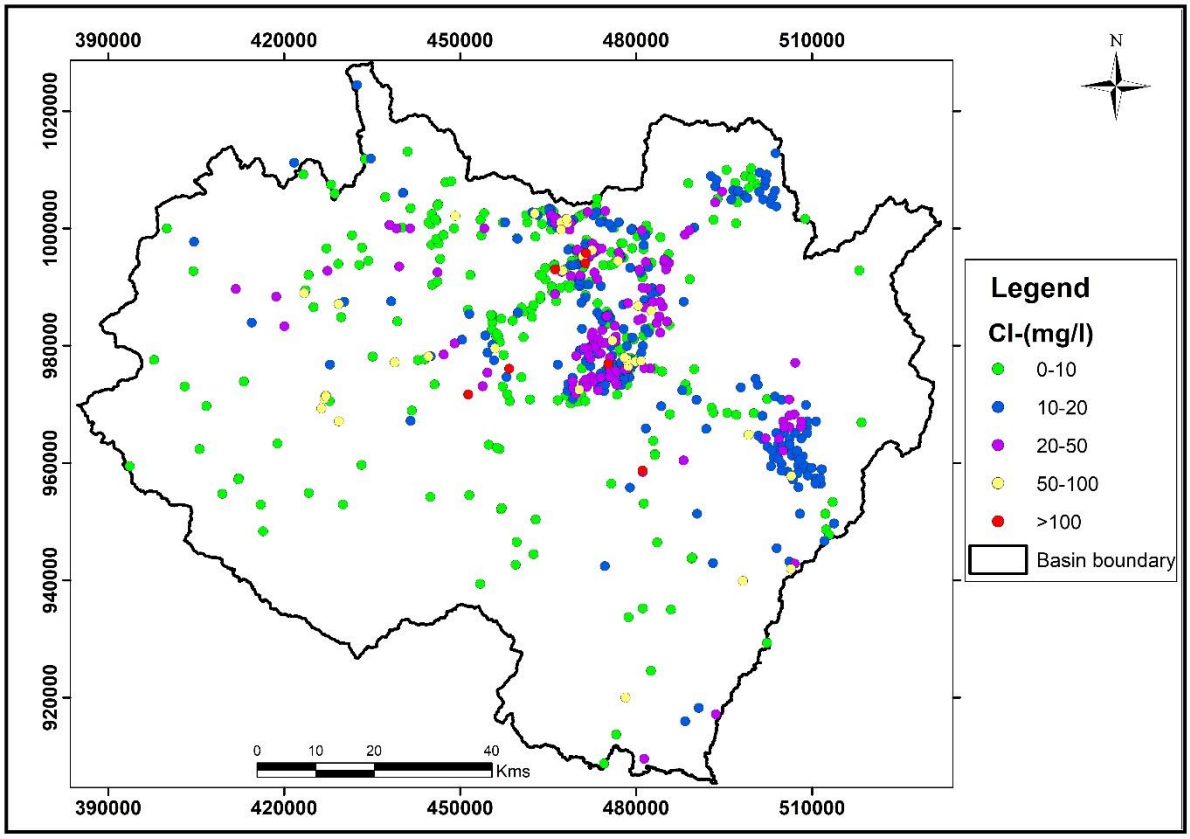

Figure 6. 16: Spatial Variation of Chloride in Groundwater

Temporal Variation of Chloride in Groundwater

Chloride is the other anion that shows spatial and temporal variation. Groundwater samples from Filwuha and Hilton Hotel wells show temporal variation of chloride concentration from 16.3mg/l to 36.9mg/l (1951-2010); in Hilton Hotel well it has increased from 0.05mg/l to 31.3mg/l in between 1967 and 2010. In addition to Filwuha wells, temporal variation of chloride concentration was recorded in Debrezeit wells such as in Debrezeit Airforce well it has increased from 9mg/l to 73.4mg/l (1981-2010); in Blue Nile plastic factory well it has increased from 14mg/l in 1982 to 21mg/l in 2010. The concentration of chloride at the Holeta water supply well in 1983 was 4mg/l, and after thirty-eight years in 2021, it has increased to 14mg/l; at Shegole well it has increased from 7.9mg/l in 2007 to 16.9mg/l in 2015 measurement.

Despite its simple variation, there is no abrupt change in chloride ions in Upper Awash Sub-Basin.

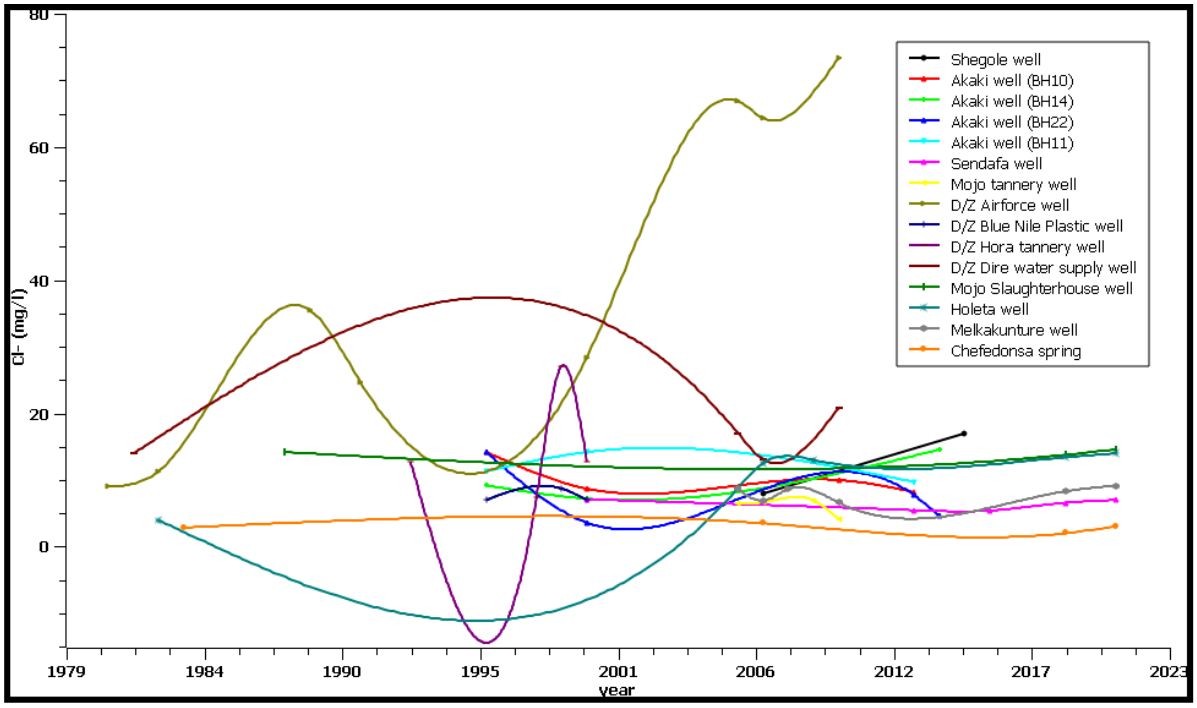

Figure 6. 17: Temporal Variation of Chloride in Groundwater

Spatial Variation of Sulfate in Groundwater

Sulfate ion in the Upper Awash groundwater is generally low. In most of the recharge areas of Entoto, Sendafa, Holeta, and the western Guraghe highlands, sulfate concentration in the groundwater is low. In areas that are highly dominated by sedimentary rocks such as gypsum, sulfate ion in such environments may be originated from the interaction of water and gypsum.

However, in areas like the Upper Awash Sub-Basin where there are no such rocks, sulfate ions in groundwater are mostly originated from anthropogenic influences including agricultural fertilizers, and industrial effluents. As shown from the distribution map, sulfate ions in groundwater with concentrations higher than 30mg/l are observed in Addis Ababa, Akaki Beseka, Debrezeit, Koka, Debregenet, and other central farmland areas. However higher concentration of SO_4^{2-} ion in groundwater close to the water divide between the Upper Awash Sub-Basin and the Blue Nile basin may be due to gypsum intercalation in deep-seated limestone and sandstone units (Tilahun Azagegn, 2014).

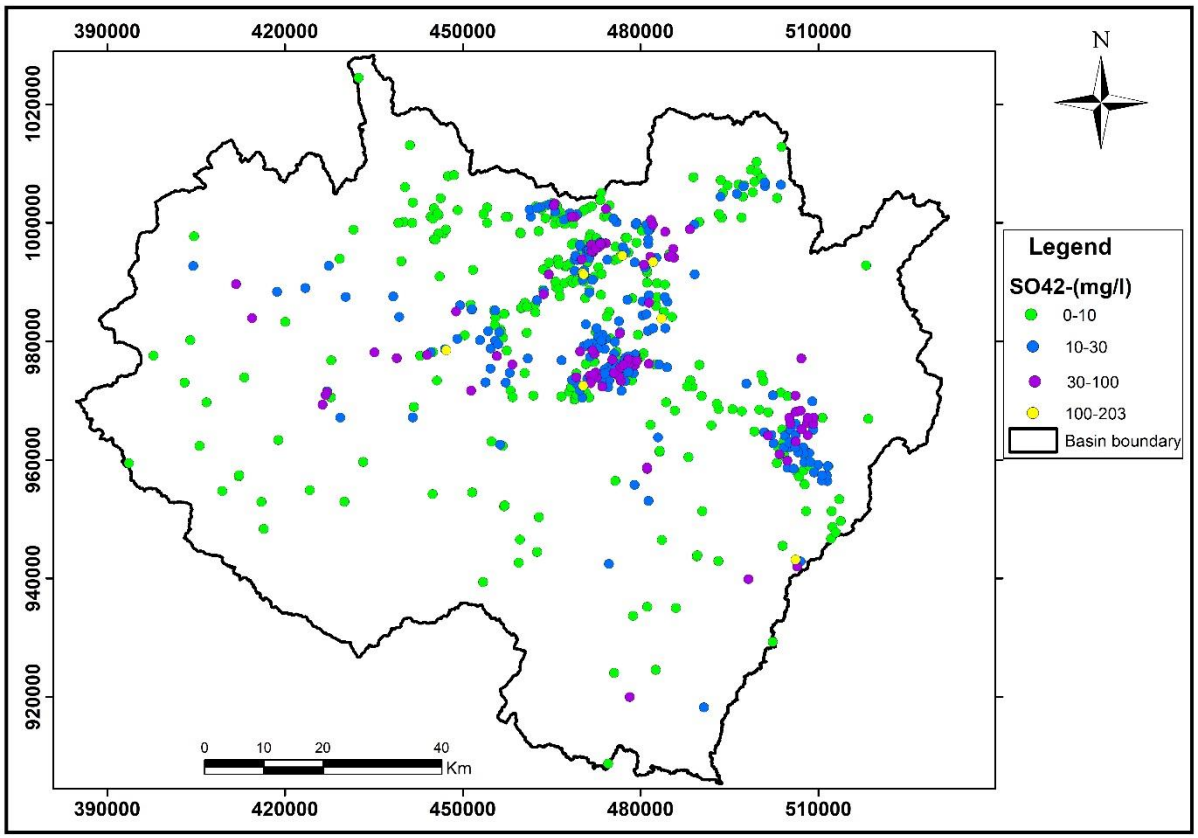

Figure 6. 18: Spatial Variation of Sulfate in Groundwater

Temporal Variation of Sulfate in Groundwater

Even though the concentration of sulfate in most groundwater samples is low, in some areas it is higher and the water type contains sulfate as an anion constituent. Sulfate concentration in Shegole well groundwater in 2007 was almost nil but after eight years in 2015, it has increased to 30mg/l. sulfate ion in one of the Akaki well groundwater was 7.4mg/l in 1996, and after seventeen years in 2013, it has increased to 28.3mg/l. The highest sulfate ion concentration in groundwater with slight temporal variation is observed in Filwuha thermal water due to the sulfur dioxide outgassing along the fault zone. The availability of high sulfur dioxide in the thermal water results in high sulfate ions in groundwater found in the area. In other wells including Chefedonsa spring, Holeta water supply well, Mojo slaughterhouse well, Hora tannery well, Blue Nile plastic factory well, Debrezeit Veterinary school well, and Debrezeit Airforce wells, sulfate in groundwater show slight increment with time but almost very low. The health-based guideline value for sulfate in drinking water is 250mg/l (WHO, 2011). All water samples in the Upper Awash Sub-Basin show that sulfate is lower than the standard value and the water is suitable for drinking.

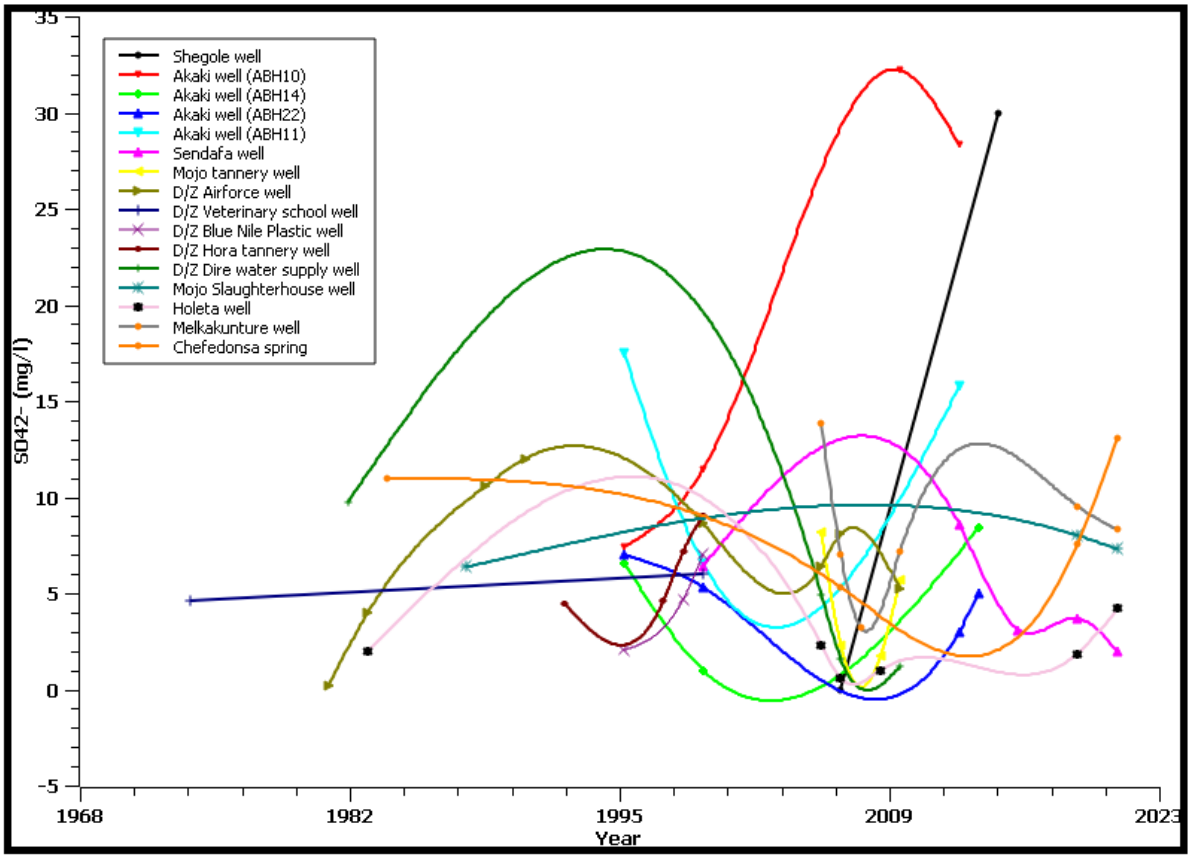

Figure 6. 19: Temporal Variation of Sulfate in Groundwater

Trace Metal Variation in Groundwater

From trace metal analysis, Cadmium and Chromium concentrations are very low with less than 0.002mg/l and 0.0012mg/l respectively. In addition to Cadmium, Iron, Manganese, Lead, and Zinc concentrations were analyzed. Iron concentration in Mojo slaughterhouse shows slight variation from two years measurement. Even though there are no health-based effects, Iron concentration above 0.3mg/l may stain plumbing fixtures and laundry. Iron concentration in Mojo slaughterhouse well has changed from 0.6mg/l to 0.8mg/l within two years as shown in the table. The concentration of Iron is changing through time as identified from Holeta, Sendafa, and Melkakunture areas.

Manganese concentration from all monitoring stations showed a slight increase from 2019 to 2021. Manganese is present in these groundwater sources below the guideline value set by WHO (0.4mg/l). On the other hand, the concentration of Lead from these monitoring stations is a bit higher than the acceptable range and shows increment with time. In the same way as Lead, Zinc is also showing increments from all monitoring stations. There is no health-based restriction for Zinc in drinking water. However, Zinc concentrations beyond 3 mg/l in drinking

water may be unacceptable by consumers. Despite its variation, Zinc concentration is even lower than its undesirable astringent taste threshold limit.

Table 6. 1: Temporal variation of trace metals in selected groundwater wells (BDL = Below Detection Limit)

Locality	Mojo		Holeta		Sendafa		Melkakunture	
SampleID	GW01		GW02		GW03		GW04	
Year	2019	2021	2019	2021	2019	2021	2019	2021
Fe (mg/l)	0.598	0.815	0.538	0.792	0.212	0.319	0.160	0.295
Mn (mg/l)	0.014	0.039	0.011	0.036	0.014	0.048	0.020	0.046
Cd (mg/l)	BDL	BDL	BDL	BDL	BDL	BDL	BDL	BDL
Pb (mg/l)	0.026	0.057	0.022	0.028	0.024	0.050	0.022	0.060
Cr (mg/l)	BDL	BDL	BDL	BDL	BDL	BDL	BDL	BDL
Zn (mg/l)	0.609	0.954	0.663	0.765	0.855	1.790	0.853	1.503

6.3. Surface-water Hydrochemistry of Upper Awash Sub-Basin

The spatial and temporal hydrochemical variation of surface-water samples were also studied. The hydrochemical variation of water supply reservoirs (Legedadi, Gefersa, and Dire lakes), Lake Abasamuel, Lake Koka and Bishoftu crater lakes, and River water samples from Mojo River upstream and at Koka inlet, Awash River at Melkakunture, Legetafo, and Holeta rivers were analyzed and the temporal hydrochemical variation was observed.

6.3.1. Temporal Variation of TDS and EC in River Water

Rivers flowing away from anthropogenic contaminant sources are safer and have stable hydrochemistry as observed from the study. River water samples taken from Awash River at Melkakunture and Holeta rivers have relatively stable TDS and EC values. The hydrochemistry of the Melkakunture River was analyzed six times in the last fifteen years (2006-2021). The maximum TDS from Awash River at Melkakunture was observed in 2019 (270mg/l) and the corresponding electrical conductivity was 540µS/cm. From 2006 onwards, the total dissolved solids, and electrical conductivity in the river show a slight increase and decrease without any significant variation over time. However other rivers like Mojo and Akaki Rivers show a significant variation of total dissolved solids and electrical conductivity through time. These rivers are vulnerable to anthropogenic influences like industrial and domestic wastes. The TDS in Mojo River increased from 310mg/l to 730mg/l in the last seventeen years (2004 to 2021) and correspondingly the electrical conductivity also increased from 620µS/cm to 1460µS/cm in the given periods. These parameters were slightly reduced downward to Lake Koka (480mg/l and 950µS/cm) due to freshwater mixing from tributaries and increasing distance from the

sources affecting its quality.

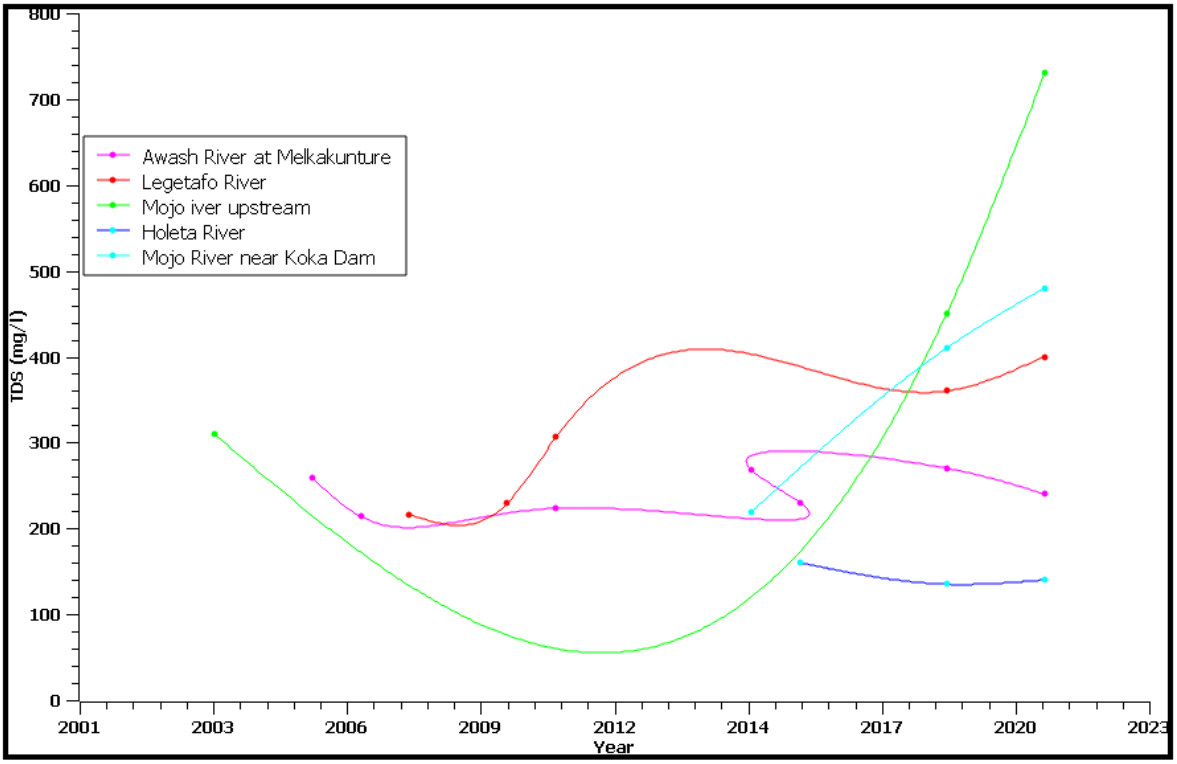

Figure 6. 20: Temporal Variation of TDS in River Water

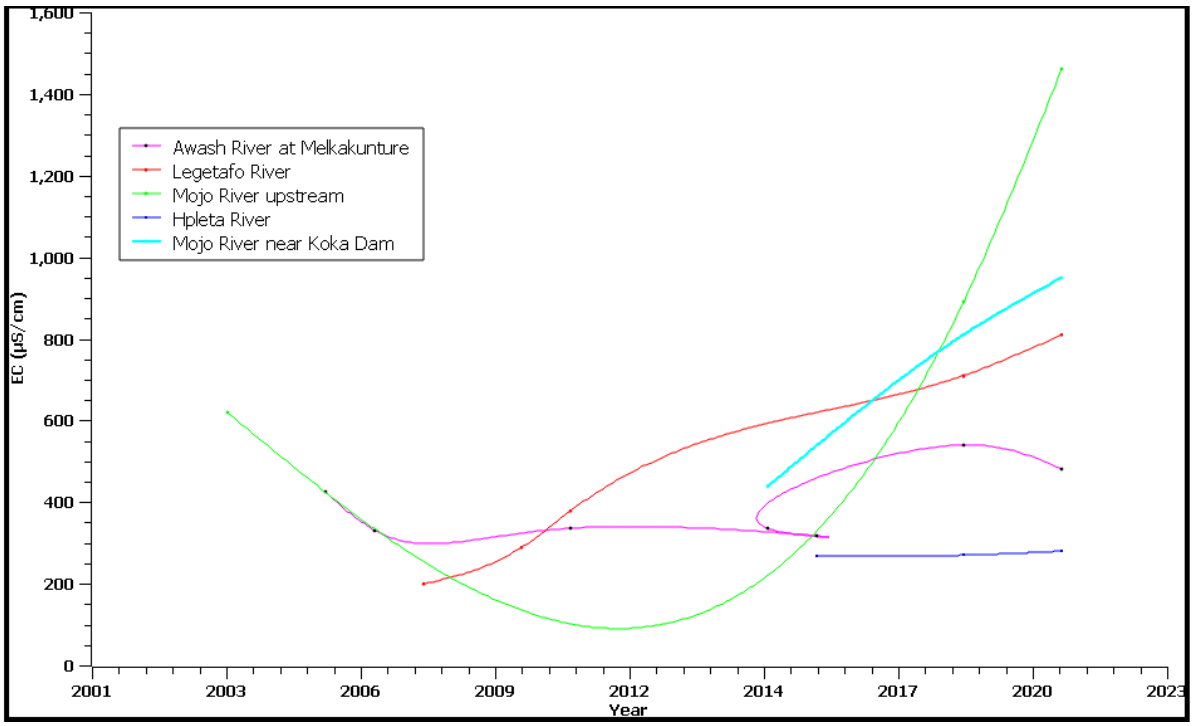

Figure 6. 21: Temporal Variation of Electrical Conductivity in Rivers

6.3.2. Major-ion Variation in the Upper Awash Rivers

The highland rivers in recharge areas are characterized by high calcium ion concentrations. Rivers that are close to the rift axis (Mojo River upstream and near Koka Dam in this case) are characterized by higher sodium ion concentrations. The temporal variation of calcium and sodium ions in River water is a bit higher than the variation in groundwater. According to Water Works Design and Supervision Enterprise (2008), sodium ion concentration at Legetafo River was 8mg/l, and in the present study, it has increased to 64mg/l. In the same way, sodium ion in the Holeta River has increased from 10.6mg/l to 75.8mg/l (2016 to 2021). As stated by the WWDSE, the concentration of sodium ion at Awash River around Melkakunture in 2006 was about 33.8mg/l, and in this study, it has increased to 86.3mg/l in 2021.

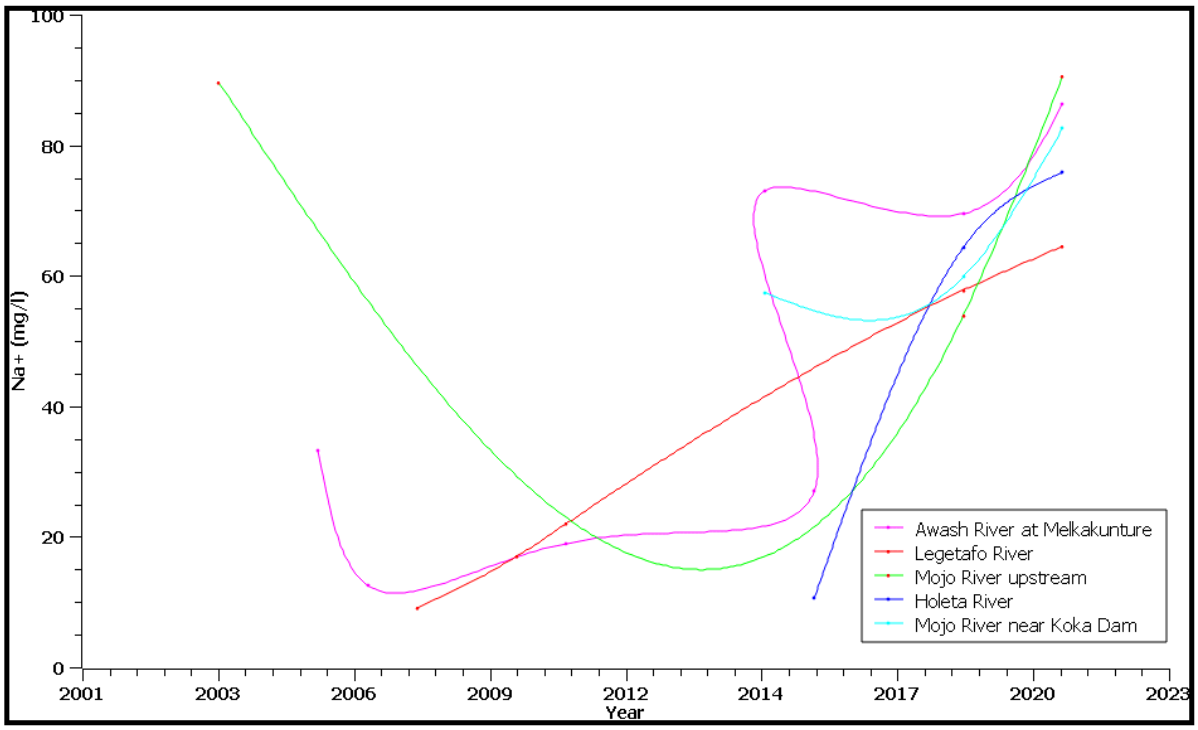

Figure 6. 22: Temporal Variation of Sodium-ion in Rivers

Calcium ion concentration at Legetafo River was about 14mg/l (WWDSE, 2008) and in 2021 (present study), it has increased to 42.3mg/l. In 2006, calcium ion in Awash River at Melkakunture was 51.4mg/l and within fifteen years duration (till 2021) the concentration has increased to 134.8mg/l. Mojo River sampled near Koka Dam also showed an increase in calcium ion concentration from 16.3mg/l to 56.8mg/l (2015 to 2021). At Holeta River, the concentration of calcium was 36mg/l (Kidist Hailu, 2016), and in the present analysis, it has increased to 72mg/l.

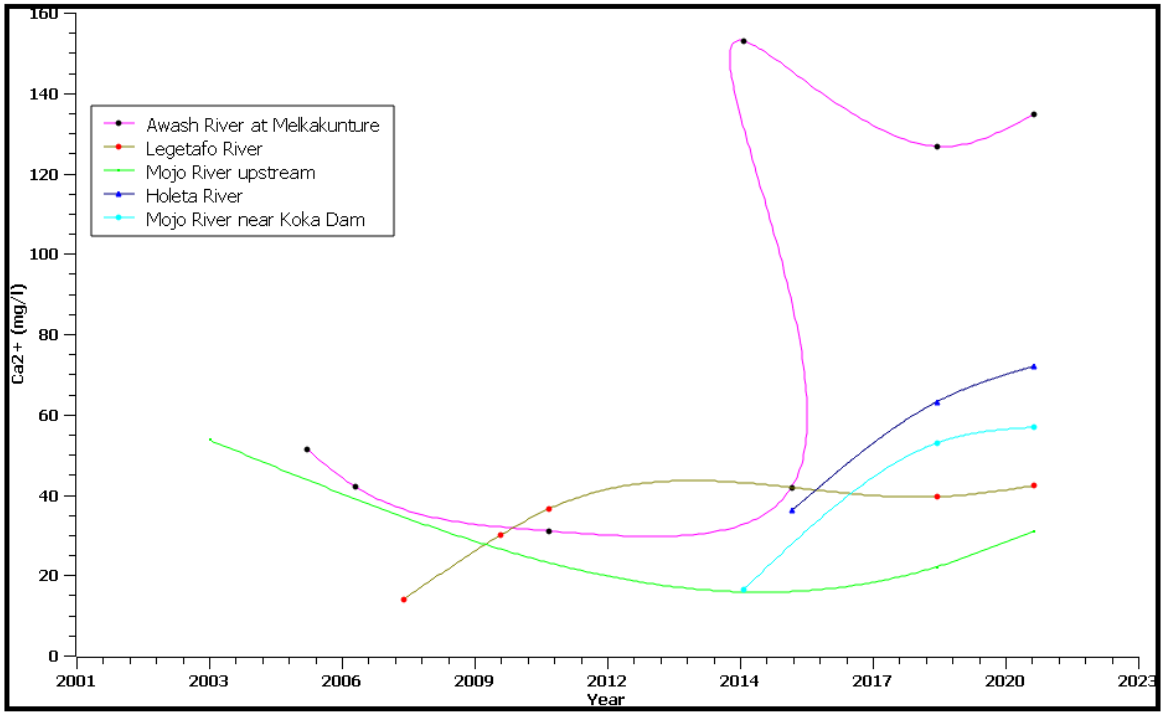

Figure 6. 23: Temporal Variation of Calcium-ion in River Waters

Heavy metal analysis of reservoirs and Rivers was conducted to understand the spatial and temporal variation.

River water samples are higher in total iron content than any other water bodies since rivers are more vulnerable to nearby anthropogenic sources. Within two years, the total Iron concentration at Mojo River near Koka reservoir increased from 1.99mg/l to 3.13mg/l. In all sampling sites, total Iron has increased within two years duration as shown in the table below. Even though it is low in concentration, a slight increment of Manganese was identified from all river water samples. Cadmium and Chromium are still below detection limits. As usual Lead and Zinc are a bit higher in concentration than other heavy metals.

Table 6. 2: Temporal variation of trace metals in river waters

Locality	Mojo River near Koka Dam				Mojo River Upstream		Holeta River		Legetafo River		Awash at Melkakunture		
SampleID	RW01				RW02		RW03		RW04		RW05		
Year	2009	2018	2019	2021	2019	2021	2019	2021	2019	2021	2009	2019	2021
Fe_tot (mg/l)			1.993	3.129	1.303	2.193	0.956	2.354	1.204	1.625		0.821	1.322
Mn2+ (mg/l)			0.022	0.068	0.026	0.033	0.024	0.060	0.017	0.050		0.020	0.025
Cd (mg/l)	0.066	BDL	BDL	BDL	BDL	BDL	BDL	BDL	BDL	BDL	0.031	BDL	BDL
Cr (mg/l)		BDL	BDL	BDL	BDL	BDL	BDL	BDL	BDL	BDL		BDL	BDL
Pb (mg/l)	5.062	0.001	0.026	0.079	0.024	0.088	0.020	0.033	0.020	0.035	1.320	0.023	0.044
Zn (mg/l)	0.150	0.080	1.158	1.471	1.150	1.955	0.755	1.258	0.755	1.739	0.089	0.660	1.463

6.3.3. Temporal Variation of TDS and EC in Lakes

The TDS and EC of the Gefersa reservoir were measured in 1982, 2010, 2019, and 2021. The

TDS has increased from 30mg/l (in 1982) to 50mg/l (in 2021) and the electrical conductivity has increased from 65µS/cm to 100µS/cm within the same time interval mentioned above. Legedadi reservoir has more or less stable TDS and EC values from 1982 to 2021 measurements and there is no significant variation of these parameters despite their fluctuation over time. On the other hand, Lake Abasamuel is fed from the Akaki River flowing across the capital city shows the temporal variation of the total dissolved solids and electrical conductivity as observed in 24 years measurement gap (1997-2021). The TDS in Lake Abasamuel has increased from 337mg/l to 530mg/l, and the EC has increased from 506µS/cm to 1060µS/cm. The total dissolved solids and electrical conductivity measurements at Lake Hora in Debrezeit from 1998 to 2011 showed a higher variation of both parameters in which the TDS has increased from 1366.4mg/l to 4349mg/l, and the Electrical conductivity has increased from 2240µS/cm to 6220µS/cm. Within the same time as Lake Hora, the total dissolved solids in Lake Bishoftu Guda have increased from 507mg/l to 772mg/l, and the corresponding electrical conductivity has increased from 831µS/cm to 1265µS/cm.

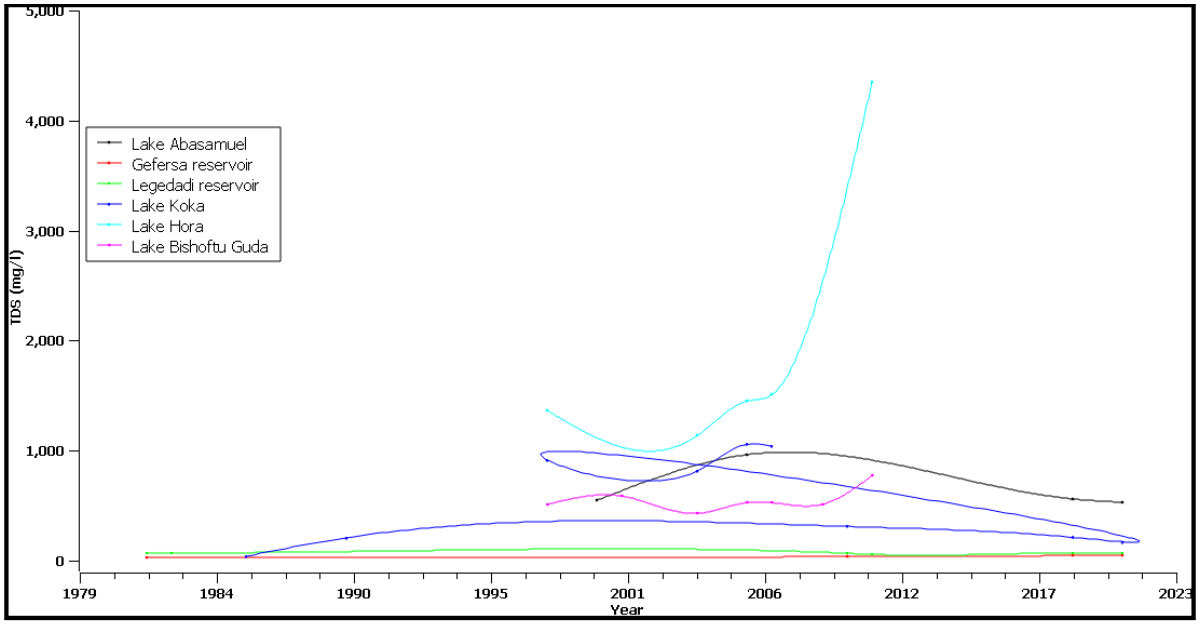

Figure 6. 24: Temporal Variation of TDS in Lakes

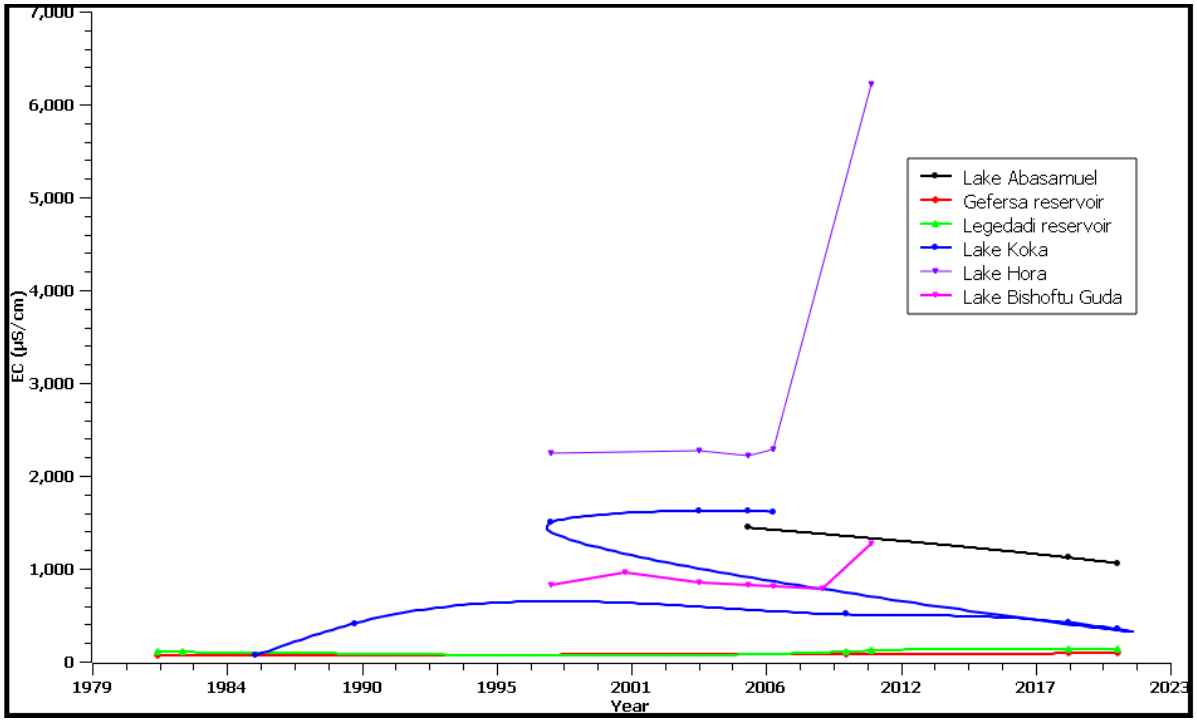

Figure 6. 25: Temporal Variation of EC in Lakes

6.3.4. Major-ion Variation of Lakes

Temporal Variation of Sodium-ion

Sodium-ion in lakes is high with a higher temporal variation. In 1997, EPA stated that the concentration of sodium ion in Lake Abasamuel was 12.6mg/l, and in the present analysis, it has increased to 99mg/l. Gefersa reservoir on the other hand shows a slightly decreasing sodium ion. Sodium-ion concentration at Lake Koka was 21.5mg/l in 1986, and after thirty-five years in 2021, it has increased to 60.13mg/l. The higher sodium ion variation with higher sodium ion variation is observed from Debrezeit crater lakes. In Lake Hora Hoda, sodium ion concentration in 1963 was 1540mg/l, and after 44 years of measurement in 2007, it has decreased to 1244mg/l. From Lake Bishoftu Guda in Debrezeit sodium ion has slightly increased from 126.5mg/l to 150mg/l (1963 to 2011). However, in other Lakes sodium ions fluctuates over time. The difference in the sodium ion in these lakes is mainly attributed to the rate of evaporative concentration (Seifu Kebede, 1999). In general, reservoirs found around Addis Ababa do not show significant ionic variation other than fluctuating over time.

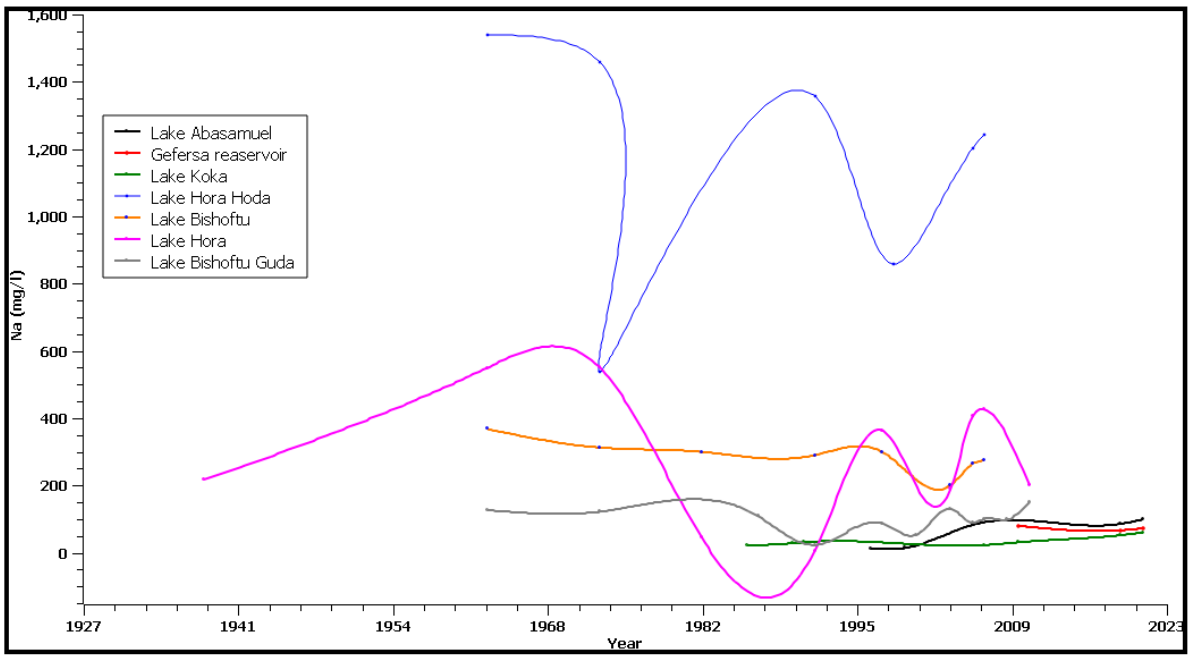

Figure 6. 26: Temporal Variation of Sodium-ion in Lakes

Temporal Variation of Calcium-ion in Lakes

Except in a few wells, calcium ions from Lakes fluctuate over time as shown in the graph. In Lake Abasamuel, the concentration of calcium was 30mg/l in 1997, and it has increased to 84mg/l in the present analysis. In Gefersa reservoir, it has increased from 8mg/l to 34.6mg/l (1982 to 2021); 9mg/l to 24.7mg/l in Legedadi reservoir (2011 to 2021).

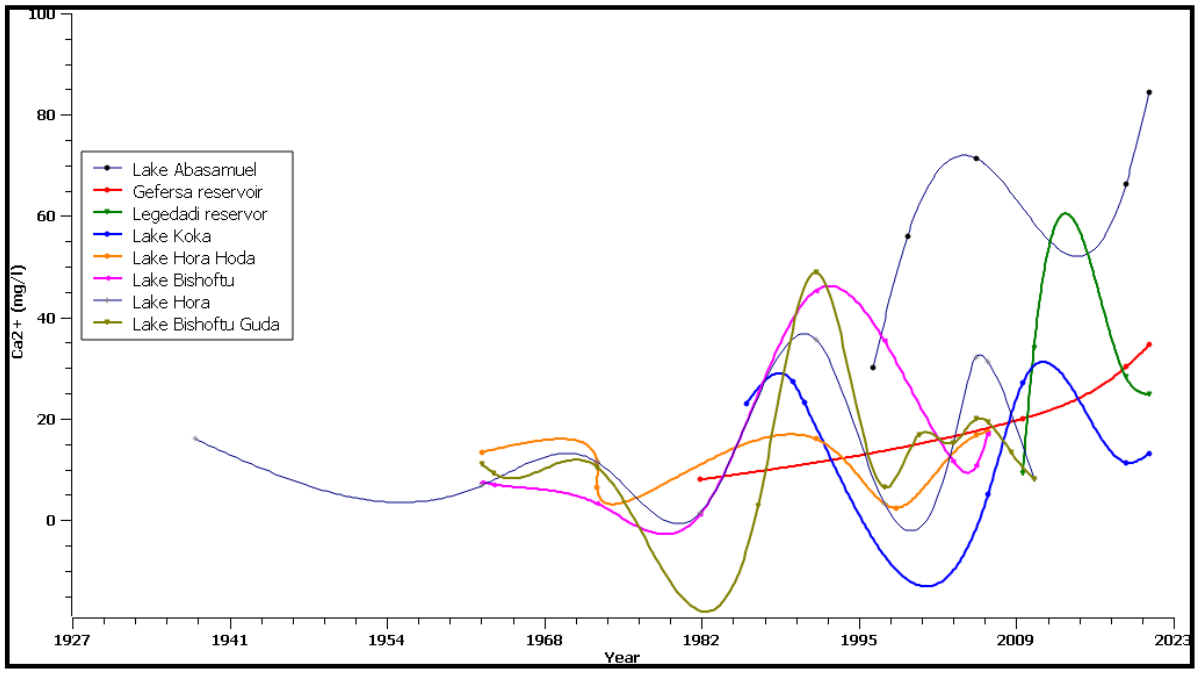

Figure 6. 27: Temporal Variation of Calcium-ion in Lakes

Temporal Variation of Chloride in Lakes

Chloride concentration in most of the lakes is almost stable. A slight increase in chloride ion is observed in Lake Hora in Debrezeit which has increased from 177mg/l to 610mg/l (1938 to 2011) due to the evaporative concentration.

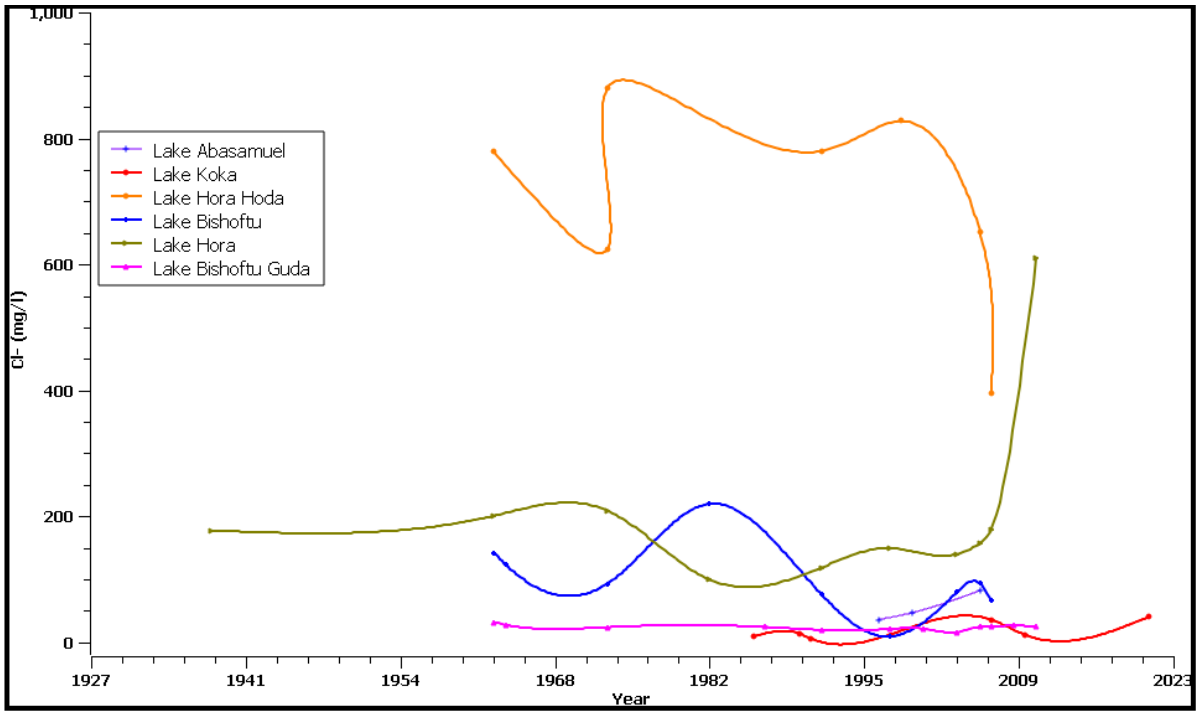

Figure 6. 28: Temporal Variation of Chloride in Lakes

The fluoride concentration is extremely high in Bishoftu crater lakes due to the influence of acidic volcanic rocks. Chloride concentration in these lakes is relatively high owing to the effect of evaporation. Lake Bishoftu Guda is relatively low in chloride concentration due to its interaction with groundwater (inflow and outflow) that makes the lake more dilute. Nitrate concentration is relatively higher in Lake Hora with a maximum concentration of 35mg/l.

6.3.5. Trace Metal Analysis of Lakes

From trace metal analysis of Lakes, iron concentration from Koka reservoir shows little variation from two years of monitoring data. At Legedadi reservoir, the concentration of Iron was increased from 0.25mg/l to 0.71mg/l. the highest concentration of Iron was identified at Gefersa reservoir having 1.1mg/l in 2019 measurement and increased to 2.98mg/l in 2021 analysis. In Lake AbaSamuel, high Iron content was detected. Even though there is no health-based guideline value regarding Iron in drinking water, its concentration above 0.3 mg/l may stain laundry and plumbing fixtures.

Manganese analysis from the Koka reservoir shows a slight increment but is still below the permissible limit. In AbaSamuel reservoir Manganese was highest in 2004 (2.04mg/l) and the starts to decline to 0.02mg/l in the present analysis. The concentration of Manganese also increased at Gefersa, Legedadi, and Dire reservoirs as shown from the table. Concentrations above the permissible limits are detected at Legedadi and Dire reservoirs from the present analysis results. Cadmium and Chromium were also analyzed from these monitoring stations but they are below the limit of detection.

In all cases, Lead was found to be more than the threshold concentration value (0.01mg/l) set by World Health Organization. Lead analysis from Legedadi, Dire, and AbaSamuel reservoirs show increment through time most likely due to anthropogenic influences. The other heavy metal analyzed was zinc. Zinc has increased in all samples taken from these reservoirs but the concentration is lower than the taste threshold (4mg/l).

Table 6. 3: Trace metal analysis of lakes (BDL= Below Detection Limit)

Locality	Koka Dam				Legedadi Reservoir			Dire Reservoir			AbaSamuel Dam						Gefersa		
SampleID	LW01				LW02			LW03			LW04						LW05		
Year	2005	2018	2019	2021	2018	2019	2021	2018	2019	2021	1997	1998	2004	2018	2019	2021	2018	2019	2021
Fe_tot (mg/l)	_	_	0.167	0.502		0.245	0.710		0.322	0.455	_	_	_	_	0.408	1.276		1.104	2.980
Mn^{2+} (mg/l)	_	_	0.018	0.030	BDL	0.042	0.089	0.240	0.016	0.026			2.040	0.504	0.013	0.020	0.020	0.125	0.289
Cd (mg/l)	_	_	BDL	BDL	BDL	BDL	BDL	0.003	BDL	BDL			0.000	0.006	BDL	BDL	BDL	BDL	BDL
Cr (mg/l)	0.003	0.005	BDL	BDL	BDL	BDL	BDL	0.003	BDL	BDL	0.000	0.030	0.000	0.007	BDL	BDL	BDL	BDL	BDL
Pb (mg/l)	0.111	1.040	0.030	0.034		0.029	0.055	0.010	0.025	0.053	0.000	0.000	0.000	0.007	0.022	0.062	0.060	0.024	0.076
Zn(mg/l)			0.850	1.446		0.826	0.914	0.009	0.828	1.593				0.029	0.835	1.360		1.161	1.686

6.4. Water Hardness

The water hardness classification was made on 527 groundwater samples; 58 samples (11%) are classified as soft water, 132 samples (25%) are moderately hard waters, 113 samples (21%) are considered as hard water and 43% of the total groundwater samples are very hard water. Since the area is characterized by basic volcanic rocks that contain high magnesium and calcium-bearing minerals, the majority of groundwater samples (64%) are classified as hard and very hard).

Groundwater from most wells does not show temporal variation of hardness. However, in Holeta well it is changed from moderately hard to very hard (1983-2021); in Mojo Slaughterhouse it has changed from hard to very hard water (1988-2021); in Sendafa well from soft to very hard water (2000-2021), and Chefedonsa Spring the change was from moderately hard water to very hard water (1984-2021).

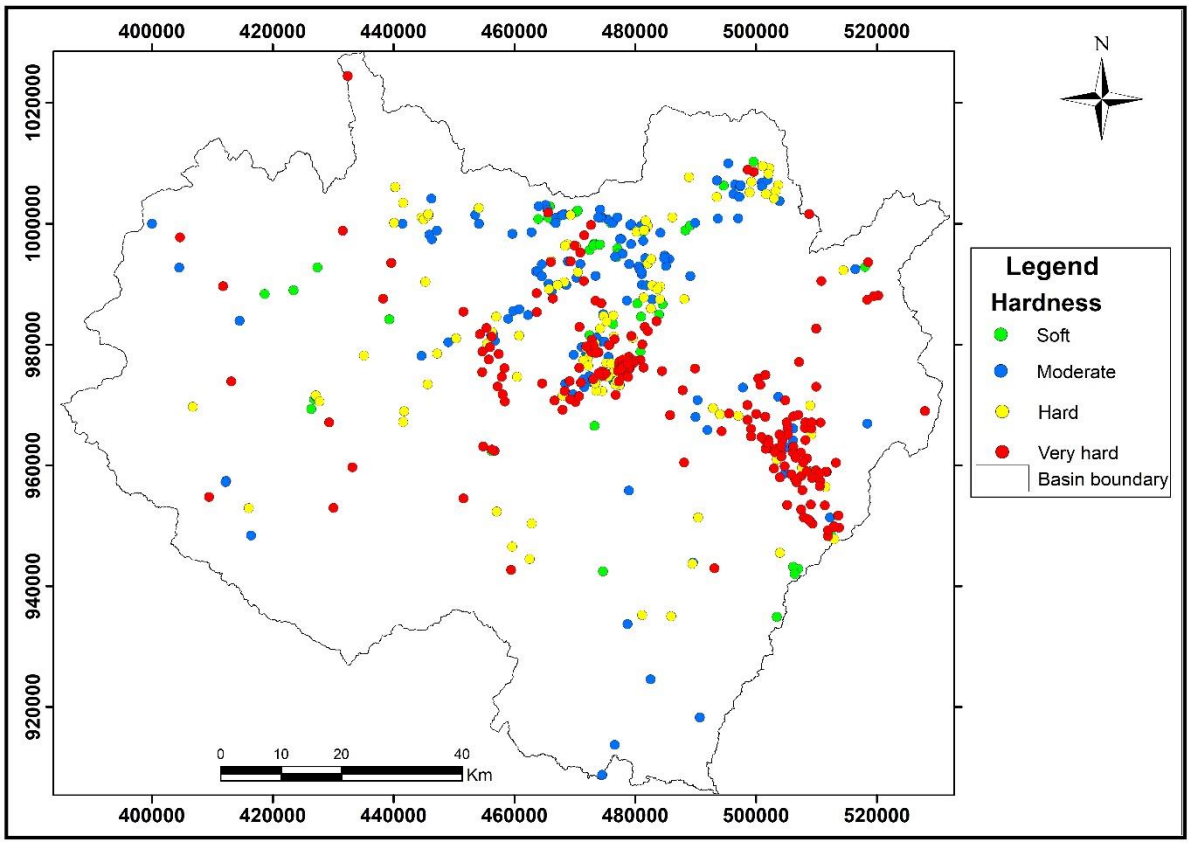

Figure 6. 29: Groundwater Hardness Classification

6.5. Groundwater Type Classification of Upper Awash Sub-Basin

Water can be classified based on the dominant major ions present in it. The ionic dominancy changes as water flow from the recharge area to the discharge area encountering various rock units. The dissolved ion concentration of water samples is mainly dependent on the lithology, regional tectonic structures as well as minor localized geological features, altitude, climatic conditions, and human activity. Consequently, the ion concentrations show significant variation throughout the area from the western plateau through the transition to the rift zone. The chemistry of groundwater does not dramatically alter along its flow path unless it comes into contact with rocks that have a completely different character. The total chemistry of groundwater at any given time and place is the consequence of dissolution, ion exchange, and precipitation processes continuing to operate. Increases in total dissolved solids and most of the major ions are common along the groundwater flow path in the saturated zone (Freeze & Cherry, 1979).

In igneous rock-dominated areas like Upper Awash, the dissolution of feldspars, micas, and other silicate minerals are greatly impacted by the chemically aggressive nature of water induced by dissolved carbon dioxide, just as it is in the chemical history of groundwater in

carbonate rocks. When CO_2-charged water with low dissolved solids come into contact with silicate minerals high in cations, aluminum, and silica, the cations and silica leach out, leaving an aluminosilicate residue with a higher Al/Si ratio. Clay minerals including kaolinite, Illite, and montmorillonite are commonly found in this residue, and Na^+, K^+, Mg^{2+}, and Ca^{2+} are the most common cations released into the water in this process (Freeze & Cherry, 1979).

In newly recharged groundwater and most probably in highland areas in Upper Awash Sub-Basin, Calcium is the dominant anion in both shallow groundwater and surface-water bodies. However deep groundwater sources in plateau areas are characterized by both calcium and sodium dominancy (Na-Ca-HCO_3 type water) with few Na-HCO_3 type water.

In the Transition and rift part of the study areas, groundwater is mostly characterized by Ca-Na-HCO_3 type water with the increasing evolution into Na-Ca-HCO_3 and Na-HCO_3 type water as we approach the rift axis. This rift-ward evolution of groundwater changes its composition and the dominant ion becomes sodium with Na-HCO_3 type water. In some areas, the anthropogenic effect, and deep circulation of groundwater increased the concentration of sulfate and chloride and that is changing the water type through time to some extent. In Akaki wellfield and some areas of Debrezeit, magnesium ion dominating water is observed in a few water samples. Water types containing chloride, sulfate, and nitrate in small amounts are found in some of Akaki wells and around the Debregenet area.

The evolution of River water is changing from calcium dominating water type (Ca-Na-HCO_3, Ca-Mg-HCO_3, Ca-Mg-Na-HCO_3, and Ca-Na-Mg-HCO_3) to sodium dominating water type (Na HCO_3 and Na-Ca-HCO_3) as we go from highland rivers to rift rivers.

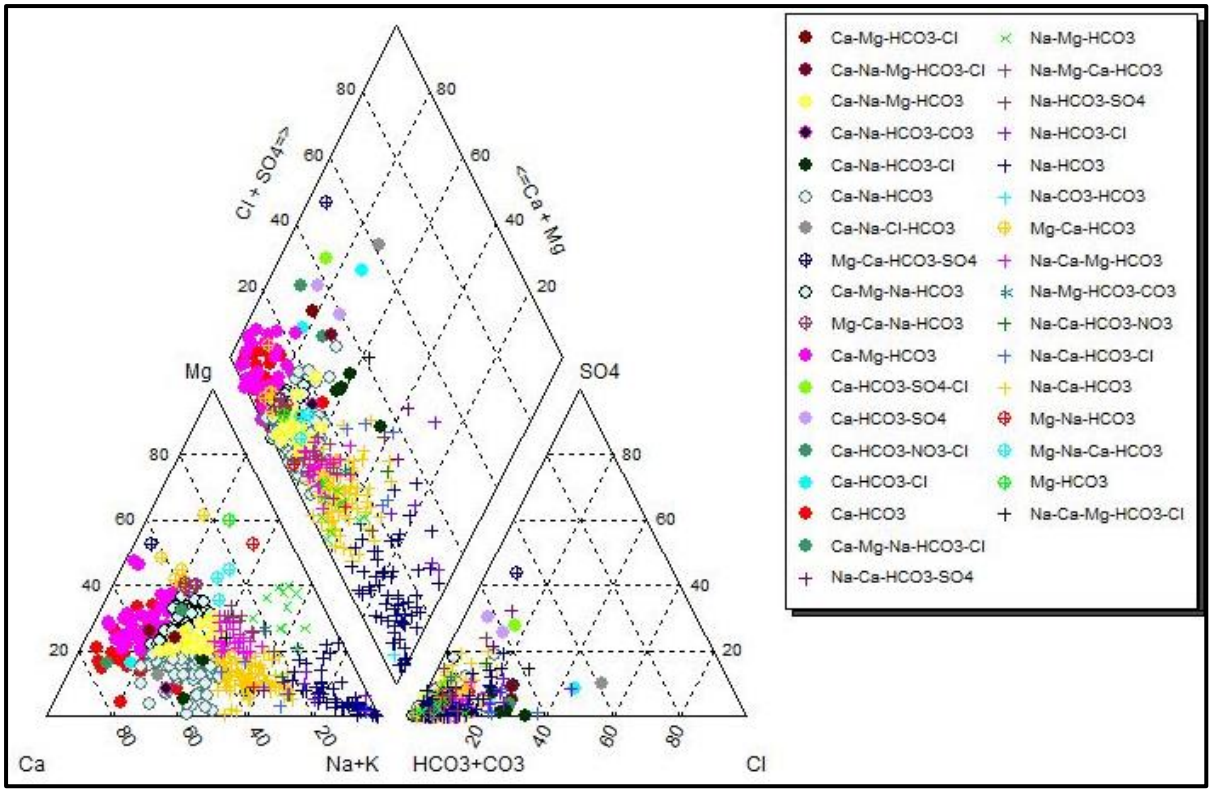

Figure 6. 30: Water Type Classification of Groundwater

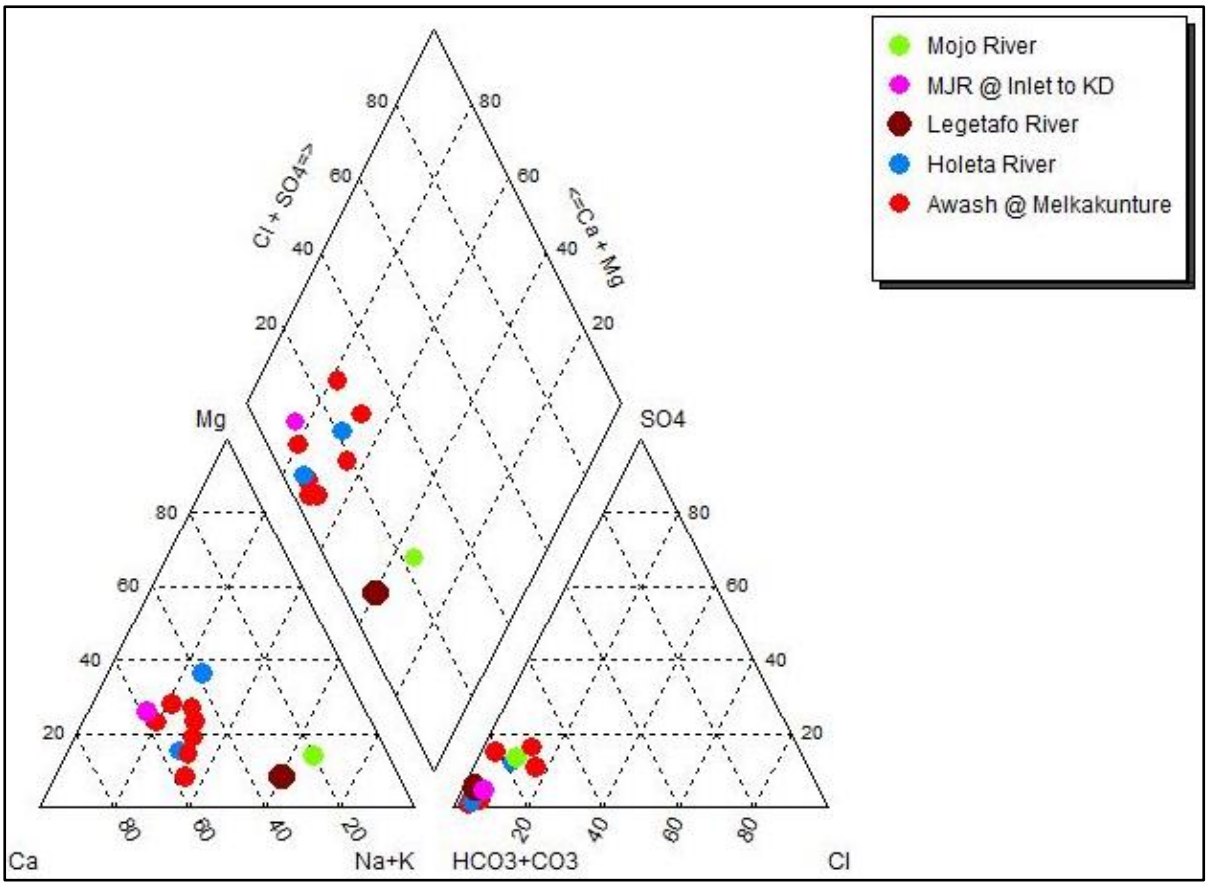

Figure 6. 31: Water Type Classification of Rivers

6.6. Water Quality

The usefulness of water for the desired purpose is determined by its chemical and biological characteristics. The physical, chemical, and biological qualities of water are necessary for every given application. Water quality monitoring provides empirical evidence for health and environmental decision-making. Water-quality requirements for various water uses, such as drinking water, irrigation, livestock watering, fisheries, leisure activities, amenities, and the preservation of river system flora and fauna, should be clearly defined. The occurrence of some ionic species in water above a certain limit may deteriorate human health and the environment. Water quality standard depends on the use of waterbody. Water designed for drinking, irrigation, industrial and aquatic life have different quality standards and these criteria are usually numerical (e.g., a precise measurement of an allowable chemical concentration, not be exceeded).

Different countries have water quality standards for the desired purpose. However, there is one general standard formulated by World Health Organization (WHO). Ethiopia has its water quality standard formulated by the Ethiopian Standards Agency in 2013.

Drinking-Water Quality of Upper Awash Sub-Basin

Most ions have a maximum permissible limit in drinking water. To assess the suitability of water for drinking purposes, the results of the chemical analyses were compared with the Ethiopian standards for drinking water prepared by the Ethiopian Standards Agency, and the Guidelines formulated by World Health Organization.

Table 6. 4: Drinking water quality of groundwater in the Upper Awash Sub-Basin

Parameter	Unit	Sample Range (min-max)	No of samples < WHO guideline	WHO Guideline	No of samples >WHO guideline	No of samples < Ethiopian standard	Ethiopian Standard	No of samples > Ethiopian standard
TDS	mg/L	98 - 3298	634	1000	22	634	1000	22
EC	(µS/cm)	147 - 6596		_			_	
pH		6 - 9.42	646	6.5-8.5	20	646	6.5 - 8.5	20
NH_4^+	mg/L	0-42		_		352	1.5	7
Na^+	mg/L	1 - 980	602	200	30	602	200	30
K^+	mg/L	0.6 - 72		_		29	1.5	489
Ca^{2+}	mg/L	0.5 - 130	491	75	31	491	75	31
Mg^{2+}	mg/L	0 - 122	624	50	0	624	50	0
Hardness	mg/L		527	500	0	512	300	15
Fe_tot	mg/L	0 - 1.7	384	0.3	40	384	0.3	40
Mn^{2+}	mg/L	0 - 6.5	355	0.4	4	355	0.5	4
F^-	mg/L	0 - 41.6	520	1.5	110	520	1.5	110
Cl^-	mg/L	0 - 155	673	250	0	673	250	0
NO_2^-	mg/L	0 - 12	346	3	4	346	3	4
NO_3^-	mg/L	0 - 230	599	50	9	599	50	9
CO_3^{2-}	mg/L	0 - 208.1		_				
HCO_3^-	mg/L	100 - 2334.5		_				
SO_4^{2-}	mg/L	0 - 203	641	250	0	641	250	0
PO_4^{3-}	mg/L	0 - 20		_			_	
Cd	mg/L		4.0	0.003	0	4	0.003	0
Cr	mg/L		4.0	0.05	0	4	0.05	0
Pb	mg/L		4.0	0.01	0	4	0.01	0
Zn	mg/L		4.0	4	0	4	5	0

As we can see from the table most of the water samples in the Upper Awash Sub-Basin fulfill the requirements for drinking purposes. However, in some wells fluoride and nitrate concentrations are above the required limit set by World Health Organization. The presence of Pumice and pyroclastic deposits in the study area cause water to have a high concentration of fluoride and that is the case for dental and skeletal problems in the society living in the area. Agricultural activities such as the misuse of inorganic nitrogenous fertilizers and manures, wastewater treatment, and the oxidation of nitrogenous waste products in human and animal excreta, including septic tanks, could all contribute to elevated nitrate levels in some groundwater samples.

Thirty water samples show sodium ion exceedance above 200mg/l. Most of the wells with high sodium ion concentrations are the thermal wells found in the Filwuha area. Despite its importance for both humans and animals, manganese concentration can have adverse effects resulting from both deficiency and overexposure. The concentration of Manganese in some areas in the Upper Awash Sub-Basin is above the permissible limit.

Water Quality for Irrigation

Water quality is thus a crucial factor in irrigated agricultural long-term sustainability, especially where salinity development is predicted to be an issue. Since salts can impair both soil structure and crop output, salinity levels are the principal water quality concern in most irrigation systems. The high salinity water is poisonous to plants and creates a salinity danger. Saline

soils are those that have a high amount of total salinity. A "physiological" drought can be caused by high salt concentrations in the soil (Fipps, 2003).

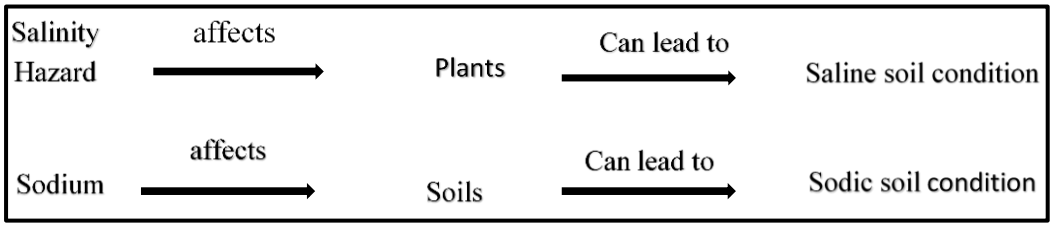

Sodium Hazard

Due to the impact of sodium on the soil, irrigation water having high levels of salt is of particular concern and constitutes a sodium hazard. Sodium hazard is usually expressed in terms of the Sodium Adsorption Ratio (SAR) which is calculated from the ratio of sodium to calcium and magnesium. The latter two ions are important since they tend to counter the effects of sodium. The United States soil laboratory proposed the following relation to calculate the effect of sodium on soil fertility (McGeorge, 1954).

$$SAR = \frac{Na^+}{\sqrt{\frac{Ca^{2+}+Mg^{2+}}{2}}}$$

Using water that has a high SAR value for irrigation results in a breakdown in the physical structure of the soil. Due to its nature, sodium can be adsorbed and becomes attached to soil particles that make the soil hard and compact when it is dried and increasingly impervious to water penetration. Soils having fine texture, especially with high clay content are vulnerable to such effects.

The other important classification of irrigation water is based on electrical conductivity (EC) and soluble sodium percentage (also known as sodium percentage), which is calculated using the formula (Wilcox, 1955):

$$\%Na = \frac{(Na^+ + K^+)}{Ca^{2+} + Mg^{2+} + Na^+ + K^+} \times 100$$

Table 6. 5: Classification of water-based on Sodium Adsorption Ratio and Percent Sodium

Equation	Range	Water class
1. $SAR = \frac{Na^+}{\sqrt{\frac{Ca^{2+}+Mg^{2+}}{2}}}$	<10 10-18 18-26 >26	Excellent Good Doubtful Unsuitable
2. $\%Na = \frac{Na^+ + K^+}{Ca^{2+} + Mg^{2+} + Na^+ + K^+} \times 100$	<20 20-40 40-60 60-80 >80	Excellent Good Permissible Doubtful Unsuitable

The United States Department of Agriculture has established a classification of water for agriculture based on the Sodium Adsorption Ratio (SAR) or percentage as a sodium hazard index and specific electrical conductivity (EC) as a salinity hazard index.

Table 6. 6: Classification of water based on electrical conductivity and sodium percentage

Water class	EC (µS/cm)	Na%
Excellent	<250	<20
Good	250-750	20-40
Permissible	750-2250	40-60
Doubtful	2210-4000	60-80
Unsuitable	>4000	>80

Table 6. 7: Classification of water based on Electrical conductivity and Sodium Adsorption Ratio (SAR)

Water class	EC (µS /cm)	SAR
Excellent	<250	<10
Good	250-750	10-18
Medium	750-2250	18-26
Bad	2210-4000	>26
Very bad	>4000	

As we can see from the map most of the groundwater have low and intermediate sodium hazard and are suitable for irrigation purpose. However, some groundwater samples from thermal wells in the Filwuha area are not suitable for agricultural activity due to very high sodium hazards. From the percent sodium analysis, about 48% of groundwater samples are suitable for irrigation (excellent to good quality), 78% can be used for irrigation in general (Excellent to Permissible). About 23% of the total samples have high sodium hazards that can affect soil fertility and crop yield.

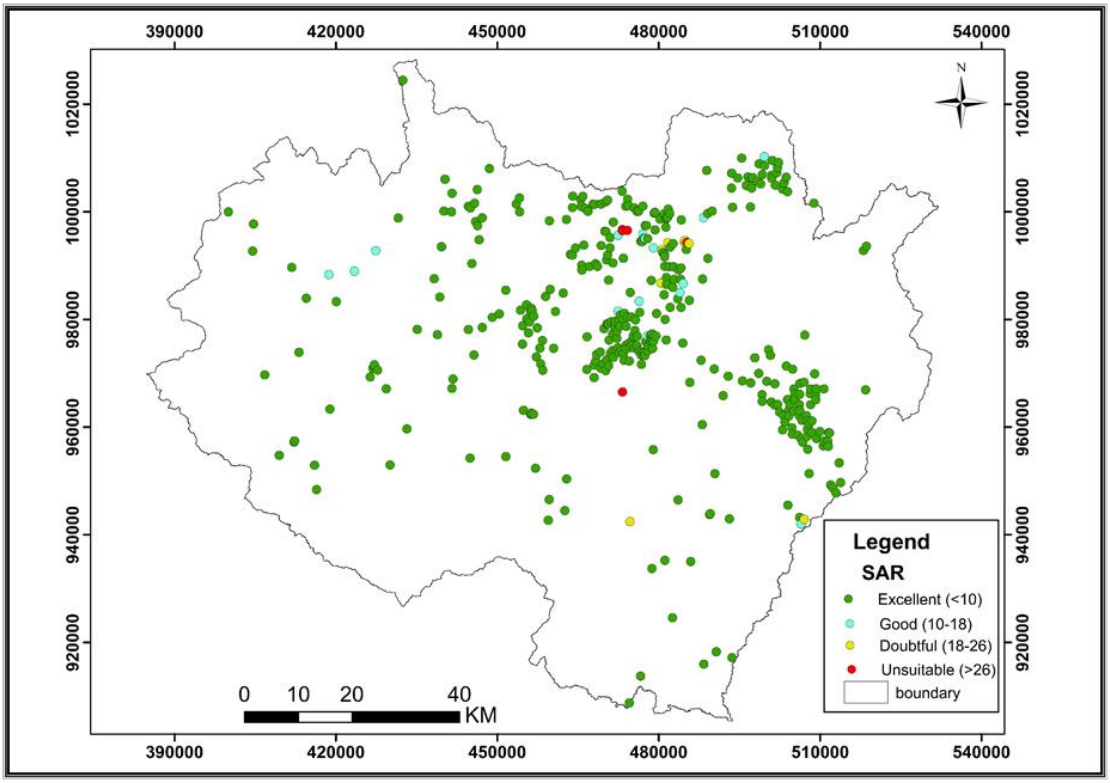

Figure 6. 32: Spatial Variation of Sodium Adsorption Ratio in the Upper Awash Sub-Basin

Table 6. 8: Upper Awash Sub-Basin water sample categorization based on its sodium percentage

%Na Range	<20	20-40	40-60	60-80	>80
Groundwater samples	57	187	147	68	51
River water samples					
Lake-water samples		6	17	15	15

Based on SAR analysis of Lake samples, Gefersa, Dire, Abasamuel, Koka, Bishoftu and Bishoftu Guda lakes have low sodium adsorption ratios and are suitable for irrigation. On the other hand, Lake Hora and Lake Hora Hoda are hazardous (unsuitable) for irrigation due to higher SAR values.

The sodium adsorption ratio of all River water samples is very low (<10) indicating that there is no sodium ion-related hazard and these rivers can be used for irrigation.

In general, except few samples from lakes and groundwater, most water bodies in the Upper Awash Sub-Basin have low to moderate sodium hazards that are suitable for irrigation purposes.

Salinity Hazard

Highly saline waters are toxic to plants and pose a salinity hazard that can result in a

"physiological" drought condition (Fipps, 2003). The salinity of the water is usually measured by the TDS (total dissolved solids) or the EC (electric conductivity). TDS is sometimes referred to as the total salinity.

Most groundwater samples have low to medium salinity and some of them have high to very high salinity hazards. Filwuha wells in Addis Ababa are highly saline which is unsuitable for plants.

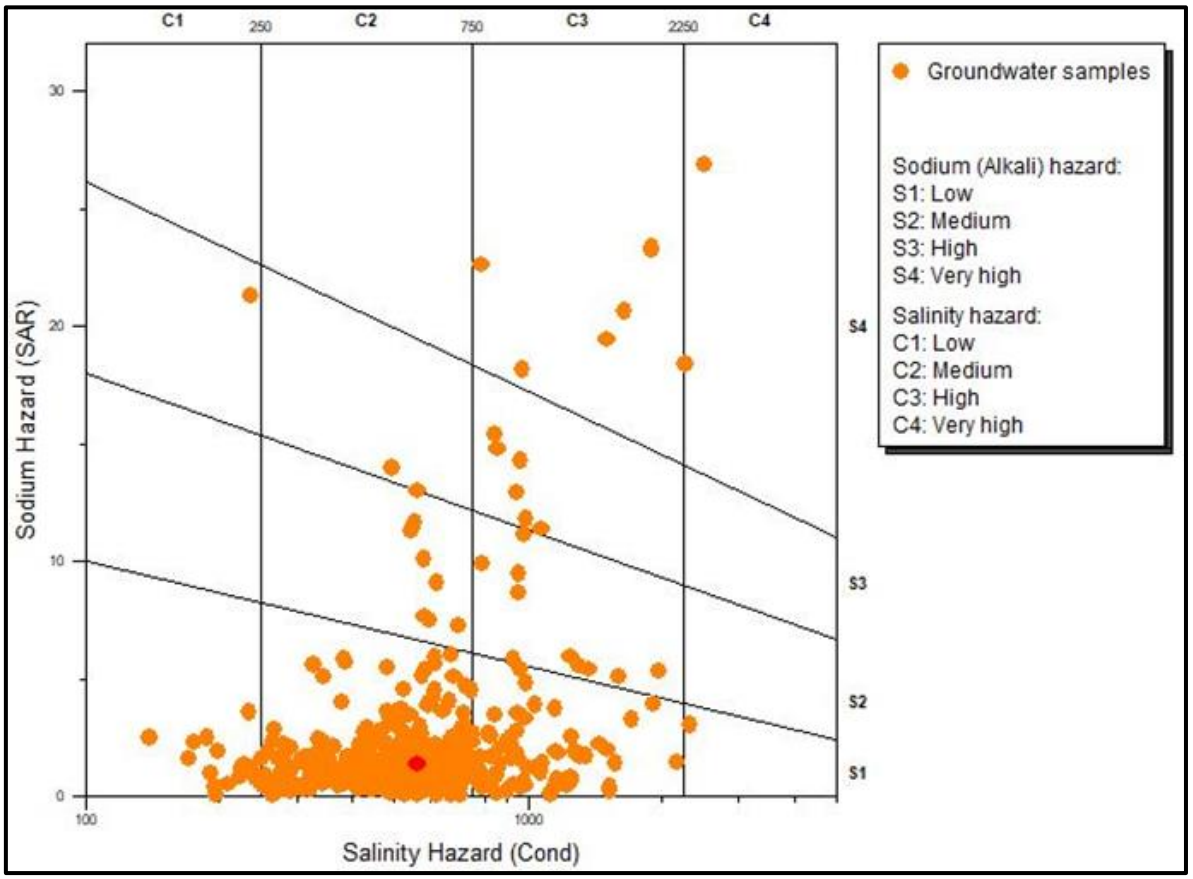

Figure 6. 33: Salinity Hazard Map of Groundwater Samples

Awash River at Melkakunture, Mojo River near Koka Dam, and Holeta River have medium salinity values suitable for agricultural purposes. Mojo River upstream and Legetafo River have high saline content that cannot be used under restricted drainage or special management for salinity control may be required, and plants with good salt tolerance should be selected. Lakes in the area have low to high salinity as shown from the salinity graph. Hora and Bishoftu Guda Lakes especially have high salinity whereas Koka and Abasamuel Lakes have relatively lower salinity.

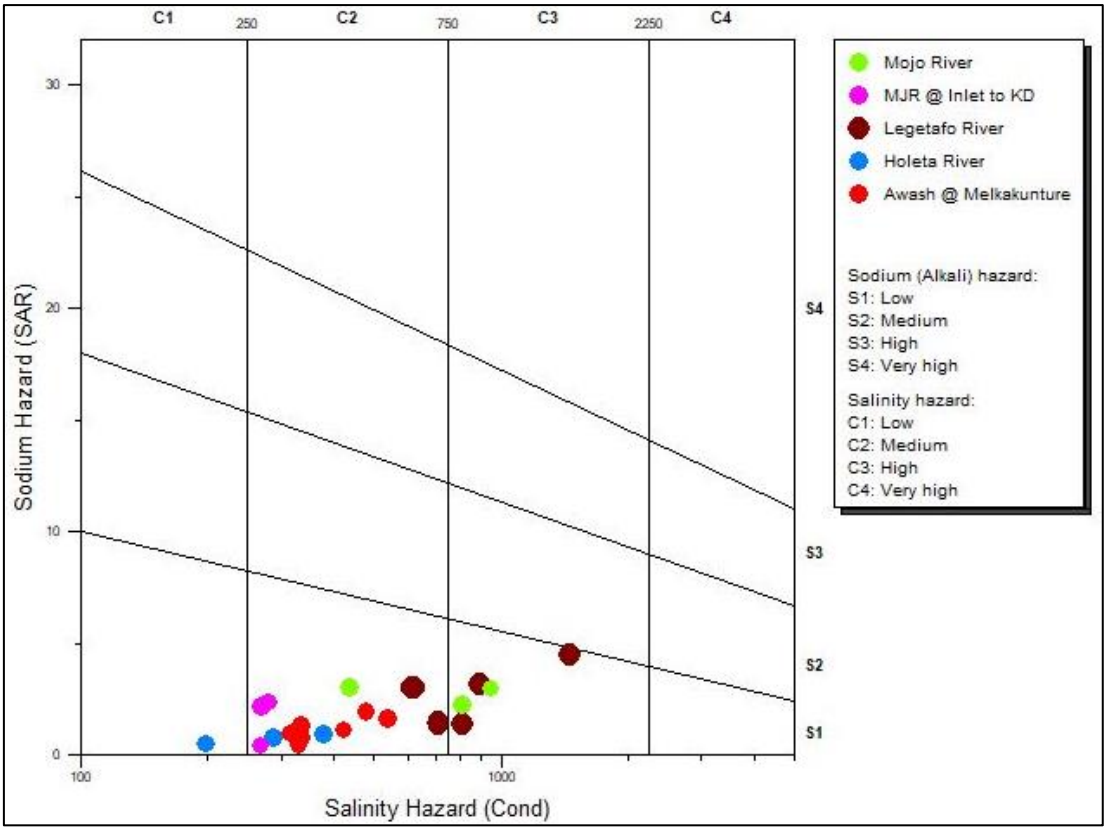

Figure 6. 34: Salinity Hazard Map of River Water Samples

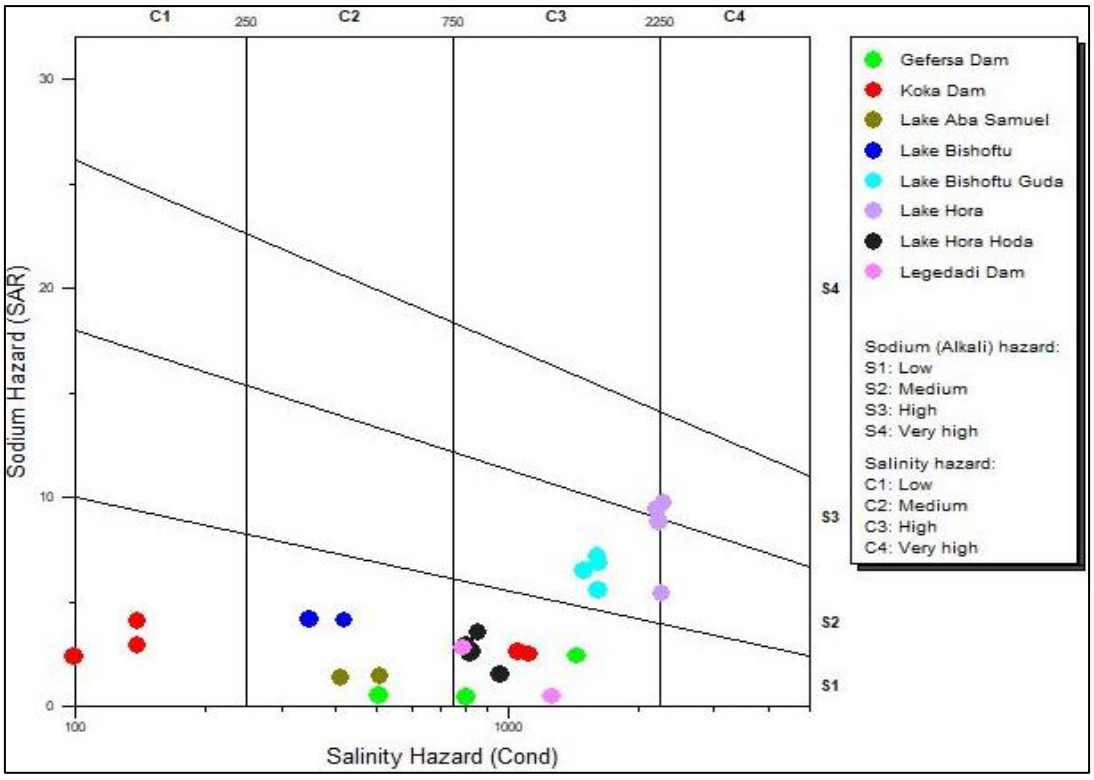

Figure 6. 35: Salinity Hazard Map of Lake Water Samples

Chapter Seven

Conclusion and Recommendation

7.1. Conclusion

This study was aimed at checking the spatial and temporal hydrochemical variations of both groundwater and surface water in the area. The spatial hydrochemical variation is greatly affected by the geology of the area, rock-water interactions related to lithology and groundwater residence time, geological structures, and climate account for the clear variation in ionic concentration in both groundwater and surface water systems.

The higher hydrochemical variations in the sub-basin are attributed to the thermal groundwater where the geological formations in such areas are affected by regional fault systems. The gradual decrease in TDS observed from Hilton Hotel wells may be due to the presence of regional fault systems resulting in permeable geological formations that allow the mixing of freshwaters with the deep high TDS thermal groundwater. Sodium and calcium are the most variable ions both spatially and temporally due to the soluble nature of sodium-bearing minerals during interaction with water. Generally, the temporal variation of these major cations in the Upper Awash Sub-Basin groundwater is mainly attributed to the residence time of groundwater in the area, and the presence of geological structures like faults that allows groundwater to easily circulate within various rocks. As the groundwater lasts a long time in the area, there will be enough time for the groundwater-rock interaction and more ions will join the groundwater.

There are a lot of reasons for the temporal variation of chloride in the Upper Awash groundwater. Among these, the first one might be due to the stagnation of deeper groundwater at compacted clay along the fault zones and recent eruption centers. The other reason might be due to the pre-recharge evaporative enrichment that may increase the concentration of chloride in groundwater. In addition to these factors, the contribution of anthropogenic factors should also be considered.

The temporal increment of sulfate, nitrate, and heavy metal concentrations may also depict the effect of anthropogenic sources. The use of fertilizers by the local farmers and for the flower farm may increase the concentration of nitrate in groundwater. Based on trace metal analysis, Rivers in Upper Awash Sub-Basin have a higher concentration of iron, manganese lead, and zinc with relative temporal and spatial variation than its variation in groundwater. Cadmium

ion concentration is generally below 0.002mg/l in all selected sites, and in the same way, zinc is also below 0.0012mg/l in all cases. A high concentration of zinc is detected in the Mojo River upstream. Iron, manganese, lead, and zinc are generally low in lakes but there is a slight temporal variation in all selected sites.

The evolution of groundwater from the recharge areas in Addis Ababa and its surrounding areas having Ca-HCO_3, Ca-Mg-HCO_3, Mg-HCO_3, Mg-Ca-HCO_3, etc. type waters gradually evolve to Ca-Na-HCO_3, Mg-Na-HCO_3, Na-Ca-HCO_3 type in the transition areas and finally evolved to Na-HCO_3 type water near the rift environment. In general, the highland recharge areas of the Upper Awash Sub-Basin are dominantly characterized by calcium, magnesium, and mixing water types. Na-Mg-HCO_3, Na-Ca-HCO_3, and Na-Ca-Mg-HCO_3 type waters are characteristics of the transitional environment. Finally, the rift and near rift areas are dominated by Na-HCO_3 water types.

The hydrochemistry of Debrezeit lakes is mainly related to their connection with the groundwater. The rate of groundwater flux affects the chemistry of these lakes. Lake Hora and Hora Hoda are least affected by groundwater flux and have highly variable chemistry. Whereas lake Bishoftu and Bishoftu Guda are affected by the groundwater flux. Therefore dilution changes the chemistry of these lakes. The hydrochemistry of reservoirs around Addis Ababa have more or less stable but Lake Aba Samuel is highly affected by anthropogenic influence since it receives water from the Akaki River. Rivers like Awash River at Melkakunture, and Holeta River are far from the city and industries, hence their chemical composition is generally stable. Whereas Akaki river and Mojo river are highly affected by anthropogenic factors. Since these perennial rivers receive water from groundwater, their chemistry is also affected by groundwater outflow.

Regarding the quality of groundwater for drinking purposes, all groundwater samples except Filwuha and some wells close to the rift are within the acceptable range. The wells which are close to the rift axis have high fluoride due to the contribution of acidic rocks.

The groundwater in most areas of the Upper Awash Sub-Basin, all sampled rivers, and reservoirs including Gefersa, Dire, Legedadi, AbaSamuel, and Lake Bishoftu, Lake Bishoftu Guda have lower Sodium Adsorption Ratio whereas Lake Hora and Hora Hoda have higher SAR that may affect soil fertility and crop yield. Regarding the salinity, groundwater in most parts of the Upper Awash Sub-Basin have low to medium salinity and some of them have high to very high salinity hazards. Filwuha wells in Addis Ababa are highly saline which is unsuitable for plants. On the other hand, Awash River at Melkakunture, Mojo River near Koka

Dam, and Holeta River have medium salinity values suitable for agricultural purposes. Mojo River upstream and Legetafo River have high saline content that cannot be used under restricted drainage or special management for salinity control may be required, and plants with good salt tolerance should be selected. Generally, Lakes in the area have low to high salinity. Hora and Bishoftu Guda Lakes especially have high salinity whereas Koka and Abasamuel Lakes have relatively lower salinity.

7.2. Recommendation

Based on the temporal and spatial hydrochemical analysis, the following recommendations are forwarded:

- Two years of hydrochemical monitoring in the Upper Awash Sub-Basin was done by Water Works Design and Supervision Enterprise in 2006-2007 but there should be regular monitoring and record-keeping on hydrochemical variation in the area.
- To reduce the salinity of Rivers and for safe irrigation water supply, wastewater should be treated before joining the rivers.
- Highly applicable and working regulation is required regarding industrial and domestic waste disposal.
- Water quality requires regular review and control, as well as an assessment of the impact of development on water quality in comparison to a set of standards.
- Most previous hydrochemical analyses in Upper Awash Sub-Basin are targeted to major ion concentrations. There should be a consideration of some toxic heavy metals with their spatial and temporal variation.
- This thesis did not cover most parts of the area due to a lack of continuous hydrochemical data despite opening roads for other interested organizations to do sound water quality monitoring for the future.

Reference

Abbate E., Bruni P., Sagri M. (2015) Geology of Ethiopia: A Review and Geomorphological Perspectives. In: Billi P. (eds) Landscapes and Landforms of Ethiopia. World Geomorphological Landscapes. Springer, Dordrecht. https://doi.org/10.1007/978-94-017-8026-1_2.

Amare Shiberu, Zenebe Kifle, & Agizew Nigussie (2017). Spatial and temporal water quality dynamics of Awash River using multivariate statistical techniques. African Journal of Environmental Science and Technology, 11(11), 565–577. https://doi.org/10.5897/ajest2017.2353.

Andarge Yitbarek, Razack, M., Tenalem Ayenew, Engda Zemedagegnehu, & Tilahun Azagegn (2012). Hydrogeological and hydrochemical framework of Upper Awash River basin, Ethiopia: With special emphasis on inter-basins groundwater transfer between Blue Nile and Awash Rivers. Journal of African Earth Sciences, 65(December), 46–60. https://doi.org/10.1016/j.jafrearsci.2012.01.002.

Assiged Getahun (2007). Geology of Addis Ababa City. Unpublished Technical Report; Ministry of Mines and Energy, Geological Survey of Ethiopia, Addis Ababa, Ethiopia. 35pp.

Bereket Fentaw and Leta Alemayehu (2019). Hydrogeological, Hydrochemical and Engineering Geology Maps of Addis Ababa Nc 37-10. Unpublished Technical Report; Geological Survey of Ethiopia, Addis Ababa, Ethiopia, 236pp.

Bereket Fentaw and Mihret Manaye (2019). Hydrogeological and Hydrochemical Maps of

Akaki Beseka NC 37 – 14 Sheet. Unpublished Technical Report; Ministry of Mines, Petroleum and Natural Gase, Geological Survey of Ethiopia, Addis Ababa, Ethiopia, 119pp.

Boccaletti, M., Mazzuoli, R., Bonini, M., Trua, T., & Bekele Abebe (1999). Plio-Quaternary volcanotectonic activity in the northern sector of the Main Ethiopian Rift: Relationships with oblique rifting. Journal of African Earth Sciences, 29(**4**), 679–698. https://doi.org/10.1016/S0899-5362(99)00124-4.

Bonini, M., Corti, G., Innocenti, F., Manetti, P., Mazzarini, F., Tsegaye Abebe, & Pecskay, Z. (2005). Evolution of the Main Ethiopian Rift in the frame of Afar and Kenya rifts propagation. Tectonics, 24(**1**), 1–21. https://doi.org/10.1029/2004TC001680.

Bretzler, A., Osenbrück, K., Gloaguen, R., Ruprecht, J. S., Seifu Kebede, & Stadler, S. (2011). Groundwater origin and flow dynamics in active rift systems - A multi-isotope approach in the Main Ethiopian Rift. Journal of Hydrology, 402(3–4), 274–289. https://doi.org/10.1016/j.jhydrol.2011.03.022.

Chebotarev, I. I. (1955). Metamorphism of natural waters in the crust of weathering-2. Geochimica et Cosmochimica Acta, 8(3), 137–170. https://doi.org/10.1016/0016-7037(55)90010-7.

Copernicus Sentinel data (2016). Retrieved from ASF DAAC (26/5/2016), processed by ESA.

Ebasa Oljira (2006). Numerical Groundwater Flow Modeling of the Akaki River Catchment. Unpublished MSc Thesis; Addis Ababa University, Addis Ababa, Ethiopia, 131pp.

Efrem Beshawered (2010). Geology of the Akaki-Beseka Area. Unpublished Technical Report; Ministry of Mines, Geological Survey of Ethiopia, Addis Ababa, Ethiopia, 93pp.

Fipps, G. (2003). Irrigation water quality standards and salinity management strategies. Texas A&M Agrilife Extension, 4(03), 1–18.

Freeze, R. A., & Cherry, J. A. (1979). Groundwater. Prentice-Hall, Inc.

Gasparon, M., Innocenti, F., Manetti, P., Peccerillo, A., & Tsegaye Abebe (1993). Genesis of the pliocene to recent bimodal mafic-felsic volcanism in the Debre Zeyt area, central Ethiopia: volcanological and geochemical constraints. Journal of African Earth Sciences, 17(2), 145–165. https://doi.org/10.1016/0899-5362(93)90032-L.

Gayathri, J. A., Raj, V. T., Sreelash, K., Maya, K., Vandana, M., & Padmalal, D. (2021). Spatiotemporal variability in groundwater chemistry of a mountainous catchment with complex geologic and climate gradients in southwest India. Environmental Earth Sciences, 80(17), 1–32. https://doi.org/10.1007/s12665-021-09862-6

Giday Woldegabriel, Aronson, J. L., & Walter, R. C. (1990). Geology, geochronology, and rift basin development in the central sector of the Main Ethiopia Rift. Bulletin of the Geological Society of America, 102(4), 439–458. https://doi.org/10.1130/0016-7606(1990)102<0439:GGARBD>2.3.CO;2.

Hayward, N. J., & Ebinger, C. J. (1996). Variations in the along-axis segmentation of the Afar Rift system. Tectonics, 15(2), 244–257. https://doi.org/10.1029/95TC02292.

HEM, J. D. (1985). Study and Interpretation of the Chemical Characteristics of Natural Water.

Development, 263pp.

Hiscock, K. M., & Bense, V. F. (2005). Hydrogeology: Principles and Practice. Blackwell Publishing, Oxford, UK., 68–70.

Kazmin, V.; Seifemichael Berhe. (1978): Geological map of Nazreth Sheet, Scale 1:250,000.Unpublished Technical Report, Geological Survey of Ethiopia, Addis Ababa, Ethiopia.

Kidist Hailu (2016). Groundwater Dynamics in Tributary Streams of Muger and Holota River Catchments. Unpublished MSc Thesis; Addis Ababa University, Addis Ababa, Ethiopia, 73pp.

Krishna Kumar, S., Hari Babu, S., Eswar Rao, P., Selvakumar, S., Thivya, C., Muralidharan, S., & Jeyabal, G. (2017). Evaluation of water quality and hydrogeochemistry of surface and groundwater, Tiruvallur District, Tamil Nadu, India. Applied Water Science, 7(5), 2533–2544. https://doi.org/10.1007/s13201-016-0447-7.

McGeorge, W. T. (1954). Diagnosis and Improvement of Saline and Alkaline Soils. Soil Science Society of America Journal, 18(3), 348. https://doi.org/10.2136/sssaj1954.03615995001800030032x.

Mekdes Nigatie (2012). Characterization of Aquifers and Hydrochemistry in Volcanic Terrain

of Central Ethiopia. Unpublished MSc thesis; Addis Ababa University, Addis Ababa, Ethiopia, 136pp.

Mockus, V., (1972b). Estimation of direct runoff from storm rainfall. Chapter 10, Section 4

(Hydrology), National Engineering Handbook. Soil Conservation Service, U.S. Dept. Agriculture.

Mohr, P. (1983). The Ethiopian flood basalt province. Continental Flood Basalts, 63–110. https://doi.org/10.1007/978-94-015-7805-9_3.

Molla Demlie, Wohnlich, S., Wisotzky, F., & Birhanu Gizaw (2007). Groundwater recharge, flow and hydrogeochemical evolution in a complex volcanic aquifer system, central Ethiopia. Hydrogeology Journal, 15(6), 1169–1181. https://doi.org/10.1007/s10040-007-0163-3.

Morán-Ramírez, J., Ledesma-Ruiz, R., Mahlknecht, J., & Ramos-Leal, J. A. (2016). Rock-water interactions and pollution processes in the volcanic aquifer system of Guadalajara,

Mexico, using inverse geochemical modeling. Applied Geochemistry, 68, 79–94. https://doi.org/10.1016/j.apgeochem.2016.03.008.

Muhammed Haji, Qin, D., Guo, Y., Li, L., Wang, D., Karuppannan, S., & Shube, H. (2021). Origin and geochemical evolution of groundwater in the Abaya Chamo basin of the Main Ethiopian Rift: application of multi-tracer approaches. Hydrogeology Journal, 29(3), 1219–1238. https://doi.org/10.1007/s10040-020-02291-y.

National Meteorological Agency of Ethiopia (2001). Initial National Communication of Ethiopia to the United Nations Framework Convention on Climate Change (UNFCCC). Unpublished Technical Report; Addis Ababa, Ethiopia, 127pp.

Omer Cooper (1930). Preliminary Investigation of the Freshwater Fauna of Abyssinia. University of Durham, England. 196-207.

Pashaeifar, M., Dehghanzadeh, R., Ramazani, M. E., Rafieyan, O., & Nejaei, A. (2021). Spatial and temporal assessment of groundwater quality and hydrogeochemical processes in Urmia Lake Basin, Iran. Water Supply, 00(0). https://doi.org/10.2166/ws.2021.180.

Pazi, I. (2008). Water mass properties and chemical characteristics in the Saros Gulf, Northeast Aegean Sea (Eastern Mediterranean). Journal of Marine Systems, 74(1–2), 698–710. https://doi.org/10.1016/j.jmarsys.2008.07.002.

Rezaei, A. R., Ismail, Z. B., Niksokhan, M. H., Ramli, A. H., Sidek, L. M., & Dayarian, M. A. (2019). Investigating the effective factors influencing surface runoff generation in urban catchments – a review. Desalination and Water Treatment, 164(January), 276–292. https://doi.org/10.5004/dwt.2019.24359.

Rooney, T. O., Furman, T., Gezahegn Yirgu, & Dereje Ayalew (2005). Structure of the Ethiopian lithosphere: Xenolith evidence in the Main Ethiopian Rift. Geochimica et Cosmochimica Acta, 69(15), 3889–3910. https://doi.org/10.1016/j.gca.2005.03.043.

Rumuri, R., & Manivannan, R. (2020). Identifying major factors controlling groundwater chemistry in a predominantly agricultural area of Kattumannarkoil taluk, India, using the hydrochemical processes and GIS. Geology, Ecology, and Landscapes, 00(00), 1–12. https://doi.org/10.1080/24749508.2020.1726560.

Seifu Kebede (2013). Groundwater in Ethiopia. Springer Heidelberg New York, 294pp.

Seifu Kebede, Travi, Y., Asfawossen Asrat, Tamiru Alemayehu, Tenalem Ayenew, & Zenaw

Tessema (2008). Groundwater origin and flow along selected transects in Ethiopian rift volcanic aquifers. Hydrogeology Journal, 16(1), 55–73. https://doi.org/10.1007/s10040-007-0210-0.

Stanton, J. S., Qi, S. L., Ryter, D. W., Falk, S. E., Houston, N. A., Peterson, S. M., Westenbroek, S. M., & Christenson, S. C. (2011). Selected approaches to estimate water-budget components of the High Plains, 1940 through 1949 and 2000 through 2009. In U.S. Geological Survey Scientific Investigations Report.

Tamiru Alemayehu (1992). Hydrogeology of Debrezeit Area. Unpublished MSc Thesis; Addis Ababa University, Addis Ababa, Ethiopia, 119pp.

Tamiru Alemayehu (2001). The impact of uncontrolled waste disposal on surface water quality in Addis Ababa, Ethiopia. In SINET: Ethiopian Journal of Science (Vol. 24, Issue 1). https://doi.org/10.4314/sinet.v24i1.18177.

Tenalem Ayenew (2006). Major ions composition of the groundwater and surface water systems and their geological and geochemical controls in the Ethiopian volcanic terrain. SINET: Ethiopian Journal of Science, 28(2), 171–188. https://doi.org/10.4314/sinet.v28i2.18253.

Tenalem Ayenew, Molla Demlie, & Wohnlich, S. (2008). Hydrogeological framework and occurrence of groundwater in the Ethiopian aquifers. Journal of African Earth Sciences, 52(3), 97–113. https://doi.org/10.1016/j.jafrearsci.2008.06.006

Tesfaye Chernet, Travi, Y., & Valles, V. (2001). Mechanism of degradation of the quality of natural water in the lakes region of the Ethiopian Rift Valley. Water Research, 35(12), 2819–2832. https://doi.org/10.1016/S0043-1354(01)00002-1.

Thornthwaite, C. W. (1948). An Approach Toward a Rational. Geographical Review, 38(1), 55–94.

Thornthwaite, C. W., & Mather, J. R. (1957). Instructions and Tables for Computing Potential Evapotranspiration and Water Balance. Publications in Climatology, 10, 185–311.

Tilahun Azagegn (2008). Hydrogeochemical Characterization of Aquifer Systems in Upper Awash and Adjacent Abay Plateau Using Geochemical Modeling and Isotope Hydrology. Unpublished MSc Thesis; Addis Ababa University, Addis Ababa, Ethiopia, 138pp.

Tilahun Azagegn (2014). Groundwater Dynamics in the Left Bank Catchments of the Middle

Blue Nile and the Upper Awash River Basins. Unpublished Ph.D. Thesis,Addis Ababa University, Addis Ababa, Ethiopia, 137pp.

Tripathee, L., Kang, S., Huang, J., Sillanpää, M., Sharma, C. M., Lüthi, Z. L., Guo, J., & Paudyal, R. (2014). Ionic composition of wet precipitation over the southern slope of central Himalayas, Nepal. Environmental Science and Pollution Research, 21(4), 2677–2687. https://doi.org/10.1007/s11356-013-2197-5.

Tsegaye Abebe, Balestrieri, M. L., & Bigazzi, G. (2010). The Central Main Ethiopian Rift is younger than 8 Ma: Confirmation through apatite fission-track thermochronology. Terra Nova, 22(6), 470–476. https://doi.org/10.1111/j.1365-3121.2010.00968.x.

Tsegaye Abebe, Mazzarini, F., Innocenti, F., & Manetti, P. (1998). The Yerer-Tullu Wellel Volcanotectonic lineament: A Transtensional structure in central Ethiopia and the associated magmatic activity. Journal of African Earth Sciences, 26(1), 135–150. https://doi.org/10.1016/S0899-5362(97)00141-3.

Wilcox, L. V. (1955). Classification and Use of Irrigation Waters. Department of Agriculture, United States. 969(Circular No. 696), 1–21. https://www.ars.usda.gov/arsuserfiles/20360500/pdf_pubs/P0192.pdf.

Water Works Design and Supervision Enterprise (2008). Evaluation of Water Resources of The Ada'a and Becho Plains. Unpublished Technical Report; Addis Ababa, Ethiopia, 147pp.

Yates, D., & Strzepek, K. (1994). Potential Evapotranspiration Methods and their Impact on the Assessment of River Basin Runoff Under Climate Change. International Institute for Applied Systems Analysis.

Appendices

Appendix 1: Mean monthly Precipitation at each station (mm/month)

Stations	Jan	Feb	Mar	Apr	May	Jun	Jul	Aug	Sep	Oct	Nov	Dec
Addis Ababa	12	20	57	80	91	152	278	294	192	32	12	10
Akaki	9	20	50	77	71	112	232	234	126	11	8	5
Sendafa	14	16	43	81	69	149	296	347	142	29	13	8
Intoto	8	19	53	74	90	173	348	335	156	27	14	9
Holeta	21	46	69	81	88	129	243	258	172	46	5	8
Sululta	10	23	53	69	78	156	323	322	167	19	11	7
Ginchi	26	26	64	79	88	155	216	222	129	28	12	11
Chefedonsa	11	17	40	62	78	100	240	253	111	10	9	4
Debrezeit	11	21	53	57	50	98	224	213	106	22	7	6
Mojo	11	20	52	64	76	107	316	259	126	31	10	5
Koka	10	15	48	47	70	86	256	232	112	18	12	10
Alem Tena	17	28	48	48	39	85	197	204	112	34	6	10
Tulubolo	13	15	51	68	107	190	255	242	110	25	5	8

Appendix 2: Average monthly Temperature at each station (ºC)

Month	Jan	Feb	Mar	Apr	May	Jun	Jul	Aug	Sep	Oct	Nov	Dec
Addis Ababa	16.75	18.11	18.94	19.09	19.07	17.78	16.6	16.43	16.9	17.11	16.51	16.06
Akaki	19.63	20.1	21.19	21.01	21.26	19.78	18.76	18.18	19.03	19.35	19.23	19.7
chefedonsa	16.69	17.38	18.33	18.21	18.68	17.73	16.65	16.62	16.44	15.96	15.27	15.38
Debrezeit	17.6	17.8	20.2	20.5	20.7	19.7	18.2	18.2	18.2	18.1	17.5	17.2
Ginchi	18.7	19.7	20.1	20	19.5	18.2	17.1	17.6	17.2	17.8	17.7	17.8
Holota	13.82	14.51	15.77	16.97	17.17	16.29	15.15	14.92	14.44	13.53	13.4	13.03
Intoto	13.47	14.58	14.71	14.25	14.41	13.4	11.96	11.29	12.09	12.93	13.35	13.37
Koka Dam	21.09	22.94	23.89	23.98	24.59	24.26	21.9	22	22.52	21.22	20.28	19.54
Mojo	20.52	20.37	21.95	21.88	22.23	21.13	19.57	19.49	19.15	19.67	19.21	19.51
Sendafa	15.8	16.7	17.7	17.6	18.2	16.7	15.5	15.6	16	16.1	15.6	15.5
Sululta	14.02	15.3	15.13	15.52	15.08	14.42	13.88	13.67	14.18	13.85	13.74	13.12
Tulubolo	17.87	19.16	19.64	19.27	18.91	18.33	17.62	17.75	16.56	15.99	15.84	16.6
Alem Tena	18.2	19.3	20.2	20.8	20.7	20.2	19.5	19.2	18.7	19.2	17.8	17.5

Appendix 3: Groundwater monitoring stations

StationID	Addis Ababa															
SampleID	Shegole (SH01)		Akaki (ABH10)				Akaki (ABH14)			Akaki (ABH22)				Akaki (ABH11)		
Year	2007	2015	1996	2000	2010	2013	1996	2000	2014	1996	2000	2013	2014	1996	2000	2013
TDS (mg/l)	174	311	438.92	292	235	302	453.43	291	320	433.42	301	225.05	238	449.57	315	355.67
EC (µS/cm)	311	845	478.7	478	489	500	476.4	476	516	494.2	494	480.5	484	516	516	546.5
pH	7.04	8.1	7.2		7.58	7.66	7.2	7.7	7.73	7.2		7.69	7.94	7.2		7.67
NH_4^+(mg/l)	0.14	0.63	0		0.07	0.37	0		0.16	0		0	0.1	0.05	0.05	0.23
Na^+ (mg/l)	8.4	212	30.6	32	30.5	28.5	27.2	27.2	35.5	27.2	27.2	20.47	27.63	30.6	30.6	38.5
K^+ (mg/l)	1.8	1.2	3.96	3.6	3.92	4.6	5.94	4.3	4.9	4.3	3.5	3.7	3.5	2.97	3.96	3.52
T. Hardness (mg/l)	157.3	71.4	215.6	227.9	220.9	212.5	228.1	235.6	213.6	220.0	239.9	257.6	272.9	224.1	215.6	231.0
Ca^{2+} (mg/l)	42	12.8	40	48.5	49	48	48.1	60.8	50	49.7	77.6	27.6	28.8	46.5	40	67.6
Mg^{2+} (mg/l)	12.75	9.6	28.2	26	24	22.56	26.3	20.4	21.6	23.35	11.2	46	49	26.3	28.2	15.12
Fe_tot (mg/l)	0.03	0.25	0		0.05	0.01	0.01		0.01	0.09		0.02	0.01	0.02		0.05
Mn^{2+} (mg/l)		Trace	0		0.01	0	0		0.04	0		0.01	0.01	0		0.01
F^- (mg/l)	1.29	7.19	0.23	0.24	0.19	0.56	0.7	0.37	0.6	0.39	0.6	0.58	0.75	0.32	0.39	0.61
Cl^- (mg/l)	7.94	16.92	14.2	8.7	10	8.18	9.2	7.2	14.56	14.2	3.6	7.7	4.6	11.3	14.2	9.7
NO_2^- (mg/l)	0.02	0.13	0.13	0.02	0	0	0		Trace	0.69		0.08	0.13	0.01	0.15	0.1
NO_3^- (mg/l)		0.59	9.2	16.7	3.5	15.58	0	9.68	7.6	13.7	6.6	4.4	4.4	21.2	3.9	27.45
Alkalinity (mg/l)					232		270		264	240		270	280	240		265
CO_3^{2-} (mg/l)	0	0	0	0	0	0	0	16.8	0	0	7.2	30	44	0	0	0
HCO_3^- (mg/l)	197	517.28	305	305	280.09	294.39	329.4	300.1	322.1	292.8	317.3	283	236	292.8	313.1	323.3
SO_4^{2-}(mg/l)	0	29.96	7.4	11.43	32.2	28.31	6.58	1	8.42	7	5.32	3	5	17.5	6.58	15.75
PO_4^{3-}(mg/l)	0.16	4.34	0	0.06	0.23	0.21	0		0.16	0		19	19	0		0.2
Water Type	Ca-Mg-HCO3	Na-HCO3	Mg-Ca-Na-HCO3	Ca-Mg-Na-HCO3	Ca-Mg-Na-HCO3	Ca-Mg-Na-HCO3	Ca-Mg-Na-HCO3	Ca-Mg-Na-HCO3	Ca-Mg-Na-HCO3	Ca-Mg-Na-HCO3	Ca-Na-HCO3	Mg-Ca-HCO3	Mg-Ca-HCO3-CO3	Ca-Mg-Na-HCO3	Mg-Ca-Na-HCO3	Ca-Na-Mg-HCO3

Continued…

StationID	Addis Ababa																	
SampleID	Filwuha well (FW01)								Hilton (HH01)					Sendafa well (GW03)				
Year	1951	1952	1962	1967	2006	2007	2008	2010	1967	1982	1986	2000	2007	2000	2013	2016	2019	2021
TDS (mg/L)					2240	2308	2190	2846.67	3298	3021	1880	2049	1769	111	226	264	245	240
EC (µS/cm)			Addis Ababa+S1:AG		3380	3550	3370	4270	4947	4531.5	3760	3359	2900	166.5	348	455	490	480
pH					9	7.3	7.49	7.32	8.3		8.3		7.13	7.3	7.14	7.2	7.47	7.74
NH_4^+(mg/L)					0		0								0.07	0.2		
Na^+ (mg/L)	715.7	717	950	980	930	949	980	963	964	948	952	953	988	6	31	32.5	46	47.5
K^+ (mg/L)	3.1	2	19	60	16	16.1	20	22.69	64.8	18	64.8	15	11.8	1.3	5.5	2.4	2.87	9.4
T. Hardness (mg/L)					11.5	12.9	31.9	10.1	56.0	16.6	56.0	23.2	12.7	56.4	127.4	191.3	188.8	185.3
Ca^{2+} (mg/L)	24.1	18.5	5.65	4	2.76	4.5	5.63	3.56	16	5	16	6	3.43	16	36	57.6	58.4	59.31
Mg^{2+} (mg/L)	1.01	1.2	1.85	2.43	1.12	0.4	4.34	0.29	3.9	1	3.9	2	1	4	9.12	11.53	10.45	9.03
Fe_tot (mg/L)					0.39		0.01					0.4			0.02	0.1	0.2118	0.3188
Mn^{2+} (mg/L)					0.07		0	0				0			0	Trace	0.0138	0.0478
F^- (mg/L)					27.6		29.6	24.34		25	26	21.1		0.3	0.69	0.6	0.71	0.75
Cl^- (mg/L)	16.3	4.4	38	71	7.68	41.6	40.98	36.98	0.05	48	0.1	43	31.3	7.1	5.46	5.4	6.58	7
NO_2^- (mg/L)					101	0	0	0				0		0.01	0	0		0
NO_3^- (mg/L)					1.9	0.03	0.03	2	0	2	0	0.04	0.04	3	0.89	1		1.1
Alkalinity (mg/L)							1913.52											
CO_3^{2-} (mg/L)	0	0	0	0	101	0	0	0	144		144	0	0	0	0	0		0
HCO_3^- (mg/L)	1873.3	1743.7	2323.5	2440	2132	2355	2334.49	2347	2186	2261	2000	2198	2391	61	207.4	287.9	329	319
SO_4^{2-}(mg/L)	60.3	46.9	72.05	54	92	53.8	21.11	64.16	156	48	156	55	45.6	6.4	8.58	3.1	3.7	2
PO_4^{3-}(mg/L)					1.03		0.25								0.4	0.3		0.6
Water Type	Na-HCO3	Na-HCO3	Na-HCO3	Na-HCO3	Na-HCO3	Na-HCO3	Na-HCO3	Na-HCO3	Na-HCO3	Na-HCO3	Na-HCO3	Na-HCO3	Na-HCO3	Ca-Mg-HCO3	Ca-Na-HCO3	Ca-Na-HCO3	Ca-Na-HCO3	Ca-Na-HCO3

Continued…

StationID	Mojo				Bishoftu									
SampleID	Mojo Tannery (MT01)				D/Z Airforce (AF01)								D/Z Veterinary ((VET01)	
Year	2006	2007	2009	2010	1981	1983	1989	1991	2000	2006	2007	2010	1974	2000
TDS (mg/L)	299.56	293.5	266	258.03				616.22	689	777.89	758.17	854	452	635
EC (µS/cm)	453.11	447.5	451	423				1000	1060	1274.78	1185.08	1307		1041
pH	7.5	7.61	7.87	8.09		7.4	7.2	7.2	7.8	7.95	7.92	8	7.4	7.87
NH_4^+(mg/L)	0.14	0.21	0.22							0.41	0.55	0.42		
Na^+ (mg/L)	42.28	47.25	53	53.53	19	25.4	44.2	44.39	64.6	197.44	175.83	204	67.5	138
K^+ (mg/L)	14.82	15.63	15.5	16.79	14	12	11.2	23.4	11.9	21.86	23.13	23.5	9.5	12
T. Hardness (mg/L	133.9	130.8	123.8	109.1	274.4	311.6	283.0	246.1	232.0	257.6	263.6	255.5	240.2	237.6
Ca^{2+} (mg/L)	40.06	39.35	39.48	34.61	54	56.1	64	51.6	44.9	40.52	43.6	42	42.6	36
Mg^{2+} (mg/L)	8.23	7.9	6.12	5.51	34	41.8	30	28.56	29.2	38.11	37.71	36.7	32.6	36
Fe_tot (mg/L)	0.08	0.04	0.02					0.01		0.03	0.04	0.13		
Mn^{2+} (mg/L)	0.01	0.04						0.1		0.05	0.01			
F^- (mg/L)	1.45	1.35	1.28	1.03	0.6	0.3	0.97	0.58	0.8	0.34	0.93	1	0.75	0.72
Cl^- (mg/L)	6.52	6.66	6.95	4.07	9	11.3	35.5	24.76	28.4	66.91	64.31	73.4	15.6	0
NO_2^- (mg/L)		0.01	0.02	0.52				0.03			0.03	0.1		
NO_3^- (mg/L)	6.15	27.06		0.31		0.5	5.9	16.28	8.9	10.67	8.01			0.44
Alkalinity (mg/L)	220.7	233.21	241.2			360	300			578.39	568.94	667.8		
CO_3^{2-} (mg/L)	0	0	0	0	0	0		0		1.2	1.09	0	0	0
HCO_3^- (mg/L)	269.26	287.03	294.3	268	380	439.2	366	392.5	402.6	703.24	691.97	714	442	625
SO_4^{2-}(mg/L)	8.14	2.26	1.71	5.68	0.2	4	10.6	12	8.64	6.4	8.08	5.2	4.6	6
PO_4^{3-}(mg/L)	0.21	0.33	0.2					0.15		0.51	0.53	0.65		
Water Type	Ca-Na-HCO3	Na-Ca-HCO3	Na-Ca-HCO3	Na-Ca-HCO3	Mg-Ca-HCO3	Mg-Ca-HCO3	Ca-Mg-Na-HCO3	Ca-Mg-Na-HCO3	Na-Mg-Ca-HCO3	Na-Mg-HCO3	Na-Mg-HCO3	Na-Mg-HCO3	Na-Mg-Ca-HCO3	Na-Mg-HCO3

Continued…

StationID	Debrezeit											Mojo		
SampleID	D/Z Blue Nile Plastic (BNP01)			Hora Tannery (HT01)				GW06				Mojo Slaughterhouse (GW01)		
Year	1996	1999	2000	1993	1998	1999	2000	1982	2006	2007	2010	1988	2019	2021
TDS (mg/L)			375		359.9	478.24			553.56	550.55	558	449	395	400
EC (µS/cm)			614		590	784			846.78	852.25	843	736.07	790	810
pH	7.69	7.45	7.69	7.4	7.12	7.15			7.25	7.26	7.49	8.3	7.04	7.16
NH_4^+(mg/L)									0.22	0.57	0.25			
Na^+ (mg/L)	34	33.7	34	57.8	59.4	63.1	57.8	63	109.33	116.33	123	69.7	85	88.09
K^+ (mg/L)	9	9.1	9	5.6	5.8	6.5	5.6	12	13.26	14.08	17	13.2	15.21	13.84
T. Hardness (mg/L)	257.6	294.6	257.6	216.1	229.8	232.3	216.1	190.6	204.2	204.9	220.4	162.6	200.8	208.6
Ca^{2+} (mg/L)	44	47.31	44	43.3	46	47	43.3	50	54.32	55.28	58	47	46.7	50.3
Mg^{2+} (mg/L)	36	43	36	26.3	28	28	26.3	16	16.69	16.27	18.4	11	20.5	20.21
Fe_tot (mg/L)							0.14		0.1	0.03	0.06	0	0.60	0.81
Mn^{2+} (mg/L)							0		0.03	3.19		0	0.01	0.04
F^- (mg/L)	0.62		0.62	0.68			0.68	0.4	4.2	10.08	6.4	0.82		
Cl^- (mg/L)	7	8.71	7	12.8	7.36	27.08	12.8	14	17.04	13.12	20.85	14.2	13.78	14.59
NO_2^- (mg/L)										0.01	0.01			
NO_3^- (mg/L)	5	11.95	5	6.7	2	24.06	6.7		8.63	4.32		0.89		
Alkalinity (mg/L)				312					409.46	442.48	475.2			
CO_3^{2-} (mg/L)	0	0	0	0	0	0	0	0	0	0	0	0	0	0
HCO_3^- (mg/L)	392	415	390	380.6	415	429	380.6	496	500	539.82	579.7	341.6	439	433
SO_4^{2-} (mg/L)	2.04	4.68	7	4.44	4.61	7.18	9	9.74	4.92	1.56	1.2	6.36	8	7.31
PO_4^{3-}(mg/L)							0.1		0.27	0.34	0.05	0		
Water Type	Mg-Ca-Na-HCO3	Mg-Ca-Na-HCO3	Mg-Ca-Na-HCO3	Na-Mg-Ca-HCO3	Na-Mg-Ca-HCO3	Mg-Na-Ca-HCO3	Na-Mg-Ca-HCO3	Mg-Na-Ca-HCO3	Na-Ca-HCO3	Na-Ca-HCO3	Na-Ca-HCO3	Na-Ca-HCO3	Na-Ca-Mg-HCO3	Na-Ca-Mg-HCO3

Continued…

StationID	Holeta						Melka Kunture						Chefedonsa			
SampleID	GW02						GW04						SP02			
Year	1983	2006	2007	2009	2019	2021	2006	2007	2008	2010	2019	2021	1984	2007	2019	2021
TDS (mg/L)	175	144	162	164	155	100	268	357	508	344.65	300	300	220	279	245	250
EC (µS/cm)	350	233	260	260	310	200	536	549	534	565	600	600	361	429	490	490
pH	8	8.7	8.9	9	8.42	9.42	7.25	7.26	7.21	7.24	6.95	6.83	7.37	7.2	7.13	7.02
NH_4^+(mg/L)	0	3.4	0.59				0.23									
Na^+ (mg/L)	17	36.8	34	50	57	57.8	38	40.2	44	45.24	47.52	50.4	7.5	29.5	35.45	38.5
K^+ (mg/L)	1.01	1.7	0.9	1	1.65	9.46	11	10.8	10.7	12.13	12.1	12.8	1.8	8.2	10.96	13.43
T. Hardness (mg/L)	84.0	117.3	138.3	139.1	165.6	173.7	213.7	211.7	213.7	218.0	235.3	252.1	119.9	152.0	193.5	207.1
Ca^{2+} (mg/L)	33	46	54	54	66	69	65.3	67.13	68.64	72.13	76.52	81.4	38.4	41.3	57.2	63
Mg^{2+} (mg/L)	0.37	0.56	0.81	1	0.1482	0.2853	12.3	10.7	10.26	9.19	10.74	11.86	5.84	11.9	12.31	12.1
Fe_tot (mg/L)		1.7	0.04		0.54	0.7918	0.2				0.1595	0.2952	0		0.1849	0.3197
Mn^{2+} (mg/L)		0.21	0		0.0114	0.0357	0.1			0	0.0196	0.0461	0		0.0163	0.0404
F^- (mg/L)	0		0.6	1			1.39		1.34	0.91			1.36			
Cl^- (mg/L)	4	8.72	12.5	13	13.4	14	8.64	6.9	8.64	6.6	8.3	9.156	2.84	3.5	2	3.02
NO_2^- (mg/L)										0.51						
NO_3^- (mg/L)	0	2.22	0.23	0		1	2.39	2.86	0.73	2.75				3.8		
Alkalinity (mg/L)																
CO_3^{2-} (mg/L)	0	7.2	10.8	12	0	0	0	0		0	0	0	0	0	0	0
HCO_3^- (mg/L)	110	121	204	247	315	316	311.47	330	339.65	358	372	410	146.4	257	305	331
SO_4^{2-} (mg/L)	2.01	2.3	0.57	1	1.84	4.2	13.8	7	3.2	7.18	9.53	8.31	11	5.3	7.54	13.1
PO_4^{3-}(mg/L)		0.29	0.15	0		0.19	0.4									
Water Type	Ca-HCO3	Ca-HCO3	Ca-Na-HCO3	Ca-Na-HCO3	Ca-Na-HCO3	Ca-Na-HCO3	Ca-Na-HCO3	Ca-Na-HCO3	Ca-Na-HCO3	Ca-Na-HCO3	Ca-Na-HCO3	Ca-Na-HCO3	Ca-HCO3	Ca-Na-Mg-HCO3	Ca-Na-HCO3	Ca-Na-HCO3

Appendix 4: River water monitoring data

Station ID	Awash @ Melkakunture							Legetafo River					Holeta River		
SampleID	RW05							RW04					RW03		
Year	2006	2007	2011	2016	2015	2019	2021	2008	2010	2011	2019	2021	2016	2019	2021
TDS (mg/l)	258.6	214	223.4	230	267.9	270	240	216.4	229.1	306	360	400	160	135	140
EC (µS/cm)	424.00	331	336	316	335.6	540	480	199	289	379	710	810	269	270	280
pH	7.68	7.89	7.75	8	7.12	7.5	7.82	6.74	7.28	7.15	7.6	8.23	7.99	7.86	7.79
NH_4^+ (mg/l)	0.16	0.611													
Na^+ (mg/l)	33.17	12.5	19	27	73	69.5	86.25	9	17	22	57.77	64.49	10.6	64.29	75.81
K^+ (mg/l)	8.30	7.2	4	6.2	4.02	11.36	14.94	3	3	6.5	1.64	3.80	1.2	1.76	3.32
Total Hardness (mg/l)	176.82	146.82	122.60	155.75	591.19	363.49	383.95	67.80	95.50	115.85	102.03	124.48	129.36	168.56	201.18
Ca^{2+} (mg/l)	51.37	42	31	41.8	153	126.7	134.80	14	30	36.5	39.5	42.25	36	63.16	72.01
Mg^{2+} (mg/l)	11.81	10.2	11	12.5	50.9	11.4	11.45	8	5	6	0.8	4.60	9.6	2.6	5.16
Fe_tot (mg/l)	0.09	0.219				0.82	1.32				1.2	1.63		0.96	2.35
Mn^{2+} (mg/l)	8.64				0.17	0.02	0.03				0.02	0.05		0.02	0.06
F^- (mg/l)	1.39	0.45	0.51	0.41	2.37	0.51	0.57	0.2	0.6	0.55			0.39		
Cl^- (mg/l)	6.38	8.94	5	5.7	25		7.35	3	9	17		28	5.96		
NO_2^- (mg/l)	0.00	0.1	0		0.06		0								
NO_3^- (mg/l)	7.63		2.2	8	3.39		4.45	15	8.4				0.78		
CO_3^{2-} (mg/l CO3)	0.00	0	0	0	0	0	0	0		0	0	0	0	0	0
HCO_3^- (mg/l)	263.09	219.6	195	233.9	184	284	248	107	123	157	267	213	150.79	223	201
SO_4^{2-} (mg/l)	5.41	3.62	3.4	1.1	21.3		36	1	15	28.5			6		
PO_4^{3-} (mg/l)	0.31	0.316	0.2				0.5								
Pb (mg/L)					3.33	0.02	0.04				0.02	0.04		0.02	0.03
Zn (mg/L)					0.07	0.66	1.46				0.8	1.74		0.76	1.26
Wter Type	Ca-Na-HCO3	Ca-Mg-HCO3	Ca-Mg-Na-HCO3	Ca-Na-Mg-HCO3	Ca-Mg-Na-HCO3	Ca-Na-HCO3	Ca-Na-HCO3	Ca-Mg-HCO3	Ca-Na-HCO3	Ca-Na-HCO3	Na-Ca-HCO3	Na-Ca-HCO3	Ca-Mg-HCO3	Ca-Na-HCO3	Ca-Na-HCO3

Continued…

Station ID	Mojo River @ Inlet to Koka Dam			Mojo River		
SampleID	RW01			RW02		
Year	2015	2019	2021	2004	2019	2021
TDS (mg/l)	219	410	480	310	450	730
EC (µS/cm)	437	810	950	620	890	1460
pH	7.12	8	7.8	8.29	7.84	7.78
NH_4^+(mg/l)						
Na^+ (mg/l)	57.4	62	82.54	89.6	53.84	90.48
K^+ (mg/l)	8.17	11.97	13.75	52	1.46	3.47
Total Hardness (mg/l)	325.29	128.32	147.33	169.42	55.61	77.92
Ca^{2+} (mg/l)	16.3	50	56.8	53.6	22.08	30.97
Mg^{2+} (mg/l)	69.4	0.81	1.3	8.64	0.1	0.12
Fe_tot (mg/l)		2	3.13	0.11	1.3	2.2
Mn^{2+} (mg/l)		0.02	0.07	0.3	0.03	0.03
F^- (mg/l)	0.59			1.72		
Cl^- (mg/l)	14.3			10		
NO_2^- (mg/l)	1.07			0.08		
NO_3^- (mg/l)	19.48			8.36		
CO_3^{2-} (mg/l CO3)	0	0	0	0	0	0
HCO_3^- (mg/l)	180	323	143	464.82	339	311
SO_4^{2-} (mg/l)	24.86			21		
PO_4^{3-} (mg/l)				0.36		
Pb (mg/L)	4	0.03	0.08		0.024	0.09
Zn (mg/L)	0.07	1.2	1.47		1.15	1.96
Wter Type	Ca-Mg-Na-HCO3	Ca-Na-HCO3	Na-Ca-HCO3	Na-Ca-HCO3	Na-Ca-HCO3	Na-Ca-HCO3

Appendix 5: Lake Water monitoring data

Station ID	Lake Aba Samuel					Gefersa Dam			
Sample ID	LW04					LW05			
year	1997	2000	2006	2019	2021	1982	2010	2019	2021
TDS (mg/l)	337	546	962	560	530	30.00	34.00	45.00	50.00
EC (µS/cm)	505.5	802.94	1443	1120	1060	65.00	77.30	90.00	100.00
pH	7	8	7.56	8.08	7.64	7.78	7.81	7.67	7.89
NH_4^+(mg/l)			1.3				0.38		
Na^+ (mg/l)	12.58	14	83	85.28	99.02		80.00	66.41	72.35
K^+ (mg/l)	12	15	23.75	11.92	11.2		12.00	10.93	13.93
T.H (mg/l)	104.93	176.90	225.91	223.39	271.64	29.84	140.20	164.55	177.99
Ca^{2+} (mg/l)	30	56	71.34	66.23	84.35	8.00	20.00	30.20	34.56
Mg^{2+} (mg/l)	7.3	9	11.6	14.1	14.82	2.40	22.00	21.72	22.34
Fe_tot (mg/l)			0.06	0.408	1.276	0.70	1.26	1.10	2.98
Mn^{2+} (mg/l)			0.14	0.0129	0.0196	0.60	0.02	0.13	0.29
F^- (mg/l)	0.6	0.6	0.48			0.60	0.00		
Cl^- (mg/l)	36	47	82.13			5.00	2.50		
NO_2^- (mg/l)		0.05				0.00	0.01		
NO_3^- (mg/l)		1	16.25			4.00	0.18		
Alk. (mg/l)			309.4			30.00	50.00		115.00
CO_3^{2-} (mg/l)	0	0	0	0	0	0.00	0.00		0.00
HCO_3^- (mg/l)	160	275	392.05	444	461.8		50.00	112.00	115.00
SO_4^{2-} (mg/l)		67	19.85				8.00		
PO_4^{3-}(mg/l)		0	1.5	1.46	2.3	0.21	0.13		
Water Type	Ca-HCO3-Cl	Ca-HCO3-SO4-Cl	Na-Ca-HCO3-Cl	Na-Ca-HCO3	Na-Ca-HCO3	Ca-Mg-HCO3	Na-Mg-Ca-HCO	Na-Mg-Ca-HCO3	Na-Mg-Ca-HCO3

Continued…

Station ID	Legedadi Dam						Koka Dam						
Sample ID	LW02						LW01						
year	1982	1983	2010	2011	2019	2021	1986	1990	1991	2007	2010	2019	2021
TDS (mg/l)	69.65	69.22	65.45	56.00	70.00	70.00	39.00	206.00			309.00	210.00	170.00
EC (µS/cm)	102.43	101.80	107.30	117.60	140.00	140.00	65.00	412.00			507	420.00	350.00
pH	7.02	6.97	7.83	7.58	7.92	7.85	7.20	7.30	8.20	8.17	7.89	7.94	8.11
NH_4^+(mg/l)	0.82	0.25		0.03									
Na^+ (mg/l)			3.20		60.42	84.56	21.50	28.00	31.00	22.80	31.00	51.97	60.13
K^+ (mg/l)			2.40		14.45	17.74	5.00	5.60	5.50	16.00	7.00	12.44	19.73
T.H (mg/l)			35.73	142.40	80.58	81.29	75.95	80.14	79.32	15.78		30.36	39.71
Ca^{2+} (mg/l)			9.11	34.00	28.15	24.71	23.00	27.30	23.20	5.00	27.00	11.34	13.06
Mg^{2+} (mg/l)			3.16	14.00	2.49	4.76	4.50	2.90	5.20	0.80	5.00	0.49	1.72
Fe_tot (mg/l)	0.25	0.12	0.82	0.12	0.24	0.71			0.00	0.00		0.17	0.50
Mn^{2+} (mg/l)	0.07	0.01	0.13	0.02	0.04	0.09						0.02	0.03
F^- (mg/l)	0.56	0.72		0.27			0.70	1.97		1.29	0.60		1.04
Cl^- (mg/l)			1.75	7.00			9.50	14.20	6.40	36.00	12.00		40.82
NO_2^- (mg/l)	0.02	0.02		0.01									
NO_3^- (mg/l)	6.22	3.08	4.02	0.15			0.00	0.00	0.00				0.33
Alk. (mg/l)													
CO_3^{2-} (mg/l)	0.00	0.00	0.00	0.00	0.00	0.00	0.00	0.00	0.00	0.00	0.00	0.00	0.00
HCO_3^- (mg/l)	55.95	54.30	57.34	42.00	64.00	100.00	140.00	158.60	154.40	166.00	176.00	200.00	242.00
SO_4^{2-} (mg/l)			6.72	0.10			9.50		14.00	3.00	15.00		5.12
PO_4^{3-}(mg/l)	0.25	0.33	409.09	0.09									
Water Type			Ca-Mg-HCO3	Ca-Mg-HCO3	Na-Ca-HCO3	Na-Ca-HCO3	Ca-Na-HCO3	Ca-Na-HCO3	Na-Ca-HCO3	Na-HCO3-Cl	Na-Ca-HCO3	Na-HCO3	Na-HCO3-Cl

Continued…

Station ID	Lake Hora Hoda							Lake Bishoftu								
Sample ID	LW06							LW07								
year	1963	1973	1973	1992	1999	2006	2007	1963	1964	1973	1982	1992	1998	2004	2006	2007
TDS (mg/l)						3557.67	3620.91						915.00	812.00	1054.78	1039.55
EC (µS/cm)						5496.67	5459.09						1500	1624.00	1620.67	1613.67
pH						9.74	9.75							9.21	9.28	9.32
NH_4^+(mg/l)						0.65	0.76							0.72	0.81	0.81
Na^+ (mg/l)	1540.33	1457.57	537.97	1356.41	857.53	1203.33	1244.17	367.84		312.43	299.80	289.67	298.87	200.00	264.89	275.00
K^+ (mg/l)	316.71	260.05	70.38	449.65	217.40	225.78	226.17	58.52		43.40	60.21	71.16	35.19	99.00	39.22	43.28
T.H (mg/l)	64.32	71.61	84.45	40.08	6.01	88.48	77.33	315.79	347.59	274.00	88.72	171.14	401.83	246.46	284.05	278.06
Ca^{2+} (mg/l)	13.43	11.42	6.51	16.03	2.40	16.70	17.48	7.41	7.01	3.21	1.25	45.29	35.27	11.60	10.76	17.00
Mg^{2+} (mg/l)	7.50	10.50	16.63			11.39	8.21	72.50	80.50	64.88	20.88	14.13	76.50	53.04	62.72	57.45
Fe_tot (mg/l)						0.07	0.07							0.21	0.08	0.06
Mn^{2+} (mg/l)						0.09	5.76							0.03	0.09	0.78
F^- (mg/l)		4.94	4.18	5.00	4.13	11.41	209.31	_	_	0.21	1.10	0.38	_	0.64	1.29	34.54
Cl^- (mg/l)	779.00	623.92	879.16	779.90	827.76	652.27	395.94	141.80	123.72	92.88	219.79	75.86	9.22	80.00	93.64	66.78
NO_2^- (mg/l)							0.04							0.00		0.03
NO_3^- (mg/l)						8.65	2.99	1.24				3.72	_	10.20	8.02	5.23
Alk. (mg/l)						2185.84	2254.50							900.00	776.27	821.33
CO_3^{2-} (mg/l)						678.87	726.00							0.00	138.67	179.80
HCO_3^- (mg/l)	3136.43	4515.48	866.48			1300.33	1160.39	1220.40	1177.69	1043.44	1582.86	1151.45	_	1098.00	664.96	626.96
SO_4^{2-} (mg/l)	33.62	0.96	7.20	1.92		1.65	3.86	16.81	_	5.76	10.57	0.96		2.00	37.37	1.12
PO_4^{3-}(mg/l)						3.45	3.16							3.40	0.34	0.23
Water Type	Na-HCO3-Cl	Na-HCO3-Cl	Na-Cl-HCO3			Na-CO3-HCO3-Cl	Na-CO3-HCO3	Na-Mg-HCO3	Mg-HCO3-Cl	Na-Mg-HCO3	Na-HCO3-Cl	Na-HCO3		Na-Mg-HCO3	Na-Mg-HCO3-CO3	Na-Mg-HCO3-CO3

Continued…

Station ID	Lake Hora									
Sample ID	LW08									
year	1938	1963	1973	1982	1992	1998	2004	2006	2007	2011
TDS (mg/l)						1366.40	1134.00	1448.20	1508.25	4349.00
EC (µS/cm)						2240.00	2268.00	2216.60	2288.33	6220
pH						8.21	8.70	8.86	8.75	8.90
NH_4^+(mg/l)							0.36	0.61	0.74	
Na^+ (mg/l)	215.88	549.46	549.69	43.91	5.98	363.00	190.00	406.30	426.25	2000.00
K^+ (mg/l)	22.29	51.22	57.09	48.09	7.82	41.20	63.90	43.70	46.83	220.00
T.H (mg/l)	72.88	218.96	362.71	67.82	335.18	319.60	231.85	350.81	360.71	
Ca^{2+} (mg/l)	16.03	6.81	11.42	1.50	35.67	3.20	15.20	32.23	31.11	8.00
Mg^{2+} (mg/l)	8.00	49.25	81.50	15.63	60.00	76.00	47.28	65.91	69.01	4.00
Fe_tot (mg/l)							0.24	0.08	0.09	
Mn^{2+} (mg/l)							0.20	0.06	0.05	
F^- (mg/l)			0.38	0.80	1.33		0.93	1.26	1.08	6.00
Cl^- (mg/l)	177.60	201.00	209.16	99.97	118.76	149.60	140.00	157.00	178.18	610.00
NO_2^- (mg/l)							0.00		0.00	
NO_3^- (mg/l)						28.00	8.36	10.25	5.40	35.00
Alk. (mg/l)							1260.00	1006.04	1105.23	
CO_3^{2-} (mg/l)						0.00	0.00	84.72	147.20	21.00
HCO_3^- (mg/l)	1311.93	1635.34	1514.52	1054.43	214.79	805.00	1537.20	1054.96	1169.87	1430.00
SO_4^{2-} (mg/l)		19.21	12.01	6.00		59.60	2.00	4.65	1.36	5.00
PO_4^{3-}(mg/l)							3.90	0.43	0.38	
Water Type	Na-HCO3-Cl	Na-HCO3	Na-Mg-HCO3	HCO3-Cl	Mg-Ca-HCO3-Cl	Na-Mg-HCO3	Na-HCO3	Na-Mg-HCO3	Na-Mg-HCO3	Na-HCO3-Cl

Continued…

Station ID	Lake Bishoftu Guda												
Sample ID	LW09												
year	1963	1964	1973	1987	1992	1998	2001	2004	2006	2007	2009	2011
TDS (mg/l)						506.91	585.6	427.00	527.30	526.17	510.00	771.50
EC (µS/cm)						831.00	960.00	854.00	818.20	805.42	787.00	1264.75
pH						8.16		7.06	9.10	9.05	9.20	8.95
NH_4^+(mg/l)							5.60	1.19	0.42	0.45	0.36	
Na^+ (mg/l)	126.45		121.85	108.05	22.99	87.00	53.60	130.00	89.50	100.50	98.00	15.00
K^+ (mg/l)	41.06		28.93	26.20	49.66	30.00	14.50	43.20	27.95	30.96	34.50	27.00
T.H (mg/l)	265.87	272.63	212.09	55.19	264.72	212.80	227.32	255.46	241.29	227.49	229.89	196.30
Ca^{2+} (mg/l)	11.02	9.22	10.42	2.81	48.90	6.40	16.80	15.20	19.88	19.30	13.40	8.00
Mg^{2+} (mg/l)	58.13	60.88	45.38	11.75	34.75	48.00	45.20	53.04	46.73	43.72	47.90	43.00
Fe_tot (mg/l)							0.00	0.32	0.08	0.10	0.05	
Mn^{2+} (mg/l)							0.00	0.40	0.10	0.05		
F^- (mg/l)			0.95	0.86	0.19			1.17	1.16	0.97	0.80	1.00
Cl^- (mg/l)	31.91	28.01	24.11	24.46	19.85	21.30	2.13	16.00	24.67	25.32	26.80	25.00
NO_2^- (mg/l)								O		0.02	0.01	
NO_3^- (mg/l)				3.10			0.00	22.00	7.52	6.71		2.20
Alk. (mg/l)								500.00	430.45	460.80	468.00	
CO_3^{2-} (mg/l)						0.00	81.00	0.00	72.24	81.20	84.00	38.00
HCO_3^- (mg/l)	622.40	659.02	567.49	507.08	414.94	298.40	155.60	610.00	396.31	375.62	400.16	450.00
SO_4^{2-} (mg/l)	4.80		9.13	0.48	0.96	0.84	196.40	3.00	4.83	1.08	1.20	5.00
PO_4^{3-}(mg/l)							0.01	5.70	0.36	0.14	0.15	
Water Type	Na-Mg-HCO3	Mg-HCO3	Na-Mg-HCO3	Na-HCO3	Mg-Ca-HCO3	Mg-Na-HCO3	Mg-Na-SO4-CO3-HCO3	Na-Mg-HCO3	Na-Mg-HCO3-CO3	Na-Mg-HCO3-CO3	Na-Mg-HCO3-CO3	Mg-HCO3